8-20-2013 12:00 AM

Analysis of Subcellular Localization Patterns Suggest Non-enzymatic Roles for Select Arogenate Dehydratases

Travis R. Howes
The University of Western Ontario

Supervisor
Dr. Susanne Kohalmi
The University of Western Ontario

Graduate Program in Biology
A thesis submitted in partial fulfillment of the requirements for the degree in Master of Science

ANALYSIS OF SUBCELLULAR LOCALIZATION PATTERNS SUGGEST NON-ENZYMATIC ROLES FOR SELECT AROGENATE DEHYDRATASES

Thesis format: Monograph

by

Travis Raymond Howes

Graduate Program in Biology

A thesis submitted in partial fulfillment
of the requirements for the degree of
Master of Science

The School of Graduate and Postdoctoral Studies
The University of Western Ontario
London, Ontario, Canada

Abstract

The final step of phenylalanine biosynthesis *in planta* is catalyzed by arogenate dehydratases (ADTs). Previously cloned *ADT-CFP* fusion genes were used to provide an in depth study of the subcellular localization of all six ADTs from *Arabidopsis thaliana*. Through co-localization of ADT-CFPs with a stroma-marker it is shown that most ADTs localize to stroma-filled projections from chloroplasts called stromules. The localization of ADT5 and ADT2 provide evidence for additional, non-enzymatic roles. In the case of ADT5, it is found to localize to the nucleus, suggestive of an uncharacterized nuclear role. The localization patterns of ADT2 are suggestive of a role in chloroplast division. This secondary role is investigated through analysis of localization patterns in *N. benthamiana*, *A. thaliana* and several chloroplast division mutants. In addition, chloroplast morphology is examined in *adt2* mutant plants, and the effect of this mutation on the localization of a known chloroplast division protein is examined.

Keywords

arogenate dehydratase, phenylalanine biosynthesis, subcellular localization, stromules, chloroplast division, agroinfiltration, transient transformation, *arc* mutants, FtsZ

Acknowledgments

I would like to thank many people for their help and support in making this thesis possible. I sincerely thank my supervisor, Dr. Susanne Kohalmi, not only for her guidance and support but also her friendship over the last two years. I also thank my advisory committee members Dr. Sashko Damjanovski and Dr. Denis Maxwell for their helpful advice.

I would also like to thank my lab mates over the past two years, 4th years Levi Karademir, Rene Boudreau, Andra Jejeran and William Pirjamali for making the lab such a great place to work in. To my fellow graduate students Megan Smith-Uffen and Sara Rad, I thank you both for support and friendship during the trials and tribulations of grad school. Life in the lab is much more enjoyable with both of you around.

There are many people I also thank for their help during my project. I thank Dr. Rima Menassa for allowing me access to Agriculture Canada and their confocal microscope facility. I would also like to thank Reza Saberianfar and Lisa Amyot for their help and patience in teaching me how to use the confocal microscope. To Dr. Gang Tian and Dr. Yuhai Cui, I thank you both for providing the nucleoporin construct. To Dr. Tengfeng Huang and Dr. Georg Jander, I thank you for providing me with *adt2* mutant seeds.

I would also like to thank Ornela Kljakic for her assistance in parts of this study. She spent many tedious hours counting chloroplasts and cells, and measuring stromules. I also thank her for assisting in the statistical analysis of data.

Lastly, I would like to thank my family, especially my parents George and Charlotte who have given me unconditional love and support over the past 24 years. Without you guys I would not be in this position. Thank you so much, I love you both.

Table of Contents

List of Tables

List of Figures

List of Abbreviations

Note: abbreviations for SI units are not listed

ABA	abscisic acid
ABRC	*Arabidopsis* Biological Resource Centre
ACT	Aspartokinase, Chorismate mutase, TyrA
ADT	arogenate dehydratase
ARC	ACCUMULATION AND REPLICATION OF CHLOROPLASTS
att	*attachment*
BDM	2,3-butanedione monoxime
CaMV	cauliflower mosaic virus
ccdB	*control of cell death B*
CFP	CYAN FLUORESCENT PROTEIN
CM	chorismate mutase
Col-0	Columbia-0
ddH_2O	double-distilled H_2O
DMSO	dimethyl sulfoxide
dnMyoXI-2	dominant negative myosin XI-2
dnMyoXI-K	dominant negative myosin XI-K
EDTA	ethylenediaminetetraacetic acid
EMS	ethyl methanesulfonate

EV	empty vector
FRAP	fluorescence recovery after photo-bleaching
FtsZ	Filamentous temperature sensitive Z
LB	lysogeny broth
L*er*	Landsberg *erecta*
MES	2-(N-morpholino)ethanesulfonic acid
NUP1	NUCLEOPORIN1
OD_{600}	optical density measured at 600 nm
PARC6	PARALOG OF ARC6
PAT	prephenate aminotransferase
PD	plastid-dividing
PDT	prephenate dehydratase
PDV	PLASTID DIVISION
PPAT	phenylpyruvate aminotransferase
PTGS	post-transcriptional gene silencing
RuBisCO	Ribulose-1,5-Bisphosphate Carboxylase/Oxygenase
SOC	super optimal growth with catabolite repression
TAE	Tris base, acetic acid, EDTA
T-DNA	transfer-DNA
TE	Tris base, EDTA

Ti-plasmid	tumor-inducing plasmid
TP	transit peptide
TP-YFP	transit peptide of the small subunit of RuBisCO fused to YFP
VIR	VIRULENCE
Ws	Wassilewskija
YEB	yeast extract and beef
YFP	YELLOW FLUORESCENT PROTEIN

1 Introduction

1.1 Phenylalanine and its significance

Phenylalanine is an aromatic amino acid that is only synthesized by plants and microorganisms (Maeda and Dudareva, 2012). Despite the human body's inability to synthesize phenylalanine it is essential for human life and must therefore be obtained through our diet (Maeda and Dudareva, 2012). Like most amino acids, phenylalanine is incorporated into proteins during their synthesis, but its importance is not limited to that role. In plants, phenylalanine serves as a precursor for the synthesis of secondary metabolites such as flavonoids (Samanta *et al.,* 2011). These are a diverse group of phenolic compounds that act as cellular signaling molecules, protect plant cells from ultraviolet-light, and are important pigments responsible for flower colour (Samanta *et al.,* 2011). Phenylalanine is also required for the synthesis of monolignols, monomers that assemble into lignin, a compound that is required for the structural integrity of plants (Liu, 2012). In mammals, phenylalanine is a precursor to the neurotransmitter dopamine and the hormones epinephrine and norepinephrine by its conversion to tyrosine followed by subsequent modifications (Fernstrom and Fernstrom, 2007; Udenfriend and Cooper, 1952) The importance of phenylalanine to humans extends beyond our inherent biological need for it, as it is an industrially important compound. For example, phenylalanine is required for the production of aspartame, an artificial sweetener, produced globally at upwards of 15,000 tons per year (Leuchtenberger *et al.,* 2005). Given the importance of phenylalanine to plant and animal life, increasing our knowledge of the enzymes and processes involved in its synthesis will be of benefit to society.

1.2 Phenylalanine biosynthesis

Phenylalanine biosynthesis (Fig. 1) is an extension of the shikimate pathway, a series of enzyme catalyzed biochemical reactions connecting the metabolism of carbohydrates to the synthesis of aromatic amino acids (Herrmann and Weaver, 1999). The end product of the shikimate pathway is chorismate, the last common precursor to the synthesis of the three aromatic amino acids tyrosine, tryptophan and phenylalanine

Figure 1. Phenylalanine biosynthesis.

Phenylalanine biosynthesis occurs downstream of the shikimate pathway. Chorismate, the last common precursor to all aromatic amino acids, is converted to prephenate by CM. Synthesis of phenylalanine from prephenate can occur through one of two pathways depending on the organism. In microorganisms phenylalanine biosynthesis predominantly occurs through the pathway shown on the left. Prephenate is dehydrated and decarboxylated by PDT to phenylpyruvate. Transamination of phenylpyruvate to phenylalanine is subsequently catalyzed by PPAT. In plants phenylalanine biosynthesis occurs predominantly through the pathway on the right, which utilizes the same biochemical reactions but in opposite order. Prephenate is transaminated to arogenate by PAT. Arogenate is then dehydrated and decarboxylated by an ADT synthesizing phenylalanine.

CM: chorismate mutase; PDT: prephenate dehydratase, PPAT: phenylpyruvate aminotransferase, PAT: prephenate aminotransferase, ADT: arogenate dehydratase.

Adapted from Cho *et al.* (2007).

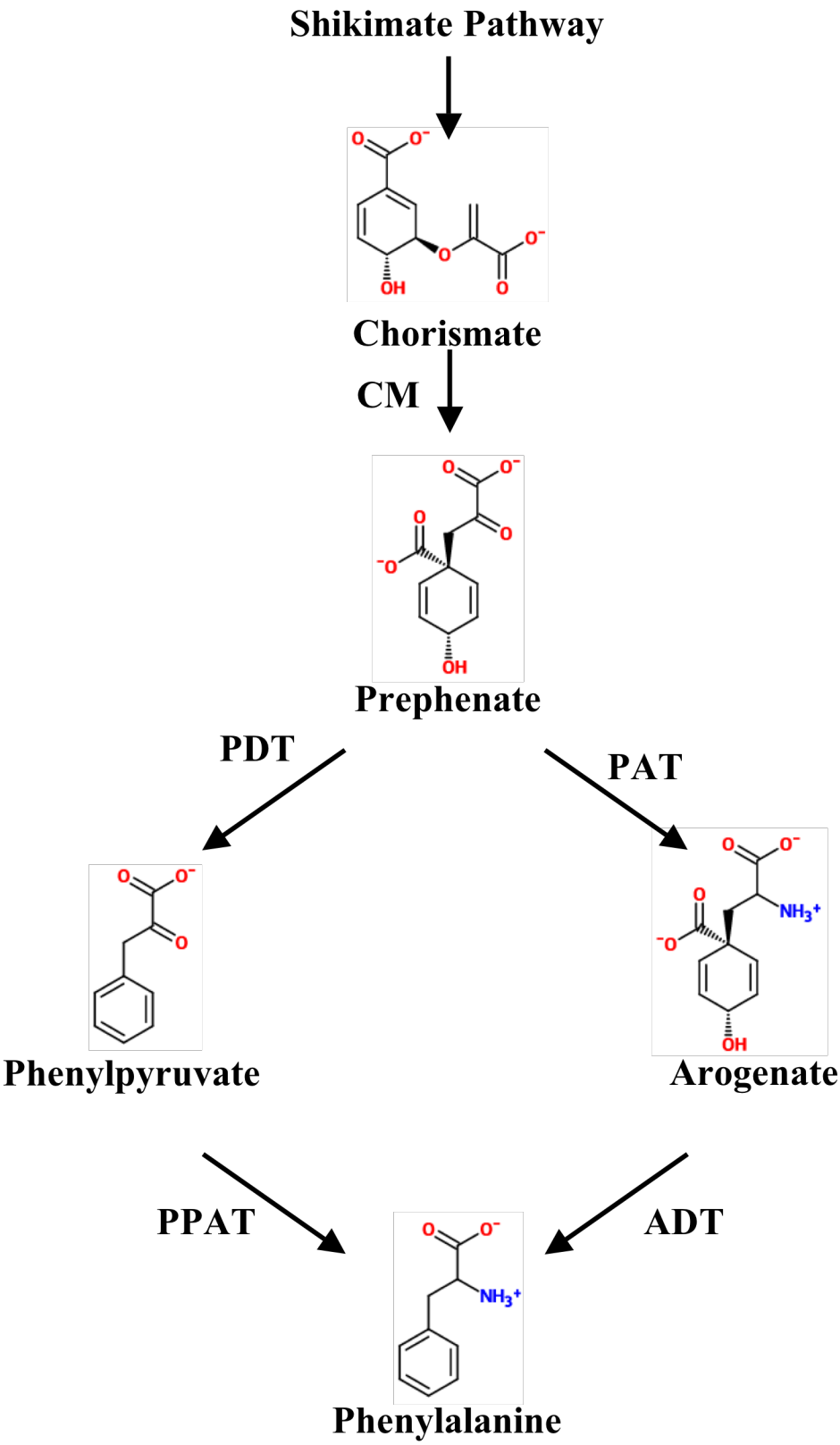
Shikimate Pathway
Chorismate
CM
Prephenate
PDT
PAT
Phenylpyruvate
Arogenate
PPAT
ADT
Phenylalanine

(Tzin and Galili, 2010). Synthesis of phenylalanine from chorismate begins with the conversion of chorismate to prephenate catalyzed by chorismate mutase (CM) (Eberhard *et al.,* 1993; Tzin and Galili, 2010). Downstream of prephenate, phenylalanine can be synthesized via one of two pathways depending on the organism (Maeda and Dudareva, 2012). In microorganisms, prephenate is dehydrated and decarboxylated by prephenate dehydratase (PDT) synthesizing phenylpyruvate (Maeda and Dudareva, 2012). A transamination of phenylpyruvate by phenylpyruvate aminotransferase (PPAT) synthesizes phenylalanine (Maeda and Dudareva, 2012). In plants, the same biochemical reactions occur, but in opposite order. Prephenate is first transaminated by prephenate aminotransferase (PAT) synthesizing arogenate (Bonner and Jensen, 1985). Arogenate is then dehydrated and decarboxylated to phenylalanine by an arogenate dehydratase (ADT) (Cho *et al.,* 2007).

1.3 AROGENATE DEHYDRATASES (ADTs)

The genome of the model plant *Arabidopsis thaliana* encodes many gene families (The *Arabidopsis* Genome Initiative, 2000). In *A. thaliana* there are six genes that code for ADTs (*ADT1: At1G11790, ADT2: At3G07630, ADT3: At2G27820, ADT4: At3G44720, ADT5: At5G22630 and ADT6: At1G08250*) (Cho *et al.,* 2007; Ehlting *et al.,* 2005). Plant ADTs have three domains: an N-terminal transit peptide, an internal catalytic domain responsible for catalyzing the dehydration/decarboxylation reaction, and a C-terminal ACT (aspartokinase, chorismate mutase, TyrA) domain (Cho *et al.,* 2007). ACT domains are a conserved feature of enzymes involved in amino acid biosynthesis, and typically regulate enzyme activity allosterically through ligand binding (Liberles *et al.,* 2005). While the ACT domains of ADTs have not been characterized in detail, bacterial PDTs are inhibited upon binding of phenylalanine, causing the enzyme to transition from an active open state to an inactive closed state (Tan *et al.,* 2008). The relationship between ADTs and bacterial PDTs extends beyond the presence of an ACT domain as they share a high degree of amino acid sequence similarity (Cho *et al.,* 2007; Ehlting *et al.,* 2005). The similarity between ADTs and PDTs led to the identification of the six *ADT*s in the *A. thaliana* genome (Ehlting *et al.,* 2005). This occurred prior to any

functional characterization of the enzymes since it was previously shown that ADT activity was present in the chloroplasts of the higher plants, *Nicotiana silvestris* and spinach, while PDT activity was absent (Jung *et al.,* 1986). ADT activity was confirmed after all six *A. thaliana* genes were cloned and expressed in *Escherichia coli* and it was determined that they could synthesize phenylalanine from arogenate (Cho *et al.,* 2007). Interestingly, ADT1, ADT2 and ADT6 are capable of using prephenate as a substrate and thus have PDT activity as well (Cho *et al.,* 2007). However, the PDT activity of these three enzymes is limited because the catalytic efficiency is much higher when arogenate is used as a substrate (Cho *et al.,* 2007).

1.3.1 Subcellular localization of ADTs

In silico analysis of amino acid sequences indicated that the N-terminal portion of ADTs is likely a transit peptide allowing for protein import into chloroplasts (Crawley, 2004), consistent with ADT activity being detected in chloroplasts (Jung *et al.,* 1986). Initial studies of ADT subcellular localization were performed in protoplasts, plant cells that have been enzymatically treated to remove the cell wall, and showed that all six ADTs localized uniformly throughout the chloroplast stroma (Rippert *et al.,* 2009). However, the cells used to generate the protoplasts were from cell suspension cultures (Rippert *et al.,* 2009) and such a system may not reflect the complexity of what is occurring *in planta*. Therefore, Bross (2011) cloned all six *ADT*s from *A. thaliana* as *CYAN FLUORESCENT PROTEIN* (*CFP*) fusion genes in pCB, a transfer-DNA (T-DNA) containing binary vector in which the expression of genes *in planta* is regulated by the Cauliflower Mosaic Virus (CaMV) *35s* promoter. After transforming *Agrobacterium tumefaciens* with pCB encoding *ADT-CFP* fusion genes, agroinfiltration was used to transiently express the fusion genes in *Nicotiana benthamiana* leaves (Bross, 2011). Confocal microscopy was used to determine the subcellular localization of each fluorescently labeled ADT (Bross, 2011). The localization of ADTs *in planta* was more complex than what had been previously observed in protoplasts (Bross, 2011; Rippert *et al.,* 2009). With the exception of ADT6, which was observed in the cytosol, all ADTs localized to tail-like structures extending from the body of chloroplasts (Bross, 2011).

Aside from localizing to these structures, ADT2 and ADT5 possessed unique localization patterns that are suggestive of additional non-enzymatic roles (Bross, 2011). In the case of ADT2, it was observed as a band across the middle of a chloroplast or as an aggregation of protein at a chloroplast pole (Bross, 2011). These localization patterns are similar to those of chloroplast division proteins (Miyagishima, 2011), and suggest that ADT2 may play a role in the division process. In the case of ADT5, it was seen to localize to globular structures resembling nuclei (Bross, 2011). Therefore, the subcellular localization patterns of ADTs *in planta* appear to be much more complex than was previously realized, and will require further examination to understand their significance.

1.4 Stromules

The tail-like structures that ADTs localize to *in planta* (Bross, 2011) are similar to a known feature of the structure of chloroplasts (Fig. 2) called stromules. Stromules (stroma-filled tubules) are stoma-filled projections of the plastid membrane (Gray *et al.,* 2001). Stromules are variable in appearance, and can be long, elaborately shaped tubules, or shorter protrusions (Gunning, 2005; Köhler and Hanson, 2000; Natesan *et al.,* 2005). They are also dynamic in nature and can extend, retract, and branch along their length (Gunning, 2005). Stromules can also create stroma-filled vesicles by budding off from their tip, a process called tip-shedding (Gunning, 2005). Visualization of stromules using confocal microscopy is not possible without the presence of stroma-targeted fluorescent proteins (Gray *et al.,* 2011). Typically, confocal microscopy identifies chloroplasts based on fluorescence from chlorophyll within the thylakoid membrane, and thylakoids are not present in stromules (Gray *et al.,* 2001; 2011).

1.4.1 Function of stromules

While stromules have been observed in a wide range of plant species (Natesan *et al*., 2005), their function has not been fully elucidated. However, there are several possible functions that have been proposed. The presence of stromules creates an increase in plastid surface area without substantially increasing plastid volume (Gray *et al.,* 2001; Natesan *et al.,* 2005). This property could, in theory, increase the capacity of plastids to

Figure 2. Structure of a chloroplast.

Chloroplasts are ovoid organelles with an outer and an inner membrane. Between the two membranes is the intermembrane space. Chloroplasts contain a protein rich fluid called stroma, where thylakoids are present. Thylakoids are membranous structures surrounding a lumen that can stack forming a granum. Contained within the thylakoid membrane is chlorophyll, a pigment required to visualize chloroplasts using confocal microscopy. Stroma-filled protrusions formed by the outer and inner membranes called stromules can extend from the body of the chloroplast, but do not contain thylakoids and therefore are not visible through chlorophyll fluoresence. Stromules are highly variable in size and shape, and are able to bud off from the chloroplast, forming vesicles.

Adapted from Bross (2011).

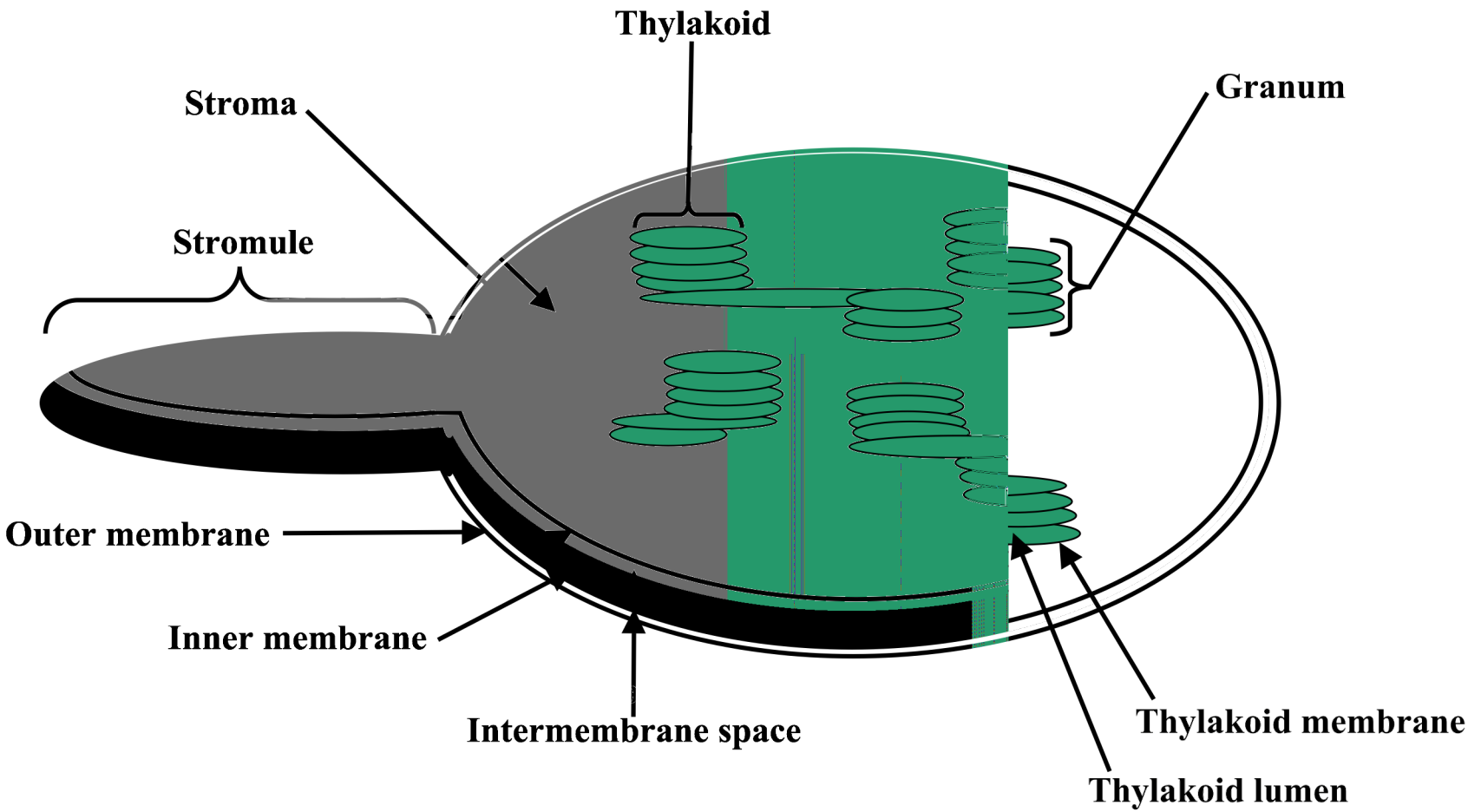
Thylakoid
Granum
Stroma
Stromule
Outer membrane
Inner membrane
Intermembrane space
Thylakoid membrane
Thylakoid lumen

transport metabolites and macromolecules to other areas of the cell (Natesan *et al.,* 2005). Consistent with a role in transport it has been shown that fluorescently labeled proteins can shuttle between plastids connected by stromules (Köhler *et al.,* 1997; Kwok and Hanson, 2004a). While supporting evidence exists only for inter-plastidic transport, stromules have been reported to associate closely with mitochondria (Gunning, 2005), endoplasmic reticulum (Schattat *et al.,* 2011) and nuclei (Kwok and Hanson, 2004b) although these remain purely qualitative observations. The close association between stromules and the nucleus raises the possibility that stromules may be capable of transporting molecules to the nucleus, facilitating communication between the two organelles (Krause *et al.,* 2012; Kwok and Hanson, 2004b). In addition, the vesicles stromules form by tip shedding (Gunning, 2005) may have functional significance. It has been speculated that they could recycle stromal proteins if the vesicle comes into contact and fuses with another plastid (Hanson and Sattarzadeh, 2011). Alternatively, these vesicles may dispose of stromal proteins by sending them to the vacuole for degradation as a way to degrade stromal proteins without degrading the entire plastid (Hanson and Sattarzadeh, 2011; Ishida *et al.,* 2008). Currently, evidence for a role of stromules in increasing metabolite transport is lacking. As ADTs synthesize phenylalanine, an amino acid needed throughout the cell, their localization to tail-like structures resembling stromules (Bross, 2011) is intriguing. Thus, it should be determined if ADTs localize to stromules by co-localizing ADT-CFP fusion proteins with a fluorescently tagged stroma-localized protein allowing stromule visualization using confocal microscopy.

1.4.2 Stromule induction and formation

While there are many hypotheses as to the function of stromules, researchers are also studying if stromules are induced under specific conditions. In a comprehensive study, it was shown that stromule formation is induced in response to abiotic stressors such as drought and high salinity (Gray *et al.,* 2012). The induction of stromules under these conditions is due to the actions of two phytohormones, abscisic acid (ABA) and ethylene (Gray *et al.*, 2012). Application of compounds inhibiting signal transduction

pathways associated with either ABA or ethylene such as $AgNO_3$, an inhibitor of ethylene signaling, can cause a reduction in stromule formation (Gray *et al.,* 2012).

While stromules can be induced under conditions of abiotic stress, this does not explain the molecular mechanisms governing their formation and movement. Stromules closely associate with actin microfilaments (Kwok and Hanson, 2004c), and are inhibited upon application of compounds that destabilize actin polymers (Kwok and Hanson, 2003), indicating stromules need the actin cytoskeleton to form. The actin-associated formation of stromules is dependant on myosins, as application of 2,3-butanedione monoxime (BDM), an inhibitor of myosin ATPase activity, nearly abolishes the presence of stromules (Natesan *et al.,* 2009). More specifically, a plant specific class of myosins (myosin XI) is responsible for stromule formation and movement (Natesan *et al.,* 2009). In *A. thaliana* there are 13 genes encoding different myosin XI sub-classes (Reddy and Day, 2001) and functional redundancy exists between them (Peremyslov *et al.,* 2008). While it is not known if stromules result from the actions of a specific sub-class of myosin XI, RNA interference against myosin XI or transient expression of tail domains of myosin XI are able to inhibit stromule formation (Natesan *et al.,* 2009). The inhibition of stromules caused by expression of myosin XI tail domains likely results from a dominant negative effect as they inhibit the function of wild-type myosin XI (Avisar *et al.,* 2008).

Much of what is known about stromule formation has been deduced from what inhibits their formation. However, as stromules are hypothesized to transport materials, it is conceivable that stromule inhibition could provide evidence for stromule-mediated transport if inhibition of stromules is found to reduce transport of a molecule or protein of interest.

1.5 Chloroplast division

Initial studies by Bross (2011) found that ADT2-CFP localizes to a band at the equatorial plane (middle) of chloroplasts or to the pole of a chloroplast. These localization patterns are interesting because they are similar to proteins involved in

chloroplast division (Miyagishima, 2011), suggesting ADT2 may have a role in this process. Chloroplast division is regulated by the size of chloroplasts (Pyke, 1999) and is initiated by the sequential formation of proteinaceous rings at the equatorial plane of a dividing chloroplast (Miyagishima and Kabeya, 2010). In *A. thaliana* there are four rings (Fig. 3) involved in the division of a chloroplast, located in both the stroma and the cytosol (Pyke, 2013).

The earliest known event in chloroplast division is the formation of the innermost division ring, the Z-ring (Miyagishima, 2011). The Z-ring is composed of the tubulin-like protein Filamentous temperature sensitive Z (FtsZ) (Vitha *et al.,* 2001). There are three FtsZ proteins encoded in the *A. thaliana* genome; FtsZ1-1, FtsZ2-1 and FtsZ2-2 (Osteryoung and Vierling, 1995; Osteryoung *et al.,* 1998). All forms of FtsZ are able to polymerize with each other, forming filaments that are assembled into the Z-ring at the equatorial plane of a dividing chloroplast (TerBush *et al.,* 2012; 2013; Vitha *et al.,* 2001).

The formation of the Z-ring is regulated by the coordinated actions of several proteins that allow the Z-ring to form only at the equatorial plane of a dividing chloroplast (Fig. 4A) (TerBush *et al.,* 2013). An important regulator of Z-ring positioning is ACCUMULATION AND REPLICATION OF CHLOROPLASTS 3 (ARC3), which inhibits FtsZ polymerization (Zhang *et al.,* 2013) and is believed to be active away from the equatorial plane, towards the poles of chloroplasts (TerBush *et al.,* 2013). As a result of ARC3 activity the Z-ring is restricted to the equatorial plane (TerBush *et al.,* 2013). Another protein involved in Z-ring placement is the transmembrane protein ARC6 (Vitha *et al.,* 2003). ARC6 spans the inner membrane, and acts to anchor and stabilize FtsZ filaments into the Z-ring (Vitha *et al.,* 2003).

The next ring to form is the inner plastid-dividing (PD) ring, located in the stroma between the Z-ring and the inner membrane (Miyagishima and Kabeya, 2010). The composition of this ring is unknown having only been visualized using electron microscopy, where it appears as a dark, electron dense region at the stromal side of the inner membrane (Miyagishima and Kabeya, 2010). Although no components of the inner

Figure 3. Cross-section of division rings at the equatorial plane of a chloroplast. Chloroplast division in higher plants requires the sequential formation of four rings at the equatorial plane of a chloroplast. There are two rings in the stroma, the Z-ring composed of FtsZ1 and FtsZ2 (orange and yellow circles) filaments and the inner PD ring of unknown composition. The remaining rings are located in the cytosol. The outer PD ring is of unknown composition in higher plants, but is composed of polyglucan filaments in *C. merolae*. The ARC5 ring provides some of the constricting force required to divide chloroplasts.

FtsZ: Filamentous temperature sensitive Z; PD: plastid-dividing; ARC5: ACCUMULATION AND REPLICATION OF CHLOROPLASTS 5

Adapted from Glynn *et al*. (2007).

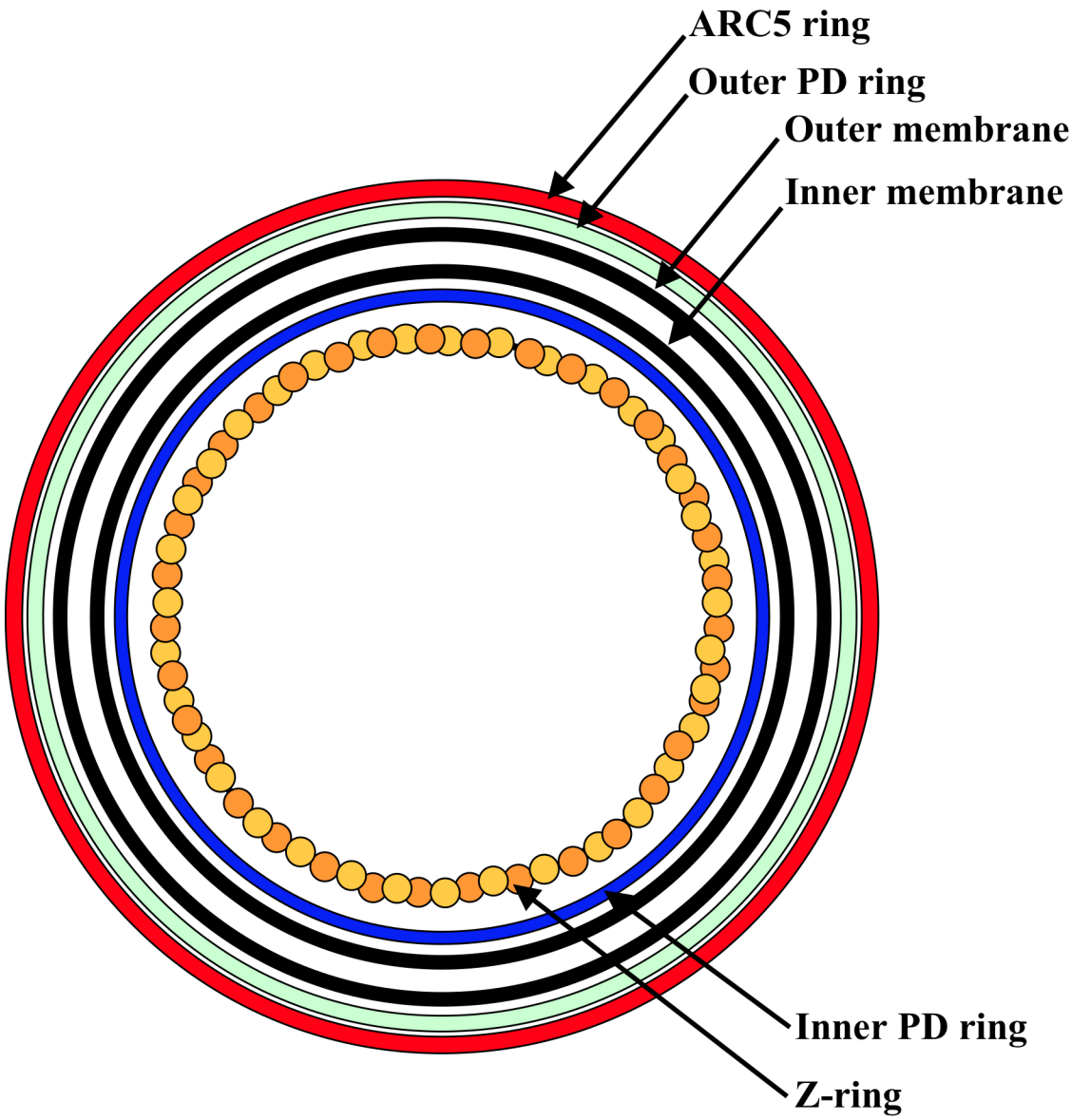
ARC5 ring
Outer PD ring
Outer membrane
Inner membrane
Inner PD ring
Z-ring

Figure 4. Overview of chloroplast division components.

This schematic is a simplified overview of chloroplast division focusing on components relevant to this thesis.

(A) The placement of the Z-ring is a regulated process. ARC3 inhibits FtsZ polymerization away from the equatorial plane, restricting Z-ring formation to this area. ARC6 spans the inner membrane and allows the Z-ring to form by stabilizing and anchoring FtsZ filaments.

Adapted from TerBush *et al.* (2013).

(B) The stromal division rings are connected to the cytosolic rings by transmembrane proteins in the inner and outer membranes. In the inner membrane ARC6 and PARC6 recruit PDV2 and PDV1 in the outer membrane. The presence of PDV1 and PDV2 act to recruit cytosolic ARC5 to the division plane.

Adapted from Glynn *et al.* (2009).

FtsZ: Filamentous temperature sensitive Z; ARC: ACCUMULATION AND REPLICATION OF CHLOROPLASTS; PARC6: PARALOG OF ARC6; PDV: PLASTID DIVISION.

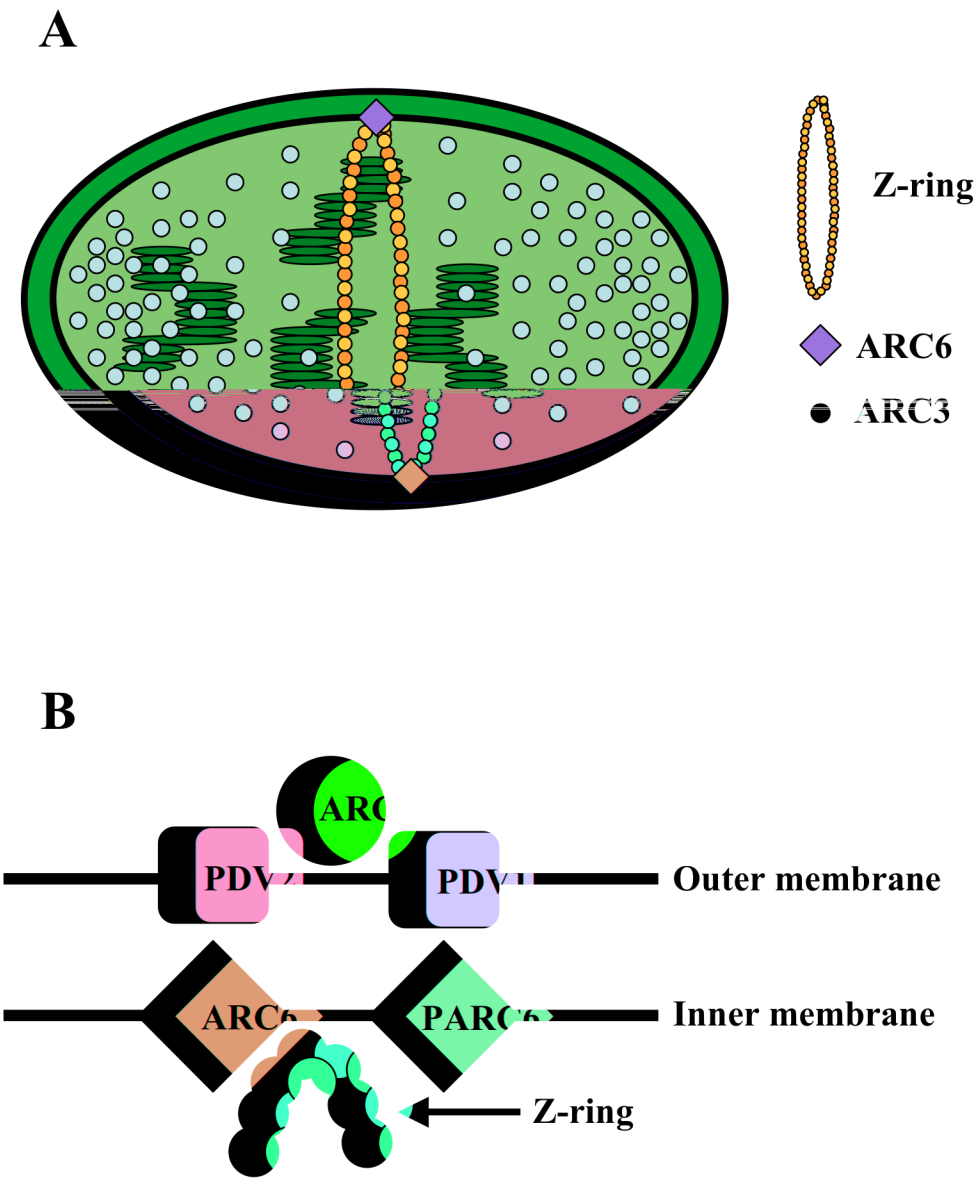
A
Z-ring
ARC6
ARC3
B
ARC
PDV
PDV
Outer membrane
ARC6
PARC6
Inner membrane
Z-ring

PD ring are known, it is hypothesized to be composed of uncharacterized chloroplast division proteins (Miyagishima and Kabeya, 2010).

The third ring to form is the outer PD ring, located at the cytosolic face of the outer membrane (Miyagishima and Kabeya, 2010; Yoshida *et al.,* 2010). Like the inner PD ring, it is of unknown composition in higher plants (Miyagishima and Kabeya, 2010). However, in the unicellular algae *Cyanidioschyzon merolae* the outer PD ring is composed of polyglucan filaments and proteins associated with these filaments (Yoshida *et al.,* 2010). In *C. merolae* these polyglucan filaments are synthesized by PLASTID-DIVISION RING1, a protein conserved in higher plants including *A.thaliana* (Yoshida *et al.,* 2010). This suggests that the outer PD ring is of similar composition in chloroplasts of plants (Yoshida *et al*., 2010).

The final, and outermost ring to form is composed of the cytosolic dynamin-like protein ARC5 (Gao *et al.,* 2003; Yoshida *et al.,* 2010). During division chloroplasts become constricted leading to the separation of the chloroplast into two smaller daughter chloroplasts (Pyke, 1999). The role of ARC5 in division is to provide some of this constricting force needed for complete division of chloroplasts (Gao *et al*., 2003; Yoshida *et al.*, 2006).

As stromal and cytosolic division rings are separated by the chloroplast membranes there needs to be a way of connecting the stromal rings, which form first, to the cytosolic rings, which form later (Glynn *et al.,* 2008; 2009; Holtsmark *et al.,* 2013; Miyagishima *et al.,* 2006). This occurs via transmembrane proteins in both the inner and outer membranes (Fig. 4B). In the inner membrane ARC6 and PARALOG OF ARC6 (PARC6) recruit PLASTID DIVISION2 (PDV2) and PDV1, respectively, in the outer membrane (Glynn *et al.,* 2008; 2009). The presence of PDV1 and PDV2 in the outer membrane at the division plane is believed to recruit ARC5 (Miyagishima *et al.,* 2006; Holtsmark *et al.,* 2013). Although the inner and outer PD rings are located between the Z-ring and the ARC5 ring (Miyagishima, 2011), their role in connecting the division rings is not understood.

The discovery of many chloroplast division components occurred after studying mutant plants with abnormal chloroplast morphology (Pyke, 2013). In *A. thaliana* the *accumulation and replication of chloroplasts* (*arc*) mutants are chloroplast division mutants generated through random mutagenesis and identified by screening for unusual chloroplast size, number or shape (Pyke and Leech 1992; 1994; Pyke *et al.,* 1994). The *arc3* (Pyke and Leech, 1992), *arc5* (Pyke and Leech, 1994) and *arc6* mutants (Pyke *et al.,* 1994) are among the best-characterized chloroplast division mutants, as the position of the Z-ring as determined by FtsZ localization is known in each (Glynn *et al.,* 2007; Vitha *et al.,* 2001; 2003).

In *arc3* mutants multiple Z-rings are able to form in a single chloroplast (Glynn *et al.,* 2007) because functional ARC3 protein is not present to restrict the Z-ring to the equatorial plane (TerBush *et al.,* 2013). As a result of Z-ring misplacement asymmetrical division can occur (Zhang *et al.,* 2013) causing *arc3* chloroplasts to be heterogeneous in size and shape, although on average they are larger in size and fewer in number per cell than wild-type (Pyke and Leech, 1992).

In *arc5* mutants, many chloroplasts are severely enlarged and centrally constricted appearing dumbbell shaped (Pyke and Leech, 1994), as the mutant arc5 protein cannot efficiently constrict and divide chloroplasts (Gao *et al.,* 2003). In *arc5* mutants the stromal division machinery is unaffected and the Z-ring remains present in the stroma at the central constriction (Vitha *et al.,* 2001).

The *arc6* mutant has a particularly severe phenotype, with mesophyll cells containing only two chloroplasts on average (Pyke *et al.,* 1994). The presence of ARC6 early in division is required for the Z-ring to form and as a result Z-rings do not form in *arc6* chloroplasts (Vitha *et al.,* 2003). Instead, FtsZ localizes to multiple short filaments that appear randomly scattered in the stroma of *arc6* chloroplasts (Vitha *et al.,* 2003).

The known position of a critical chloroplast division protein such as FtsZ in *arc3* (Glynn *et al.,* 2007), *arc5* (Vitha *et al.,* 2001) and *arc6* mutants (Vitha *et al.,* 2003) makes them useful tools for investigating the role of a putative chloroplast division

protein such as ADT2. By expressing ADT2-CFP in these mutants its localization patterns can be compared with those of FtsZ to provide evidence for a possible role in division.

1.6 *Agrobacterium*-mediated transgene expression

A. tumefaciens is a soil bacterium that can induce tumor formation in plants (Gelvin, 2003). Its ability to do so relies on sequences contained on a tumor-inducing plasmid (Ti-plasmid) (Gelvin, 2003). The Ti-plasmid encodes *VIRULENCE* (*VIR*) genes and contains the T-DNA, a region defined by the left-border and right-border sequences that flank it (Gelvin, 2003). Proteins encoded by *VIR* genes allow *A. tumefaciens* to sense chemicals, such as acetosyringone, that are released by the plant in response to wounding (Statchel *et al.,* 1985). This initiates a signal cascade mediated by VIR proteins resulting in the transfer of the T-DNA to plant cells where it can be expressed (Gelvin, 2003). The T-DNA encodes genes involved in phytohormone synthesis that cause uncontrolled cell growth when expressed *in planta* (Escobar and Dandekar, 2003), and genes involved in the synthesis of opines, compounds *A. tumefaciens* can metabolize to obtain nutrients (Zupan *et al.,* 2000).

For use in molecular biology, sequences on the Ti-plasmid are modified and partitioned into two separate plasmids: a helper Ti-plasmid and a T-DNA containing binary vector (Bevan, 1984; Hoekema *et al.,* 1983). The helper Ti-plasmid encodes *VIR* genes but does not contain a T-DNA and is present in strains of *A. tumefaciens* developed for molecular biology (Hoekema *et al.,* 1983). The T-DNA is contained on a separate binary vector, and the phytohormone and opine synthesis genes are replaced with sequences of interest (Bevan, 1984; Hoekema *et al.,* 1983). Once the T-DNA containing binary vector is transformed into *A. tumefaciens* carrying a helper Ti-plasmid the bacteria now contains the *VIR* genes and the T-DNA required for expression of a gene of interest *in planta* (Bevan, 1984; Hoekema *et al.,* 1983).

Agrobacterium-mediated plant transformations can create stably transformed plants, that is, plants with a copy of the T-DNA within the genome of every cell using

methods such as the floral dip (Clough and Bent, 1998). Stable transformation allows for transgene expression in all tissues, but is also time consuming and relies on random integration of T-DNA into the genome, which can result in positional effects (Clough and Bent, 1998; Gelvin, 2003). *A. tumefaciens* can also be used to transiently transform plants using methods such as agroinfiltration (Yang *et al.,* 2000). This involves pressure infiltrating *A. tumefaciens* into the underside of leaves using a blunt ended syringe. Although transgene expression is limited to leaf cells, the time until transgene expression can be analyzed is measured in days rather than months (Yang *et al.,* 2000). Agroinfiltration is commonly performed in relatives of tobacco, such as *N. benthamiana*, while its effectiveness has historically been limited in *A. thaliana* (Wroblewski *et al.,* 2005).

1.7 Hypotheses and objectives

Initial studies of ADT subcellular localization *in planta* (Bross, 2011) were brief. However, the complexity of the observed subcellular localization patterns raises questions as to what these patterns represent. This thesis intends to re-examine the subcellular localization of all ADTs through agroinfiltration of *N. benthamiana* and *A. thaliana*.

This thesis will address three main hypotheses:

Firstly, the localization of ADTs to tail-like structures appearing outside of the body of chloroplasts (Bross, 2011) leads to the hypothesis that ADTs localize to stromules. This hypothesis will be tested by co-expressing ADT-CFP fusion proteins with a fluorescently labeled stroma-marker allowing for stromule visualization using confocal microscopy.

Secondly, the localization of ADT5-CFP to globular structures resembling nuclei (Bross, 2011) leads to the hypothesis that ADT5 localizes to the nucleus. This hypothesis will be tested by co-expressing ADT5-CFP with a fluorescently tagged nuclear marker allowing for visualization of the nucleus using confocal microscopy.

Finally, the observation that ADT2-CFP is visualized at the equatorial plane or pole of chloroplasts (Bross, 2011) leads to the hypothesis that ADT2 is involved in chloroplast division. To investigate a possible secondary role for ADT2, multiple approaches will be used. Firstly, ADT2-CFP localization patterns will be extensively observed to determine ADT2-CFP localization in dividing chloroplasts. Chloroplasts in an *adt2* mutant will be visualized for the first time, to determine if a link can be established between ADT2 function and chloroplast division. ADT2-CFP will also be expressed in *arc3*, *arc5* and *arc6* chloroplast division mutants to determine if its localization patterns are altered in response to mutations affecting chloroplast division. Finally, a fluorescently tagged chloroplast division protein will be developed to determine if chloroplast division proteins are misplaced in an *adt2* mutant.

2 Materials and Methods

2.1 Media, media supplements, solutions, and buffers

2.1.1 Media

Media was prepared in double-distilled H_2O (ddH_2O) in either solid or liquid form. In the case of solid media, 15 g of agar was added per litre. Media was autoclaved for 20 minutes at 121°C.

Agrobacterium-induction media

To 1 L of YEB media (see recipe below): 10 mL 1 M 2-(N-morpholino)ethanesulfonic acid (MES) and 500 μL 200 mM acetosyringone.

Lysogeny broth (LB) media

For 1 L: 10 g tryptone, 5 g yeast extract and 10 g NaCl.

Super optimal growth with catabolite repression (SOC) media

For 1 L: 20 g tryptone, 5 g yeast extract, 0.5 g NaCl, 20 mL 1 M glucose, 10 mL 0.25 M KCl, and 5 mL 2 M MgCl. pH adjusted to 7.0 with NaOH.

Yeast extract and beef (YEB) media

For 1 L: 5 g peptone, 5 g beef extract, 5 g sucrose, 1 g yeast extract, 0.49 g $MgSO_4$.

2.1.2 Media supplements

Media was supplemented with appropriate antibiotics for selection.

Antibiotic Stock Solutions

Stock solutions of kanamycin (60 mg/mL), streptomycin (50 mg/mL), gentamycin (50 mg/mL) and spectinomycin (100 mg/mL) were prepared by dissolving the antibiotic in ddH_2O followed by filter sterilization. Stock solutions of rifampicin (25 mg/mL) were

prepared by dissolving the antibiotic in dimethyl sulfoxide (DMSO). All stock solutions are stored at -20°C.

Antibiotics were supplemented in media at the following concentrations. Gentamycin: 15 μg/mL; kanamycin: 60 μg/ml; rifampicin: 10 μg/mL; spectinomycin: 100 μg/mL; streptomycin: 50 μg/mL.

2.1.3 Solutions

Acetosyringone Stock Solution

Acetosyringone stock solution was prepared in DMSO at 200 mM, and stored at -20°C.

$AgNO_3$ stock solution

$AgNO_3$ stock solutions was prepared in ddH_2O at 120 mM. The solution was filter sterilized and stored at room temperature.

Alkaline lysis solution I

For 100 mL: 5 mL 1 M glucose, 2.5 mL Tris-HCl (pH 8) and 200 μL 0.5 M ethylenediaminetetraacetic acid (EDTA) (pH 8) was added to ddH_2O. The solution was autoclaved and stored at 4°C.

Alkaline lysis solution II

For 5 mL: 200 μL 5 M NaOH and 500 uL 10% w/v sodium dodecyl sulfate was added to ddH_2O. The solution was prepared fresh prior to use.

Alkaline lysis solution III

For 100 mL: 60 mL potassium acetate and 11.5 mL of glacial acetic acid was added to ddH_2O. The solution was autoclaved and stored at 4°C.

2,3-butanedione monoxime (BDM) stock solution

BDM stock solution was prepared in ddH_2O at 100 mM. The solution was filter sterilized and stored at room temperature.

Gamborg's Solution

For 1 L: 3.2 g Gamborg's B5 medium with vitamins and 20 g sucrose was added to ddH_2O. Solution was autoclaved, after which 10 mL 1 M MES and 1 mL acetosyringone stock solution were added and was stored at room temperature.

L-ascorbic acid stock solution

L-ascorbic acid stock solution was prepared in ddH_2O at 1 M. The solution was filter sterilized and stored at room temperature.

2.1.4 Buffers

Buffers were prepared in concentrated forms (50X or 10X) and diluted with ddH_2O for use at 1X.

50X Tris base, acetic acid, EDTA (TAE) buffer

For 1 L: 242 g Tris base, 57.1 mL glacial acetic acid and 100 mL 0.5 M EDTA (pH 8.0) was added to ddH_2O.

10X Tris base, EDTA (TE) buffer

For 1L: 100 mL 1M Tris-Cl (pH 8.0) and 20 mL 0.5 M EDTA (pH 8.0) was added to ddH_2O.

2.2 Bacterial strains

2.2.1 *A. tumefaciens* strains

All transient transformations of plants were performed using *A. tumefaciens* strain LBA4404 (Hoekema *et al*., 1983) or strain GV3101 (Koncz and Schell, 1986).

2.2.2 *E. coli* strains

E. coli strains DH5α, DH10B, and DB3.1 (Invitrogen catalogue number 11319-019, 13033-015, and 11782-018) were used for the propagation of plasmids for cloning purposes. Plasmid DNA containing the *control of cell death B* (*ccdB*) gene for negative selection were propagated in *E. coli* strain DB3.1, while non-*ccdB* containing plasmids were propagated in *E. coli* strain DH5α or DH10B.

2.3 Plants

2.3.1 *A. thaliana*

Three accessions of *A. thaliana* were used: Columbia-0 (Col-0), Landsberg *erecta* (L*er*) and Wassilewskija (Ws). Seeds were obtained from the *Arabidopsis* Biological Resource Center (ABRC), stock numbers CS1092 (Col-0), CS20 (L*er*) and CS915 (Ws). Plants were grown in soil (pro-mix) and were vernalized for 4 days at 4°C prior to being placed in a Conviron CMP 4030 growth chamber. Plants were grown with a 16 hour light (150 μM photons/m^2/s) and 8 hour dark cycle. The temperature during the light cycle was 24°C and during the dark cycle was 22°C. *A. thaliana* were watered with a 20 mM solution of L-ascorbic acid.

Several mutant lines of *A. thaliana* were also used in transient transformation assays. The growth conditions were identical to what was described for wild-type accessions. The mutations are described in detail below.

<u>*adt2* mutants</u>

The *adt2* plants are homozygous for the *adt2-1D* allele, which has a point mutation in the ACT domain that results in a serine to alanine substitution (Huang *et al.,* 2010). As a result the enzyme is insensitive to feedback inhibition by phenylalanine (Huang *et al.,* 2010). Seeds of homozygous *adt2* plants (accession Col-0) were generously provided by Dr. Tengfang Huang and Dr. Georg Jander (Boyce Thompson Institute for Plant Research, Ithaca, New York).

arc3 mutants

The *arc3* plants are homozygous for the *arc3-1* allele, an ethyl methanesulfonate (EMS) induced point mutation that causes a guanine to adenine transversion in the 13th exon (Pyke and Leech, 1992; Shimada *et al.,* 2004). This results in a premature stop codon, creating a truncated protein (Shimada *et al.,* 2004). Seeds for *arc3* mutant plants (accession L*er*) were obtained from the ABRC (stock number CS264) thanks to the original donation by Kevin Pyke (Pyke and Leech, 1992).

arc5 mutants

The *arc5* plants are homozygous for the *arc5-1* allele, an EMS induced point mutation that causes a guanine to adenine transversion in the 5th exon resulting in a premature stop codon (Gao *et al.,* 2003; Pyke and Leech, 1994). Seeds for *arc5* mutant plants (accession L*er*) were obtained from the ABRC (stock number CS1633) thanks to the original donation by Kevin Pyke (Pyke and Leech, 1994).

arc6 mutants

The *arc6* plants are homozygous for the *arc6-1* allele, a point mutation that causes a cytosine to thymine transition in exon 3 resulting in a premature stop codon (Pyke *et al.,*1994; Vitha *et al.,* 2003). Seeds for *arc6* mutant plants (accession Ws) were obtained from the ABRC (stock number CS286) thanks to the original donation by Rachel Leech (Pyke *et al.,* 1994).

2.3.2 *N. benthamiana*

N. benthamiana seeds were generously provided by Hong Zhu and Dr. Rima Menassa (Agriculture Canada, London, Ontario). Seeds were sown in soil (pro-mix) and *N. benthamiana* plants were grown in a Conviron CMP 4030 growth chamber. Plants were grown with a 16 hour light (100 μM photons/m^2/s) and 8 hour dark cycle. The temperature during the light cycle was 24°C and during the dark cycle was 22°C.

2.4 Plasmids

Plasmids used in this study are either T-DNA containing binary vectors used for transient transformation of plants or Gateway® compatible vectors used for cloning.

2.4.1 *ADT-CFP* plant expression vectors

All six *A. thaliana ADT*s were previously cloned in pCB, a derivative of pEZT-NL (Carnegie cell imaging project, http://deepgreen.stanford.edu) that has the *ENHANCED GREEN FLUORESCENT PROTEIN* coding sequence replaced with the *CFP* coding sequence (Bross, 2011). *In planta* expression of *ADT-CFP* fusion genes encoded in pCB is regulated by the CaMV *35s* promoter. In bacteria, the presence of pCB can be selected for using kanamycin.

2.4.2 *p19* plant expression vector

The p19 vector encodes the p19 protein from tomato bushy stunt virus, a suppressor of post-transcriptional gene silencing (PTGS) (Silhavy *et al.,* 2002). The p19 vector is of unknown origin. In this study *p19* is present in all transient transformations, as expression of p19 increases transgene expression by decreasing PTGS (Voinnet *et al.,* 2003).

2.4.3 Vector encoding a stroma-marker

The T-DNA containing binary vector pt-yk was obtained from the ABRC (stock number CD3-997), thanks to the original donation by Andreas Nebenführ (Nelson *et al.,* 2007). The vector contains a T-DNA encoding the plastid transit peptide of the small-subunit of ribulose-1,5-bisphosphate carboxylase/oxygenase (RuBisCO) from tobacco fused to the *YELLOW FLUORESCENT PROTEIN* (*YFP*) coding sequence. Expression is regulated *in planta* by the CaMV double-enhanced *35s* promoter, and the vector allows for selection in bacteria using kanamycin. As this fusion protein is targeted to the stroma it allows for visualization of stromules (Nelson *et al.,* 2007). In this study, this construct will be referred to as TP-YFP.

2.4.4 Vector encoding a nuclear marker

The T-DNA containing binary vector pEarleygate301-YFP encoding *A. thaliana NUCLEOPORIN1* fused to *YFP* (*NUP1-YFP*) was generously provided by Dr. Gang Tian and Dr. Yuhai Cui (Agriculture Canada, London, Ontario). The expression of *NUP1-YFP* is regulated *in planta* by its native promoter, and the vector allows for selection in bacteria using kanamycin (Lu *et al.,* 2010). As the NUP1-YFP fusion protein localizes to the nuclear pore it allows for visualization of the nuclear membrane.

2.4.5 Dominant negative myosin XI expression constructs

A. tumefaciens GV3101 containing plasmid pCB302 encoding dominant negative forms of *N. benthamiana* myosin XI-2 and XI-K were generously provided by Jamie McNeil and Dr. Rima Menassa (Agriculture Canada, London, Ontario) (Avisar *et al.,* 2008). Each construct encodes the globular tail domain of each myosin XI. Expression of the dominant negative constructs in pCB302 is regulated *in planta* by the nopaline synthase promoter (Avisar *et al.,* 2008; Xiang *et al.,* 1999). The presence of the vector can be selected for in bacteria with kanamycin (Xiang *et al.,* 1999).

2.4.6 Gateway® compatible vector encoding *FtsZ2-1*

Vector pLIC6 encoding *A. thaliana FtsZ2-1* cDNA was obtained from the ABRC, (stock number DKLAT2G36250), thanks to the original donation by Dr. Savithramma Dinesh-Kumar (Popescu *et al.,* 2007). The *FtsZ2-1* insert is flanked by *attachment*B (*att*B) sites allowing recombination with a donor vector using Gateway® technology (Popescu *et al.,* 2007). The vector allows for selection in bacteria using spectinomycin.

2.4.7 Donor vector

The donor vector pDONR221 (Invitrogen catalogue number 12536-017) contains the *ccdB* negative selectable marker gene flanked by *att*P sites allowing for recombination with *att*B sites using Gateway® technology. The vector allows for selection in bacteria using kanamycin.

2.4.8 Destination vector

E. coli DB3.1 harboring the T-DNA containing destination vector pEarleygate101 (ABRC stock number CD3-683; Earley *et al.,* 2006) were generously provided by Dr. Gang Tian and Dr. Yuhai Cui (Agriculture Canada, London, Ontario). The vector contains the *ccdB* negative selectable marker gene flanked by *att*R sites allowing for recombination with *att*L sites in an entry vector using Gateway® technology (Earley *et al.,* 2006). In pEarleygate101, inserted genes are expressed as C-terminally tagged YFP fusion proteins by the CaMV *35s* promoter (Earley *et al.,* 2006).

2.5 Cloning methodology

2.5.1 Plasmid isolation, digestion, gel electrophoresis and purification

Isolation of plasmid DNA was performed using the mini-prep alkaline lysis method as described in Sambrook and Russell (2001). Isolated plasmid DNA was stored at -20ºC in TE buffer. Restriction digests of plasmid DNA, were performed using Fermentas FastDigest restriction enzymes according to the manufacturers instructions. Digested plasmid DNA was size separated using gel electrophoresis. Gels were prepared as 0.8% agarose in TAE buffer, stained with ethidium bromide and visualized under ultraviolet light. Isolation of gel fragments of interest were performed using a PureLink™ Quick Gel Extraction Kit (Invitrogen catalogue number K2100-12) according to the manufacturer's instructions.

2.5.2 Gateway® technology

BP reactions were performed using 6 μl of gel purified *att*B flanked *FtsZ2-1* fragments combined with 2 μL of isolated pDONR221 and 0.5 μL of Gateway® BP Clonase™ II enzyme mix (Invitrogen catalogue number 11789-020).

LR reactions were performed using 6 μl of gel purified *att*L flanked *FtsZ2-1* fragments combined with 2 μL of isolated pEarleygate101 and 0.5 μL of Gateway® LR Clonase™ II enzyme mix (Invitrogen catalogue number 11791-020).

Both BP and LR reactions were left to incubate overnight at room temperature for approximately 12 hours.

2.6 Transformation procedures

2.6.1 Bacterial Transformations

E. coli DH5α made chemically competent using a modification of the method described by Hanahan (1983) were transformed using the heat shock method as described in Sambrook and Russell (2001). Cells recovered for 1.5 hours at 37°C in non-selective SOC media. Successful transformants were selected on solid LB media supplemented with appropriate antibiotics. *E. coli* stocks were snap frozen with liquid nitrogen in 25% glycerol and stored at -80ºC.

A. tumefaciens LBA4404 made electrocompetent according to Wise *et al.* (2006) were transformed using the Gene Pulser® II electroporator (Bio-rad). Settings used for electroporation were 2.5 kV, a capacitance of 25 μF and a resistance of 400 Ω. Following electroporation *A. tumefaciens* recovered at 28ºC in non-selective YEB media for 2 hours. Successful transformants were selected on solid YEB media with appropriate antibiotics. *A. tumefaciens* stocks were snap frozen with liquid nitrogen in 25% glycerol and stored at -80ºC.

2.6.2 Plant transformations

Agroinfiltration (Yang *et al.,* 2000) was used for all plant transformations. Two days prior to infiltration, a 3 mL starter culture of YEB media containing appropriate antibiotics was inoculated with *A. tumefaciens* containing a construct of interest, while a separate culture was inoculated with *A. tumefaciens* containing a construct encoding *p19*. These cultures were grown at 28ºC in an incubator-shaker (250 rpm) for approximately 20 hours. After this time, 50 μL of the starter culture was used to inoculate a 50 mL culture of *Agrobacterium*-induction media containing appropriate antibiotics. This culture was then grown at 28ºC in an incubator-shaker (250 rpm) for 20 to 22 hours. The 50 mL cultures were pelleted by centrifugation at 3000 rpm for 30 minutes at room temperature.

After discarding the supernatant the pelleted bacteria were resuspended in Gamborg's solution to an optical density at 600 nm (OD_{600}) of approximately 1.0 unless specified otherwise. The resuspended bacteria were then placed in a shaker (250 rpm) at room temperature for an hour. After this time resuspended *A. tumefaciens* containing a construct of interest were mixed with *A. tumefaciens* containing the *p19* construct in a 1:1 ratio unless specified otherwise. The mixed *A. tumefaciens* are then pressure infiltrated into the underside of leaves using a blunt ended 1 mL tuberculin syringe.

For co-infiltrations where two transgenes of interest are expressed the procedure is identical, except *A. tumefaciens* containing an additional construct is also grown and infiltrated. The ratios of *A. tumefaciens* used for co-infiltrations were 1:1:1 (*p19*:*construct1*:*construct2*) unless specified otherwise.

Infiltrations were performed in both *N. benthamiana* and *A. thaliana*. The procedure used for transformation of each species was similar, although differences exist in the age of plants used for the transformation. *N. benthamiana* plants used for transformations were between 4 and 6 weeks of age, while *A. thaliana* used for transformations were between 3 and 4 weeks of age. In addition, *A. thaliana* used for transformations were watered from seed with 20 mM L-ascorbic acid and were transferred to fresh soaked soil immediately following infiltration.

2.7 Measurements and statistics

Stromules and chloroplasts were measured in this study using the measure tool from ImageJ 1.45s (Rasband, 2007-2013). Stromules were considered to be any extension from the chloroplast greater than 1 μm in length. For non-linear stromules several measurements were taken to account for bends and curves and subsequently added together to provide a more accurate measurement of stromule length. Chloroplasts were measured in a straight line across their longest axis. Average stromule and chloroplast lengths were compared between groups using a student's t-test, while the proportion of chloroplasts with stromules and cells with ADT5 in nuclei were compared using a two-proportion Z-test.

2.8 Confocal microscopy

Visualization of the subcellular localization of fusion proteins was performed using a Leica SP2 confocal laser scanning microscope located at Agriculture Canada (London, Ontario). Samples of leaf tissue were punched from intact plant leaves and placed on a glass slide on top of a water droplet. A cover slip with Vaseline around the edges was then placed on top of the leaf section to form a watertight seal with the glass slide. A 63x water immersion objective lens was used for all imaging. A 405 nm blue diode laser was used to excite CFP and chlorophyll. Emission of CFP fluorescence was detected from between 440-485 nm (CFP channel) and chlorophyll fluorescence was detected from between 630-690 nm (chlorophyll channel). When YFP was also present in a sample it was subsequently excited using a 514 nm argon laser. Emission of YFP fluorescence was detected from between 540-550 nm (YFP channel). All images were taken 5 days post-infiltration unless otherwise specified. All scaling, merging and processing of images were performed using ImageJ 1.45s (Rasband, 2007-2013).

3 Results

3.1 ADT-CFP subcellular localization in *N. benthamiana*

Initial studies of ADT localization *in planta* observed that ADT-CFPs localize to tail-like structures outside of the region of chlorophyll fluorescence (Bross, 2011). However, this study only briefly examined the subcellular localization of ADTs, and most images obtained were low magnification overviews. Prior to re-examining ADT-CFP subcellular localization, several controls were performed to ensure that detectable fluorescence will only result from the presence of fluorescent proteins and chlorophyll. The following controls were performed: agroinfiltration with *A. tumefaciens* containing a construct encoding *p19* (a suppressor of PTGS expressed in all transient transformations) and an empty pCB vector; infiltration with *A. tumefaciens* only containing an empty pCB vector; and uninfiltrated *N. benthamiana* leaves. In all controls only chlorophyll fluorescence was detected and no fluorescence was observed in the CFP and YFP channels (Fig. 5A-C). This ensures that any fluorescence detected in the CFP and YFP channels in the ensuing experiments will only result from the presence of fluorophores.

To re-examine the *in planta* subcellular localization of all six ADTs, agroinfiltration was used to transiently express them as ADT-CFP fusion proteins in the leaves of *N. benthamiana*. Confocal imaging of ADT-CFP localization was performed with emphasis on obtaining more detailed, higher magnification images. The subcellular localization of ADT-CFP fusion proteins was consistent with data obtained by Bross (2011) (Fig. 6A-F). ADT-CFPs frequently localize to tail-like structures near the chloroplast but not directly overlapping with chlorophyll fluorescence (Fig. 6A-E). The only exception to this was ADT6-CFP, which localized in the cytosol (Fig. 6F). The shape and length of these structures were variable, ranging from short protrusions from the chloroplast body (Fig. 6C-D) to long and narrow ones (Fig. 6A-B, E). This variation was observed for each ADT-CFP, as they were all observed in tail-like structures of different shapes and lengths. While the fluorescence observed was generally highest in

Figure 5. Transformation controls for *N. benthamiana*.

Prior to expression of fluorescently labeled fusion proteins, it must be ensured that any detected fluorescence will be due to the presence of the desired fluorophores. Controls were performed using:

(A) Uninfiltrated plants.

(B) Plants infiltrated with *A. tumefaciens* only containing an empty pCB vector (EV).

(C) Plants infiltrated with *A. tumefaciens* containing p19 and an EV.

A 405 nm blue diode laser was used to excite CFP and chlorophyll, while a 514 nm argon laser was subsequently used to excite YFP. Fluorescence was collected from 440-485 nm for CFP, from 540-550 nm for YFP and from 630-690 nm for chlorophyll. The parameters described above are used for all confocal imaging and will no longer be specified in each figure legend.

(A-C) In all control transformations and uninfiltrated plants only chlorophyll fluorescence was detected.

Scale bars are 20 μm.

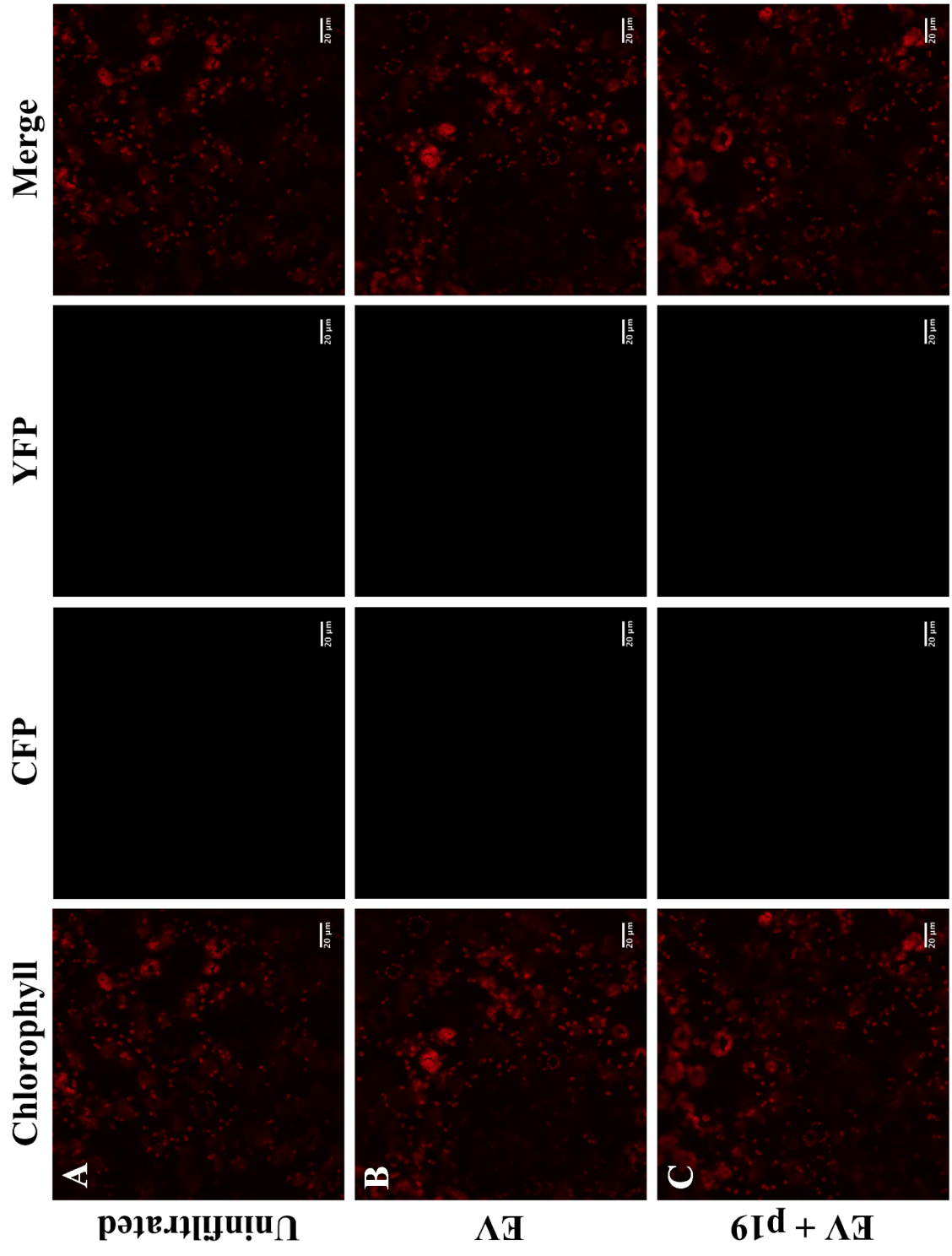
Chlorophyll
CFP
YFP
Merge
Uninfiltrated
EV
EV + p19
A
B
C
20 µm

Figure 6. Subcellular localization of ADT-CFPs in *N. benthamiana.*

All six ADTs were transiently expressed as ADT-CFP fusion proteins in *N. benthamiana*. Images of chlorophyll fluorescence (left) and ADT-CFPs (middle) are displayed separately and merged (right) for each ADT-CFP.

(A) ADT1-CFP.

(B) ADT2-CFP.

(C) ADT3-CFP.

(D) ADT4-CFP.

(E) ADT5-CFP.

(F) ADT6-CFP.

(A-F) With the exception of ADT6 in the cytosol **(F)**, all ADTs localize to tail-like structures outside of the main body of the chloroplasts **(A-E)**. The appearance these structures is variable, from long and narrow **(A-B, E)** to short and pointed **(C-D)**. Although fluorescence is generally highest in these structures fluorescence is also present in the body of the chloroplasts **(A, C-E)** suggesting that protein is present in the stroma.

Scale bars are 5 μm.

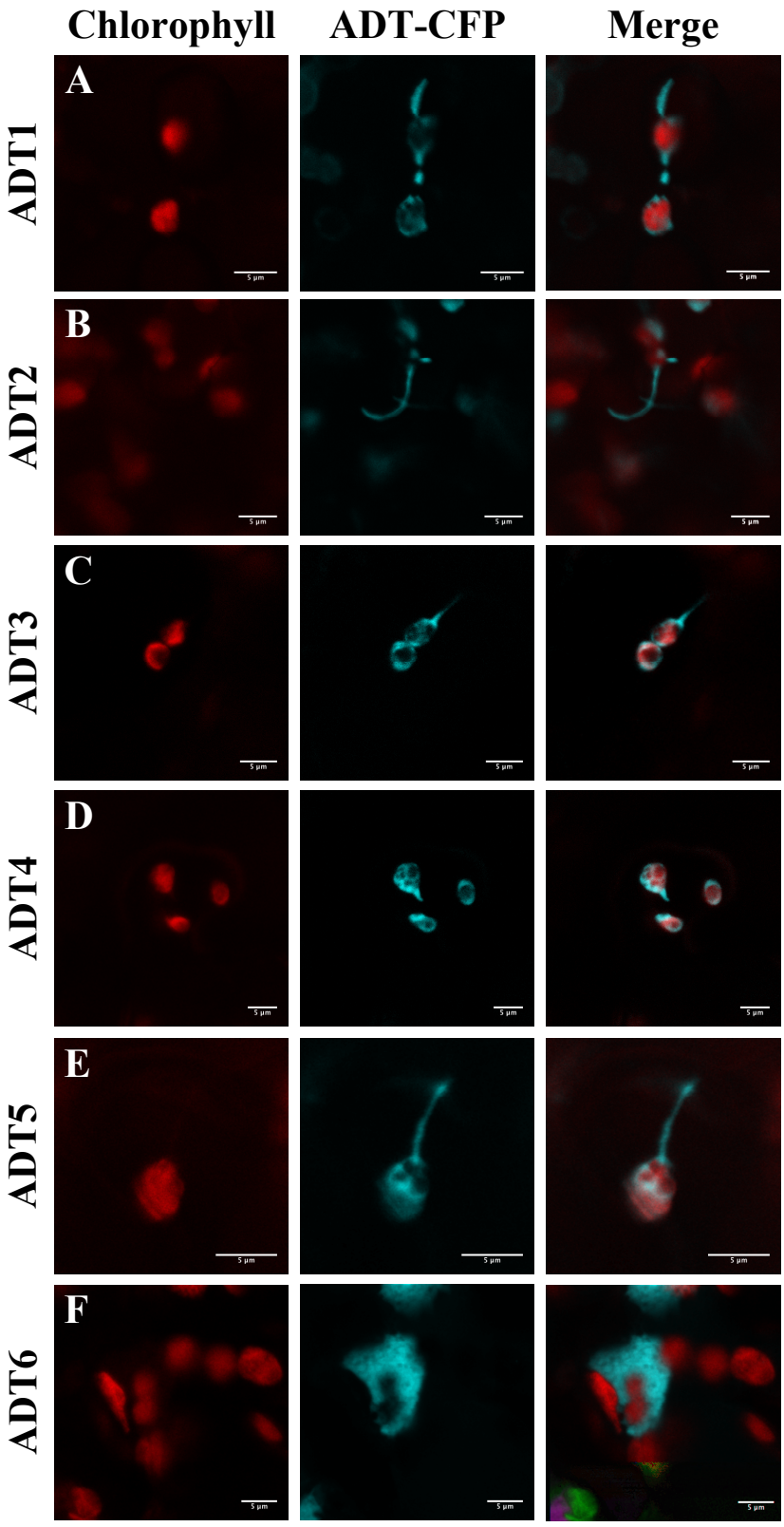
Chlorophyll
ADT-CFP
Merge
ADT1
ADT2
ADT3
ADT4
ADT5
ADT6
A
B
C
D
E
F
5 µm

these structures there was often some ADT-CFP fluorescence within the body of the chloroplast (Fig. 6A,C-E), suggesting that some protein is present in the stroma.

3.2 Co-expressing ADT-CFPs with a stroma marker

The presence of ADT-CFP fusion proteins in structures appearing to extend from chloroplasts led to the hypothesis that ADT-CFPs are localizing to stromules. The transit peptide of the small subunit of RuBisCO C-terminally fused to YFP (TP-YFP) localizes to the stroma allowing for stromules to be visualized (Nelson *et al.,* 2007) and will be used to test this hypothesis. Thus, the plasmid pt-yk encoding *TP-YFP* was transformed into *A. tumefaciens* LBA4404 and all six ADT-CFP fusion proteins were co-expressed with TP-YFP to determine if ADT-CFPs localize to stromules or are aggregating outside of chloroplasts.

Prior to co-expressing the two fusion proteins it must be ensured that any detected fluorescence in the CFP and YFP channels are the result of only the desired fluorophore. To determine if crosstalk between CFP and YFP would be an issue agroinfiltration was used to transiently express ADT2-CFP (representative of CFP fluorescence) and TP-YFP (representative of YFP fluorescence) individually in *N. benthamiana*. Each fusion protein was excited sequentially with a 405 nm blue diode laser followed by a 514 nm argon laser. Excitation of CFP with the 405 nm laser resulted in detectable CFP fluorescence in the CFP and YFP channels indicating that crosstalk is occurring (Fig. 7A). However, excitation of CFP with the 514 nm laser resulted in no detectable CFP fluorescence in any channel (Fig. 7A). Excitation of YFP with a 405 nm laser resulted in no detectable YFP fluorescence in any channel, while excitation with the 514 nm laser resulted in detectable YFP fluorescence only in the YFP channel, and TP-YFP localized to the stroma and stromules of chloroplasts (Fig. 7B). Thus, the only crosstalk observed was CFP crossing into the YFP channel when excited with a 405 nm laser (Fig. 7A). Therefore, crosstalk can be avoided by sequential excitation and fluorescence detection. The 405 nm laser will be used for CFP and chlorophyll excitation, while the 514 nm laser will be used sequentially excite YFP because no CFP fluorescence enters the YFP

Figure 7. Testing for crosstalk.

ADT2-CFP **(A)** and TP-YFP **(B)** were transiently expressed individually to assess detection of CFP and YFP fluorescence, respectively. Images of chlorophyll fluorescence, CFP, and YFP are shown individually from left to right.

(A) Excitation of CFP with the 405 nm blue diode laser allows for strong detection of CFP fluorescence in the CFP channel and residual fluorescence in the YFP channel. Excitation of CFP with the 514 nm argon laser does not result in detectable CFP fluorescence in any channel. Chlorophyll fluorescence is detectable upon excitation with either laser.

(B) Excitation of YFP with the 405 nm argon laser does not result in detectable YFP fluorescence in any channel. Excitation of YFP with the 514 nm argon laser results in detection of YFP fluorescence only in the YFP channel. TP-YFP localizes to the stroma allowing for visualization of stromules (arrow). Chlorophyll fluorescence is detectable upon excitation with either laser.

Scale bars are 5 μm.

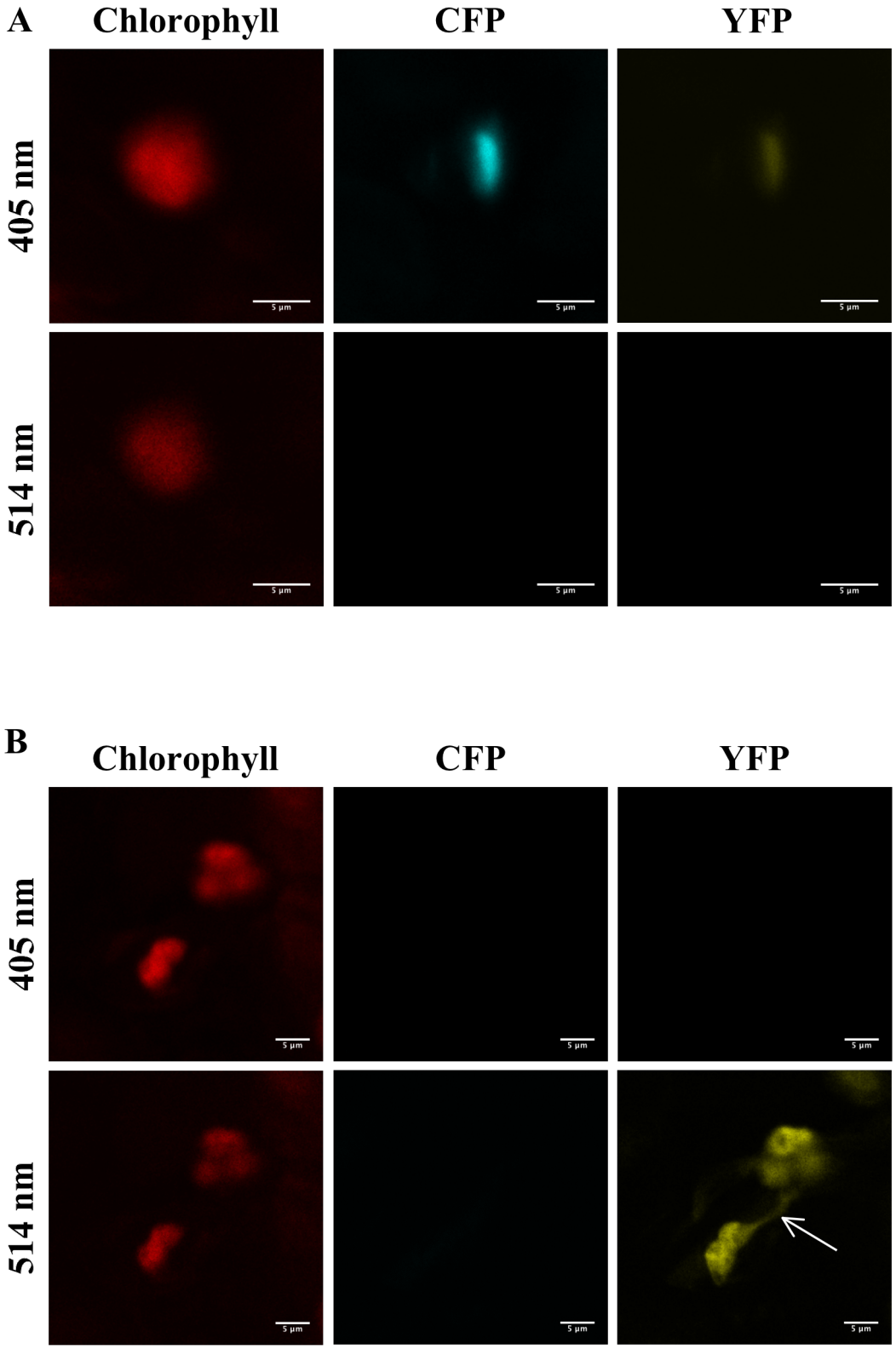
A
Chlorophyll
CFP
YFP
405 nm
514 nm
5 µm
B
Chlorophyll
CFP
YFP
405 nm
514 nm
5 µm

channel when this laser is used (Fig. 7A).

All six ADT-CFP fusion proteins were then co-expressed with TP-YFP in *N. benthamiana*. Initial attempts using agroinfiltration with the described ratios of *A. tumefaciens* (Section 2.6.2) resulted in very strong TP-YFP fluorescence compared to ADT-CFP fluorescence, which was often undetectable (data not shown). Comparable levels of fluorescence were obtained by altering the agroinfiltration protocol. A 1:1 ratio of *A. tumefaciens* containing an *ADT-CFP* fusion construct to *A. tumefaciens* encoding *p19* was infiltrated a day before a 1:1 ratio of *A. tumefaciens* containing the *TP-YFP* construct to *A. tumefaciens* encoding *p19*. In addition, *A. tumefaciens* containing the *TP-YFP* construct was infiltrated at a lower OD_{600} of approximately 0.5. Visualization of subcellular localization was performed 4 days post-infiltration with TP-YFP (5 days post-infiltration with an ADT-CFP).

Upon visualization of both fusion proteins the tail-like structures that ADT-CFPs localize to were also found to contain TP-YFP fluorescence (Fig. 8A-E). As TP-YFP is contained within the stroma, this result indicates that ADT-CFPs are as well. Thus, these tail-like structures are stromules as opposed to an aggregation of protein outside of chloroplasts. ADT6-CFP was the only exception to this, as ADT6-CFP and TP-YFP clearly localize to different areas (Fig. 8F). This is consistent with observations of ADT6-CFP in the cytosol (Fig. 6F) (Bross, 2011).

3.3 ADT-CFP subcellular localization in *A. thaliana*

Prior to this study, all data for the *in planta* localization of *A. thaliana* ADTs were obtained from *N. benthamiana* leaves. Thus, it was important to ensure that the localization patterns observed in *N. benthamiana* are also observed in *A. thaliana*, the native plant of these *ADT*s. Agroinfiltration was used to transiently express all *ADT-CFP* fusion genes in *A. thaliana* Col-0. ADT-CFP localization in *A. thaliana* is consistent with the localization patterns observed in *N. benthamiana*. ADT-CFPs commonly localized to stromule-like structures appearing to extend from the chloroplast, with varying levels of

Figure 8. Co-expression of ADT-CFP fusion proteins with TP-YFP stroma marker. All six ADT-CFP fusion proteins were co-expressed with the TP-YFP stroma marker to determine if ADTs localize to stromules. Images of chlorophyll fluorescence and ADT-CFPs are shown together in the left column. Images of TP-YFP are displayed in the middle column. The right column is a merge of chlorophyll fluorescence and areas where ADT-CFPs co-localize with TP-YFP, which are indicated in green **(A-E)**. For ADT6-CFP **(F)** the right column is a merge of ADT6-CFP, TP-YFP and chlorophyll fluorescence.

(A-E) ADT1-CFP, ADT2-CFP, ADT3-CFP, ADT4-CFP and ADT5-CFP co-localize with TP-YFP in stromules.

(F) ADT6-CFP localizes outside of chloroplasts in the cytoplasm.

Scale bars are 5 μm.

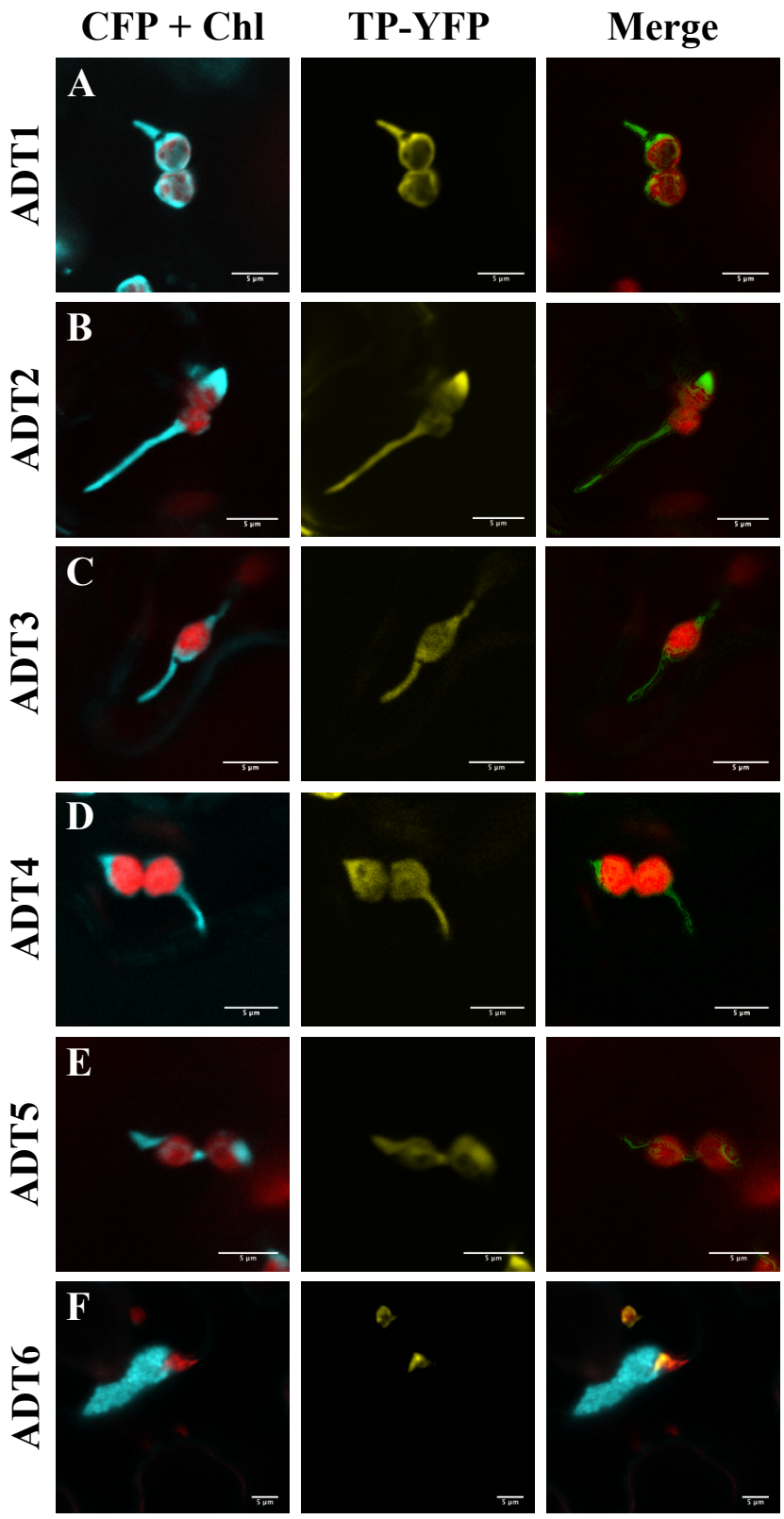
CFP + Chl
TP-YFP
Merge
ADT1
ADT2
ADT3
ADT4
ADT5
ADT6
A
B
C
D
E
F

ADT-CFP fluorescence in the stroma (Fig. 9A-E). As observed in *N. benthamiana* ADT6-CFP localizes outside of the chloroplast to the cytosol (Fig. 9F).

3.4 Nuclear localization of ADT5

Earlier studies of ADT5 localization found that it is observed in globular structures resembling nuclei 5 days post-infiltration (Bross, 2011). To re-examine this localization pattern agroinfiltration was used to express ADT5-CFP in *N. benthamiana* and *A. thaliana* Col-0. These globular structures resembling nuclei were observed in both plants (Fig. 10A-B). To determine if ADT5-CFP localizes to the nucleus it needed to be co-localized with a nuclear marker. NUCLEOPORIN-1 (NUP1) is a component of a nuclear pore complex in *A. thaliana* and was previously demonstrated to localize to the nuclear membrane as a YFP fusion protein (Lu *et al.,* 2010). The plasmid pEarleygate301-YFP encoding *NUP1-YFP* was transformed into *A. tumefaciens* LBA4404. Agroinfiltration was then used to transiently co-express ADT5-CFP and NUP1-YFP fusion proteins in the leaves of *N. benthamiana*.

Confocal imaging of the localization of each fusion protein determined that NUP1-YFP localized around ADT5-CFP (Fig. 10C). As NUP1-YFP localizes to the nuclear membrane, this result confirms that ADT5-CFP is contained within the nucleus and appears to localize uniformly throughout the nucleoplasm.

3.5 Stromule inhibition and ADT5 nuclear localization

Author's note: All experiments in section 3.5 were performed with Ornela Kljakic, a second year student working under my supervision as part of her scholar's elective research project. Ornela performed the agroinfiltrations under my supervision, I performed the confocal microscopy, and both of us measured stromules and cells with ADT5-CFP nuclear localization, while Ornela performed the statistical analysis.

From Fig. 11 one can observe that nuclei containing ADT5-CFP are often surrounded by chloroplasts that appear connected to the nucleus through stromules. This observation led to the hypothesis that ADT5 nuclear localization may be dependant on

Figure 9. Subcellular localization of ADT-CFPs in *A. thaliana* Col-0.

All six ADT-CFP fusion proteins were transiently expressed in *A. thaliana* Col-0. Images of chlorophyll fluorescence and ADT-CFPs are displayed separately in the left and middle columns, respectively, and merged in the right column.

(A-E) ADT1-CFP, ADT2-CFP, ADT3-CFP, ADT4-CFP and ADT5-CFP localize to structures resembling stromules of varying shapes and lengths, with varying levels of fluorescence in the stroma.

(F) ADT6-CFP localizes outside of chloroplasts in the cytosol.

Scale bars are 5 μm.

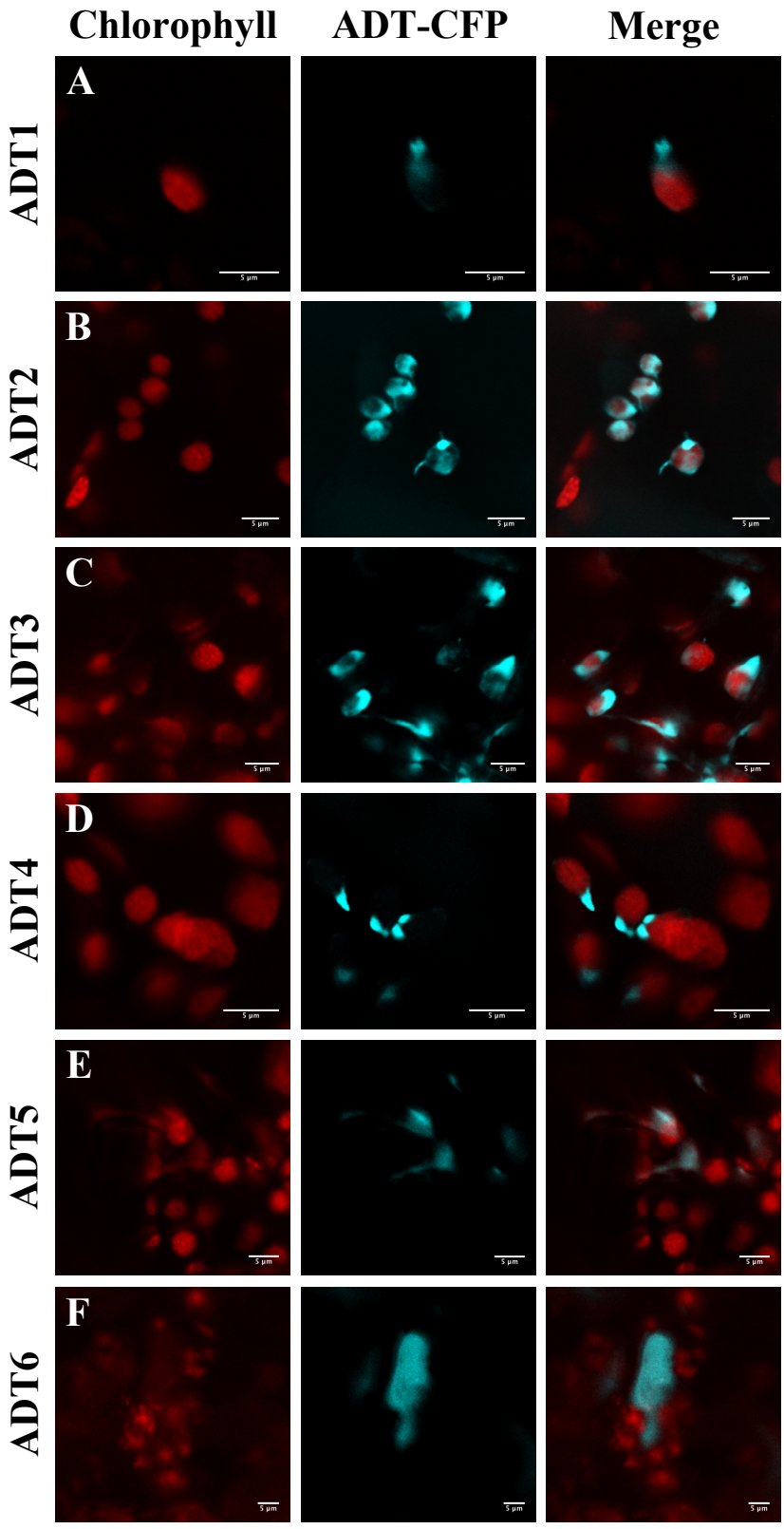
Chlorophyll
ADT-CFP
Merge
ADT1
ADT2
ADT3
ADT4
ADT5
ADT6
A
B
C
D
E
F

Figure 10. ADT5-CFP nuclear localization.

ADT5-CFP was transiently expressed in *N. benthamiana* **(A)**, and *A. thaliana* Col-0 **(B)**

(A-B) ADT5-CFP and chlorophyll fluorescence are shown merged.

(A) ADT5-CFP localizes to globular structures resembling nuclei in *N. benthamiana.*

(B) ADT5-CFP localizes to globular structures resembling nuclei in *A. thaliana* Col-0.

(C) To determine if ADT5-CFP localizes to the nucleus it was co-expressed with NUP1-YFP in *N. benthamiana*. Images of chlorophyll fluorescence and ADT5-CFP are shown merged (left). NUP1-YFP is shown alone (middle) and merged with ADT5-CFP and chlorophyll fluorescence (right). NUP1-YFP localizes to the nuclear membrane and surrounds ADT5-CFP confirming that it localizes to the nucleus.

Scale bars are 5 μm.

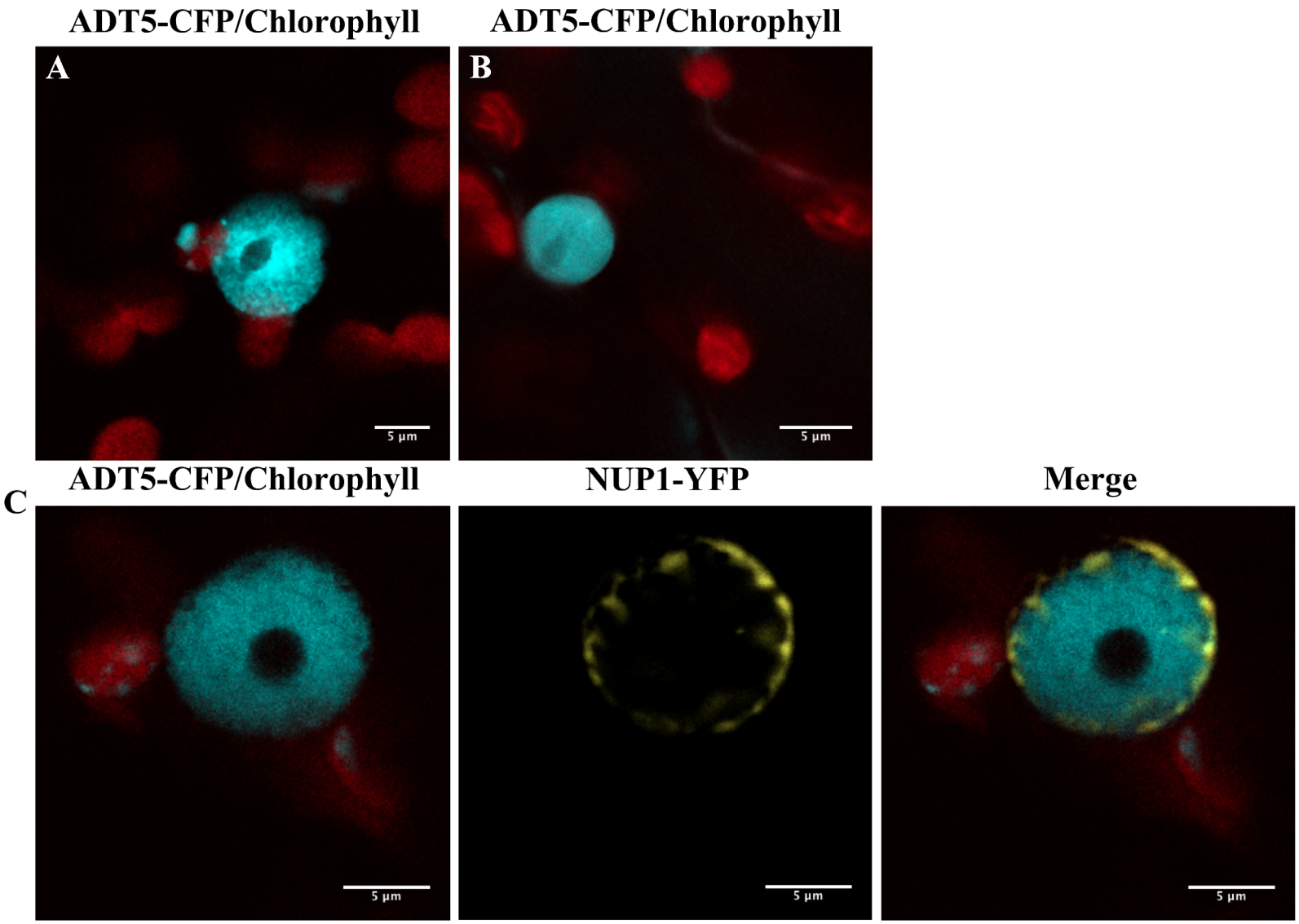
ADT5-CFP/Chlorophyll
A
5 µm
ADT5-CFP/Chlorophyll
B
5 µm
C
ADT5-CFP/Chlorophyll
5 µm
NUP1-YFP
5 µm
Merge
5 µm

Figure 11. ADT5-CFP in stromules connecting to the nucleus.

ADT5-CFP localized to nuclei that were often surrounded by chloroplasts, and in this image stromules (arrows) appear to connect the chloroplasts to the nucleus. Images of chlorophyll fluorescence (left) and ADT5-CFP (middle) are displayed separately and merged (right).

Scale bars are 5 μm.

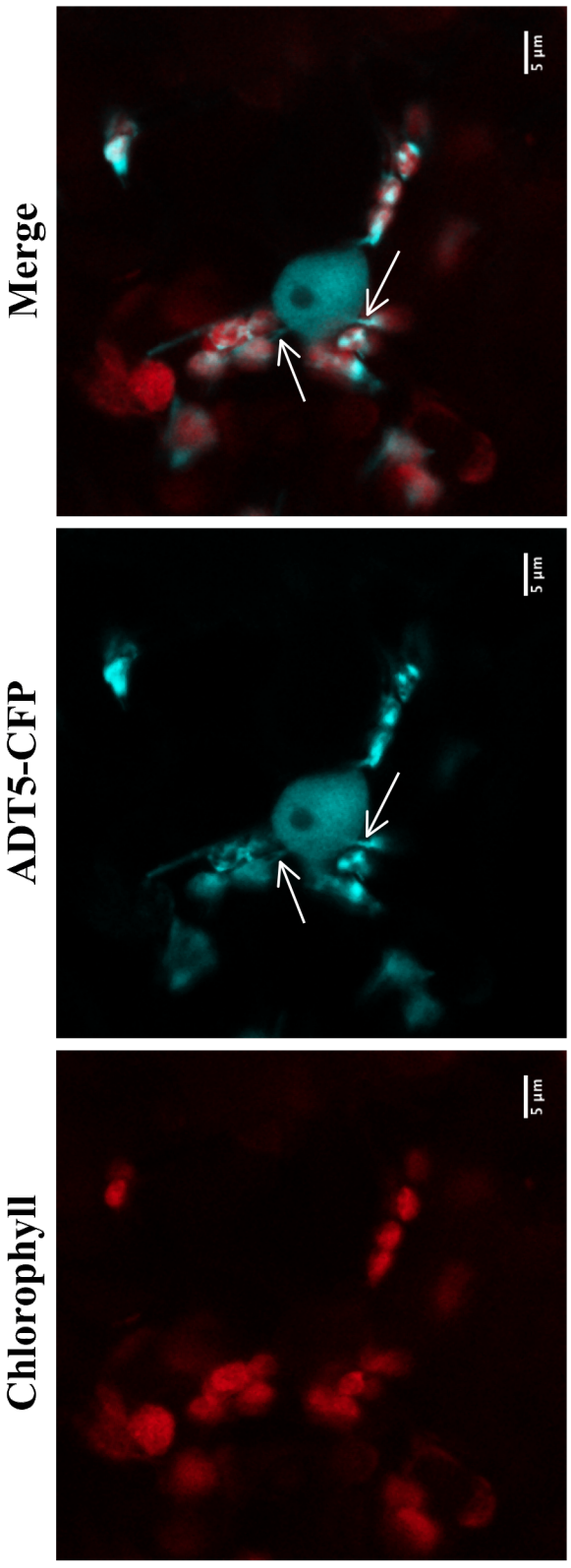
Merge
ADT5-CFP
Chlorophyll
5 µm
5 µm
5 µm

stromule-mediated transport. To test this hypothesis a stromule inhibitor was needed to decrease the frequency of chloroplasts with stromules or to decrease stromule length, and subsequently test if ADT5 nuclear localization is decreased in response. Inhibition of stromule formation has been attained in past studies using $AgNO_3$ (Gray *et al.,* 2012), 2,3-butanedione monoxime (BDM), or expression of myosin XI tail domains (Natesan *et al.,* 2009). Therefore these three approaches were used to determine if stromule inhibition could be attained.

In order to test the efficacy of these three approaches, a sensitive system to detect stromule inhibition was needed. Bross (2011) observed that the transit peptide of ADT2 fused to CFP (TP-ADT2-CFP) localized to especially long stromule-like extensions from chloroplasts. To confirm this observation agroinfiltration was used to express TP-ADT2-CFP in *N. benthamiana* and long extensions were observed (Fig. 12A), supporting results by Bross (2011). To ensure that these were stromules, agroinfiltration was performed to transiently co-express TP-ADT2-CFP and TP-YFP. The two fusion proteins were co-localized confirming that these extensions are stromules (Fig. 12B). Thus, the length of stromules visualized by TP-ADT2-CFP will provide a sensitive marker to detect stromule inhibition and all three approaches were tested.

3.5.1 $AgNO_3$

Incubation of tobacco seedlings in 120 μM $AgNO_3$ for 16 hours was previously shown to significantly reduce the percentage of plastids with stromules (Gray *et al.,* 2012). As ADT5 nuclear localization typically occurs 5 days post-infiltration (Bross, 2011) stromule inhibition should be sustained over this period of time. Incubating plants in 120 μM $AgNO_3$ for 5 days is not practical, instead *N. benthamiana* were grown from seed in soil watered with 120 μM $AgNO_3$. Plants grown under this condition did not display an adverse phenotype, and agroinfiltration was performed to transiently express TP-ADT2-CFP. Visualization of TP-ADT2-CFP localization revealed long and extensive stromules present throughout the infiltrated tissue indicating this treatment was not effective in reducing stromules (results not shown). Another approach was used to test

Figure 12. Localization of TP-ADT2-CFP and co-localization with TP-YFP.
TP-ADT2-CFP was transiently expressed alone **(A)** and co-expressed with TP-YFP **(B)**.
(A) Images of chlorophyll fluorescence (left) and TP-ADT2-CFP (middle) are displayed separately and merged (right). TP-ADT2-CFP localizes to long extensions from the chloroplast.
(B) Images of chlorophyll fluorescence and TP-ADT2-CFP are shown merged (left). Images of chlorophyll fluorescence and TP-YFP are shown merged (middle). Regions where TP-ADT2-CFP and TP-YFP fluorescence overlapped are shown in green, merged with chlorophyll fluorescence (right). TP-ADT2-CFP co-localizes with TP-YFP in a stromule.

Scale bars are 5 μm.

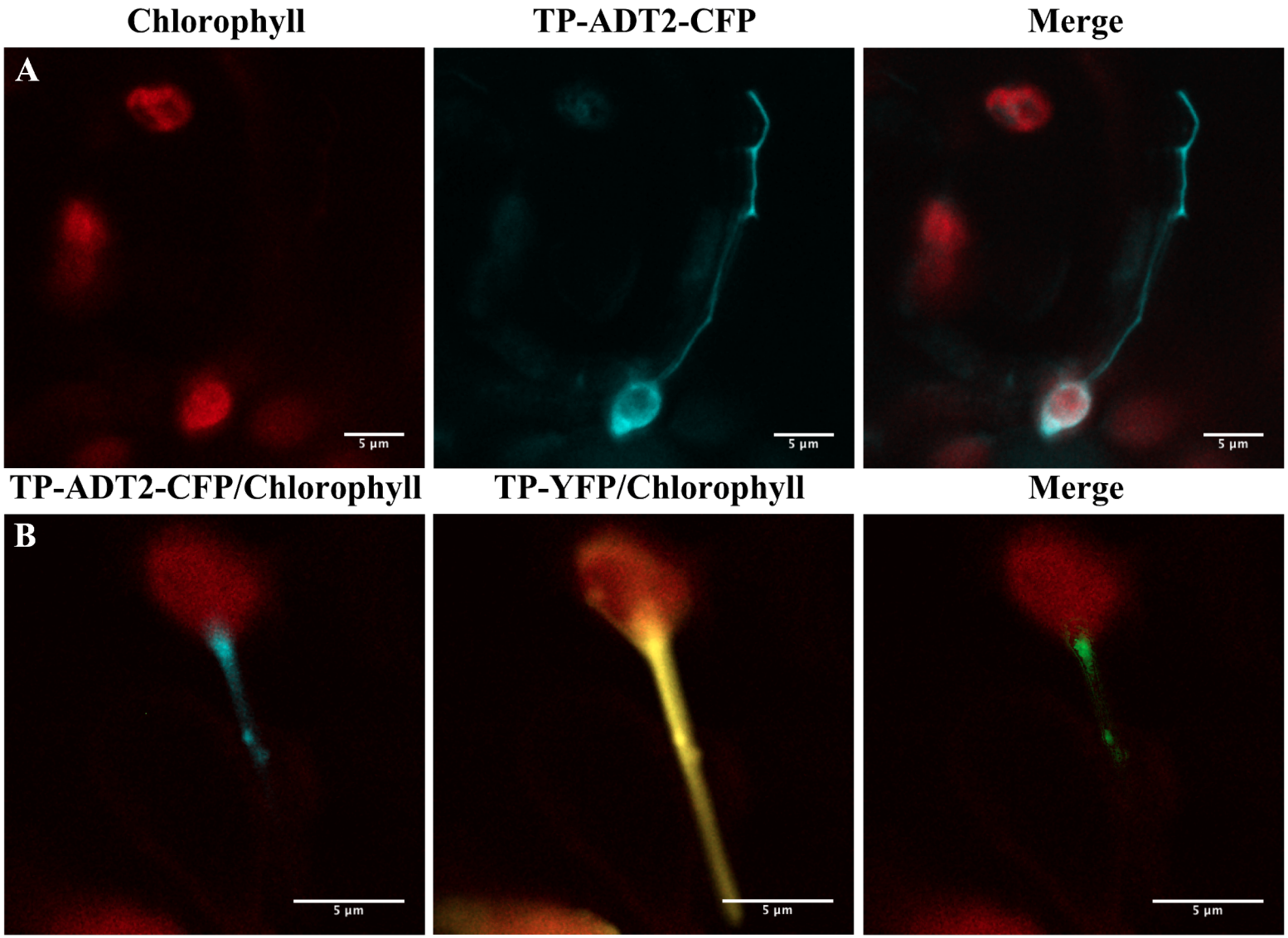
Chlorophyll
TP-ADT2-CFP
Merge
A
5 µm
5 µm
5 µm
TP-ADT2-CFP/Chlorophyll
TP-YFP/Chlorophyll
Merge
B
5 µm
5 µm
5 µm

the efficacy of $AgNO_3$ on stromule inhibition. After agroinfiltration with *A. tumefaciens* encoding *TP-ADT2-CFP* leaves were infiltrated with 120 μm $AgNO_3$ every 24 hours for 5 days. This treatment stained the leaves a dark purple colour and caused necrosis of leaf tissue preventing confocal visualization. As a result, $AgNO_3$ was judged not to be a suitable stromule inhibitor.

3.5.2 BDM

Application of 1 mM BDM to lower epidermal peels of tobacco was shown to significantly reduce the percentage of plastids with stromules and the average length of stromules two hours after application (Natesan *et al.,* 2009). As stromule inhibition should be sustained for 5 days to test the effect on ADT5 nuclear localization this procedure was modified. After agroinfiltration with *A. tumefaciens* encoding *TP-ADT2-CFP* leaves were infiltrated with 1 mM BDM every 24 hours for 5 days. Unfortunately, this treatment caused necrosis of leaves after 2 to 3 days preventing visualization and as a result, BDM was judged not to be a suitable stromule inhibitor.

3.5.3 Transient expression of myosin XI tail domains

Inhibition of stromule formation has previously been accomplished through transient expression of myosin XI tail domains (Natesan *et al.,* 2009), which inhibit the function of wild-type myosin XI by creating a dominant negative effect (Avisar *et al.,* 2008). *A. tumefaciens* containing constructs for the tail domains of myosin XI-2 and myosin XI-K (Avisar *et al.,* 2008) were used to test if a similar strategy could be effective. These constructs will henceforth be referred to as *dominant negative myosin XI-2* (*dnMyoXI-2*) and *dnMyoXI-K*. Control agroinfiltrations were performed in *N. benthamiana* using *A. tumefaciens* containing the *TP-ADT2-CFP* construct and an empty pCB vector. Control infiltrations were performed on three occasions, and a total of 554 chloroplasts were analyzed. Chloroplasts were analyzed if they contained any visible TP-ADT2-CFP fluorescence and were determined to have a stromule if the projection was longer than 1 μm. It was determined that in control plants 26.9% of chloroplasts had stromules (Fig. 13A) and the average length of these stromules was 4.62 μm (Fig. 13B).

Figure 13. Effect of dnMyoXI-2 and dnMyoXI-K on stromules.

Dominant negative myosin XI-2 and myosin XI-K (dnMyoXI-2 and dnMyoXI-K) were co-expressed with TP-ADT2-CFP to determine if they affect the percentage of chloroplasts having stromules **(A)** or the average length of stromules **(B)** compared to co-expression with an empty vector.

(A) In the empty vector control (orange) 554 chloroplasts were analyzed from three plants and 26.9% had stromules. In the treatment with dnMyoXI-2 (green) 395 chloroplasts were analyzed from three plants and 22.3% had stromules. In the treatment with dnMyoXI-K (purple) 579 chloroplasts were analyzed from three plants and 14.3% had stromules. Significant differences ($P<0.05$) as determined by a two-proportion Z-test are indicated by different letters.

(B) In the empty vector control (orange) 166 stromules were measured from three plants and the average length was 4.62 μm. In the dnMyoXI-2 treatment (green) 93 stromules were measured from three plants and had an average length of 2.71 μm. In the dnMyoXI-K treatment (purple) 91 stromules were measured and had an average length of 3.48 μm. Significant differences ($P<0.05$) as determined by a t-test are indicated by different letters.

Error bars show 95% confidence intervals.

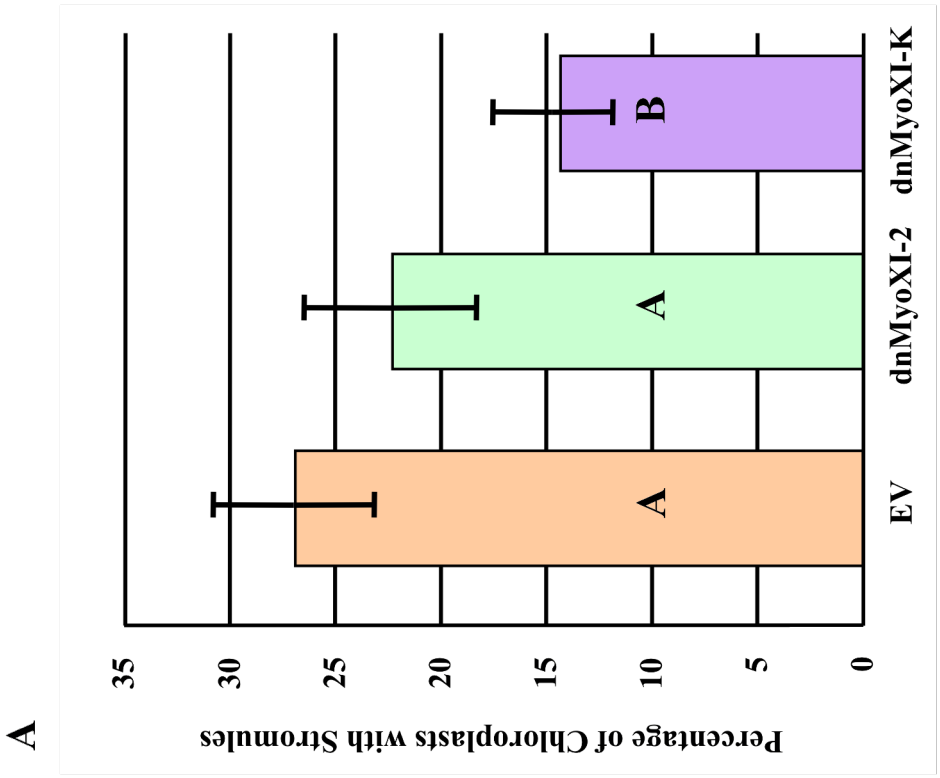
A
Percentage of Chloroplasts with Stromules
0
5
10
15
20
25
30
35
A
A
B
EV
dnMyoXI-2
dnMyoXI-K

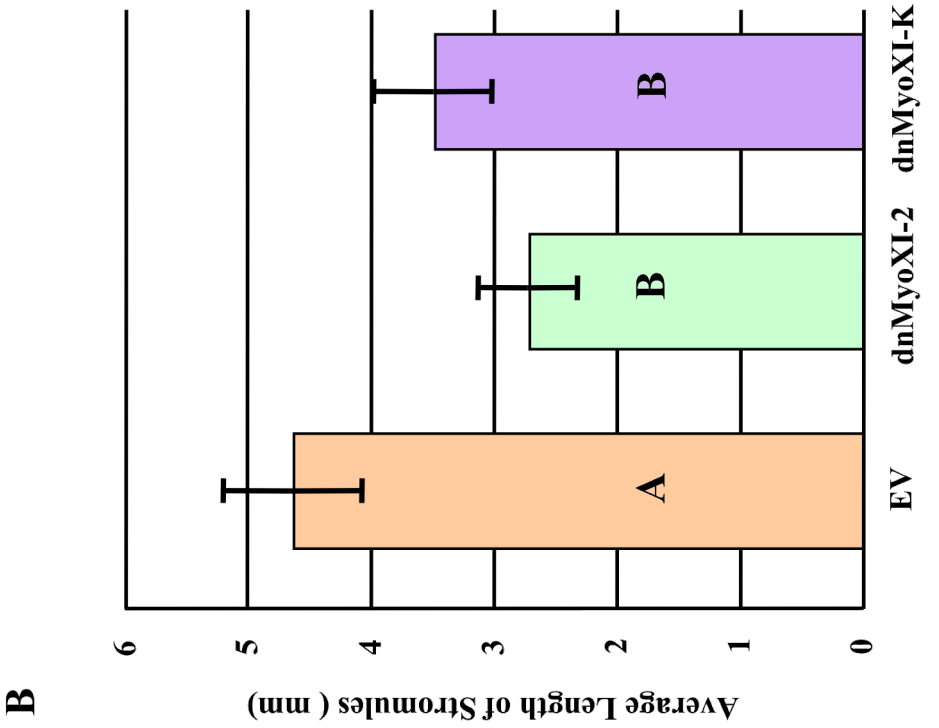
B
Average Length of Stromules (mm)
0
1
2
3
4
5
6
A
B
B
EV
dnMyoXI-2
dnMyoXI-K

To test if expression of dnMyoXI-2 or dnMyoXI-K has an effect on the proportion of chloroplasts having stromules or the average length of stromules agroinfiltration was performed using *A. tumefaciens* encoding TP-ADT2-CFP and either dnMyoXI-2 or dnMyoXI-K. Infiltrations were performed on three occasions for both dnMyoXI-2 and dnMyoXI-K treatments. For the dnMyoXI-2 treatment 395 chloroplasts were analyzed while for the dnMyoXI-K treatment 579 chloroplasts were analyzed. Treatment with dnMyoXI-2 non-significantly decreased ($P>0.05$) the percentage of chloroplasts with stromules to 22.3% (Fig. 13A). However, dnMyoXI-2 significantly reduced ($P<0.05$) the average length of stromules to 2.71 μm (Fig. 13B). Treatment with dnMyoXI-K significantly decreased ($P<0.05$) the percentage of chloroplasts with stromules to 14.3% (Fig. 13A) and also significantly decreased ($P<0.05$) the average length of stromules to 3.48 μm (Fig. 13B).

It followed that I wanted to determine if these constructs could also cause a decrease in ADT5-CFP nuclear localization by co-expressing dnMyoXI-2 and dnMyoXI-K with ADT5-CFP. Control agroinfiltrations were performed using *A. tumefaciens* encoding *ADT5-CFP* and an empty pCB vector. The percentage of cells with ADT5-CFP detected in the nucleus was used to determine the extent of ADT5-CFP nuclear localization and cells were analyzed only if ADT5-CFP fluorescence was present. Control infiltrations were performed on three occasions representing a total of 131 cells, of which 24.9% had ADT5-CFP fluorescence visible in the nucleus (Fig. 14).

Agroinfiltration was then performed with *A. tumefaciens* encoding *ADT5-CFP* and either *dnMyoXI-2* or *dnMyoXI-K*. This was performed on three occasions for both dnMyoXI-2 and dnMyoXI-K treatments. For the dnMyoXI-2 treatment 190 cells were analyzed and ADT5-CFP was detected in the nucleus in 5.79% of cells (Fig. 14), a significant decrease ($P<0.05$) from the control. For the dnMyoXI-K treatment 358 cells were analyzed and ADT5-CFP was detected in the nucleus in 3.91% (Fig. 14) of the cells, again a significant decrease ($P<0.05$) from the control.

Figure 14. Effect of dnMyoXI-2 and dnMyoXI-K on ADT5-CFP nuclear localization.

To test if expression of dnMyoXI-2 or dnMyoXI-K affects ADT5-CFP nuclear localization, they were co-expressed with ADT5-CFP and compared to co-expression of ADT5-CFP with an empty vector. In the empty vector control (orange) 131 cells were analyzed from three plants and ADT5-CFP was detected in the nucleus of 24.6% of these cells. In the treatment with dnMyoXI-2 (green) 190 cells were analyzed from three plants and ADT-CFP was visible in the nucleus of 5.76% of the cells. In the treatment with dnMyoXI-K (purple) 358 cells were analyzed from three plants and 3.91% had ADT5-CFP visible in the nucleus. Significant differences ($P<0.05$) as determined by a two-proportion Z-test are indicated by different letters.

Error bars are 95% confidence intervals.

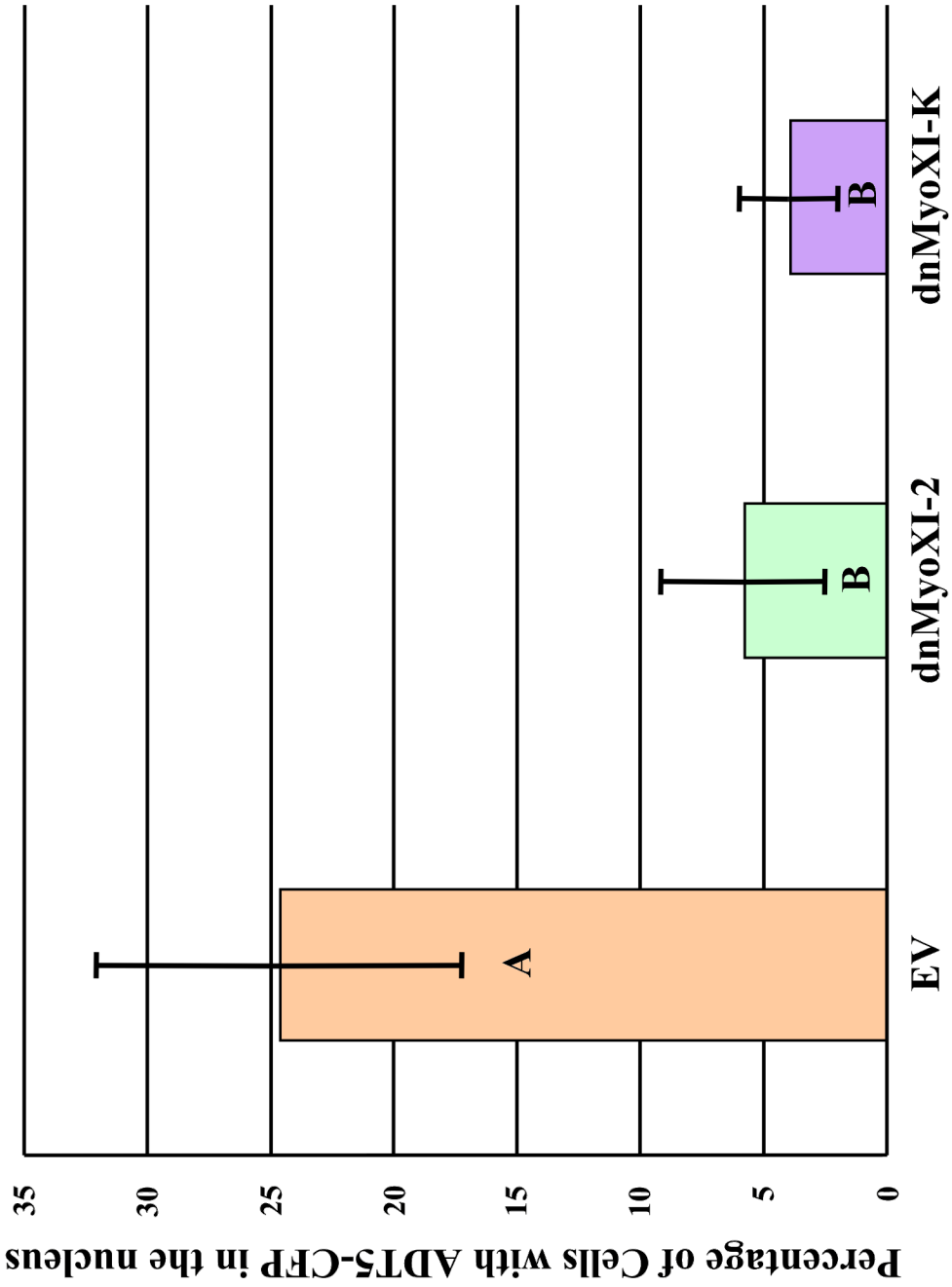
Percentage of Cells with ADT5-CFP in the nucleus
35
30
25
20
15
10
5
0
A
B
B
EV
dnMyoXI-2
dnMyoXI-K

Therefore, expression of dnMyoXI-2 and dnMyoXI-K were found to inhibit stromules and reduce the percentage of cells with ADT5-CFP in the nucleus, providing indirect evidence for stromule-mediated transport of ADT5 to the nucleus.

3.6 ADT2 and chloroplast division

In addition to stromules, ADT2-CFP was also found at the equatorial plane and poles of chloroplasts (Bross, 2011) suggesting a role in chloroplast division. Initially, only these two patterns were observed (Bross, 2011), which do not represent all stages of chloroplast division. During division, chloroplasts increase in size and become constricted at the equatorial plane before they separate into two daughter chloroplasts (Pyke, 1999). To further investigate a possible role for ADT2 in chloroplast division, agroinfiltration was used to transiently express ADT2-CFP in *N. benthamiana*. In chloroplasts with no apparent central constriction ADT2-CFP localizes to a band around the equatorial plane (Fig. 15A). In elongated chloroplasts with a slight indentation, suggestive of early division, ADT2-CFP localizes as a band around the middle of the elongation (Fig. 15B). In chloroplasts with a clear indentation, indicative of a later stage of division, ADT2-CFP is found at the site of constriction (Fig. 15C). ADT2 localization to the poles of chloroplasts (Fig. 15D) is consistent with remnants of the division ring on daughter chloroplasts (Miyagishima, 2011). These localization patterns are consistent with a role in chloroplast division from the beginning of the process through the constriction stages until separation of chloroplasts occurs (Fig. 15E).

The size of chloroplasts appears to dictate when they divide, as prior to division chloroplasts increase in size (Pyke, 1999). If chloroplasts with ADT2-CFP at a pole represent recently divided chloroplasts, and those with ADT2-CFP as a band are in the process of dividing they should be smaller and larger than average chloroplasts, respectively. While chloroplast volume would be the most accurate way to measure chloroplast size it is difficult to determine, therefore, chloroplast size was measured as the length of a chloroplast across its longest axis. Uninfiltrated *N. benthamiana* plants were used to determine the average size of a chloroplast because they should contain

Figure 15. ADT2-CFP localization and chloroplast division.

Transient expression of ADT2-CFP in *N. benthamiana* was used to determine ADT2 localization in chloroplasts at different stages of chloroplast division **(A-D)**. Images of chlorophyll fluorescence (left) and ADT2-CFP (middle) are shown separately and merged (right).

(A) ADT2-CFP is observed as a band around the equatorial plane of chloroplasts without significant elongation or constriction.

(B) ADT2-CFP is observed as a band at the equatorial plane of elongated chloroplasts.

(C) ADT2-CFP is observed at the site of constriction of highly constricted chloroplasts.

(D) ADT2-CFP localizes to a pole of chloroplasts.

(E) Diagram corresponding to different stages of chloroplast division. Left to right: division ring forms before constriction occurs **(A)**; the chloroplast becomes elongated and a small indentation occurs indicating constriction is beginning **(B)**; constriction proceeds such that the chloroplast is highly indented and dumbbell shaped **(C)**; after division, remnants of the division ring remain on chloroplast poles **(D)**.

(E) Adapted from Miyagishima (2011).

Scale bars are 5 μm.

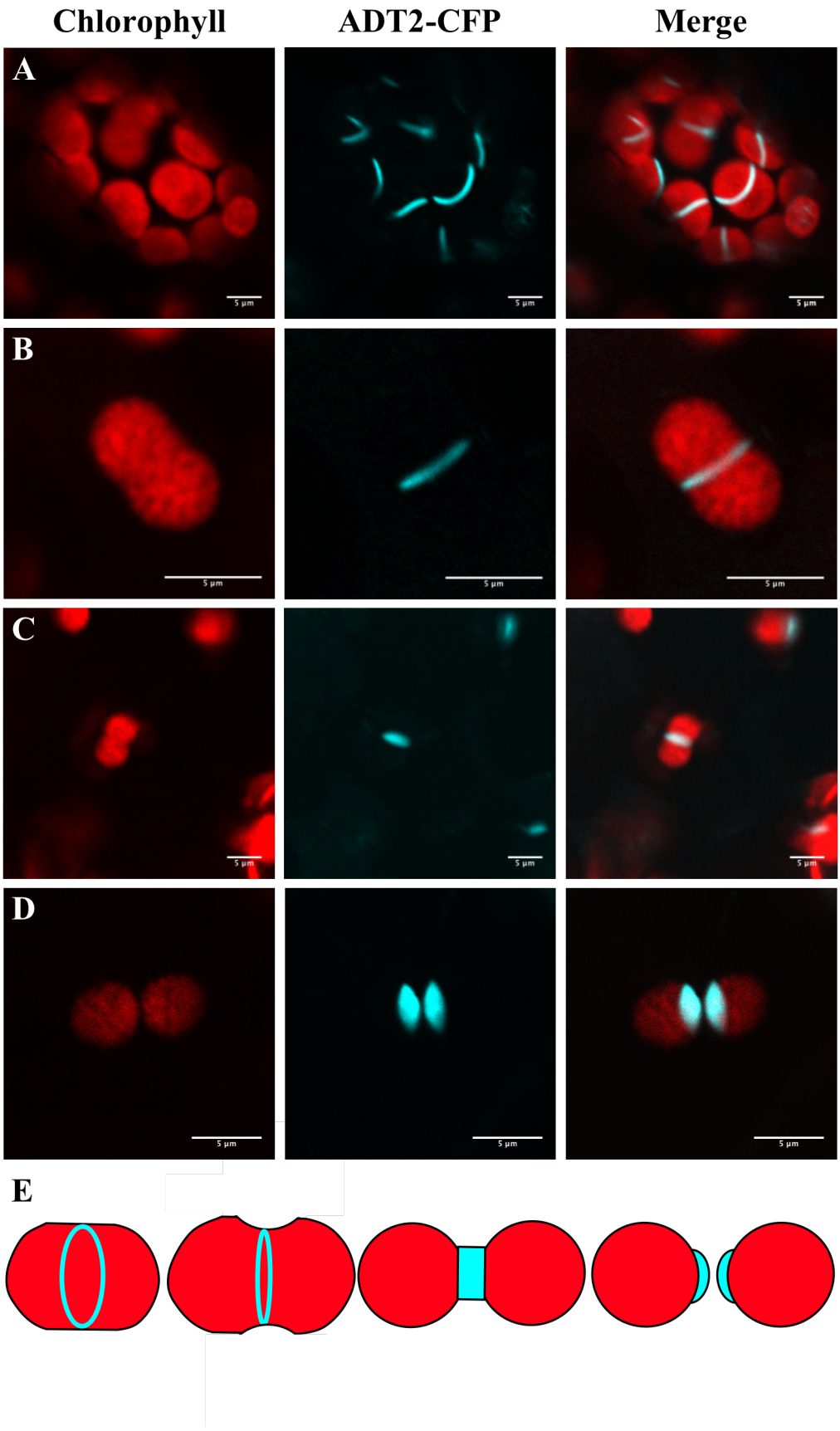
Chlorophyll
ADT2-CFP
Merge
A
B
C
D
E
5 µm

chloroplasts at many different developmental stages, and thus sizes. A total of 68 chloroplasts were measured from three uninfiltrated plants and they had an average length of 5.08 μm (Table 1). In chloroplasts with ADT2-CFP present on a pole 75 chloroplasts were measured from three different plants and the average length of these chloroplasts was significantly shorter ($P<0.05$) at 4.24 μm (Table 1). Lastly, in chloroplasts with ADT2-CFP localized to a band at the equatorial plane, 35 chloroplasts were measured from five plants with an average length of 6.69 μm (Table 1), significantly longer ($P<0.05$) than in uninfiltrated plants. The standard deviation from the mean also differed between the groups. Chloroplasts from uninfiltrated plants had the largest standard deviation, consistent with a mixed population of chloroplasts, while chloroplasts with ADT2-CFP at a pole had the lowest standard deviation, indicating that they are similar in size, consistent with newly divided chloroplasts (Table 1). The standard deviation of chloroplasts with ADT2 visualized as a band was larger than that of the polar group but smaller than chloroplasts from uninfiltrated plants (Table 1) as would be expected given that division occurs in stages (Pyke, 1999). These data support the hypothesis that different localization patterns are indicative of different chloroplast division stages.

Until this study, ADT2-CFP patterns consistent with chloroplast division have only been shown in *N. benthamiana*. To determine if the same patterns are observed in *A. thaliana* agroinfiltration was used to transiently express ADT2-CFP in the rosette leaves of *A. thaliana* Col-0, L*er*, and Ws accessions. In all three accessions ADT2-CFP was observed as either a band at the equatorial plane of a chloroplast or at a pole (Fig. 16) confirming that ADT2-CFP localization is consistent with a role in chloroplast division in *A. thaliana*, the native plant of these ADTs.

3.7 Chloroplast morphology in an *adt2* mutant

The localization patterns of ADT2 strongly suggest a role in chloroplast division. Hence, it was hypothesized that a mutation to ADT2 would affect chloroplast division. While no known knockout lines exist for ADT2 (Corea *et al.,* 2012) an *adt2* mutant was

Table 1. Comparison of chloroplast lengths.

Chloroplast Group	Chloroplasts Measured	Average Length (μm)	Standard Deviation
Uninfiltrated	68	5.08	1.12
ADT2: pole	75	4.24*	0.60
ADT2: band	35	6.69*	0.85

* significantly different from the uninfiltrated control ($P<0.05$) as determined by a t-test.

Figure 16. ADT2-CFP localization in three *A. thaliana* accessions.
ADT2-CFP was transiently expressed in three accessions of *A. thaliana*: Columbia-0 (left), Landsberg *erecta* (middle), and Wassilewskija (right). All images show ADT2-CFP and chlorophyll fluorescence merged. In each accession ADT2-CFP was visualized as a band at the equatorial plane (top images) or to the pole of a chloroplast (bottom images).

Scale bars are 5 μm.

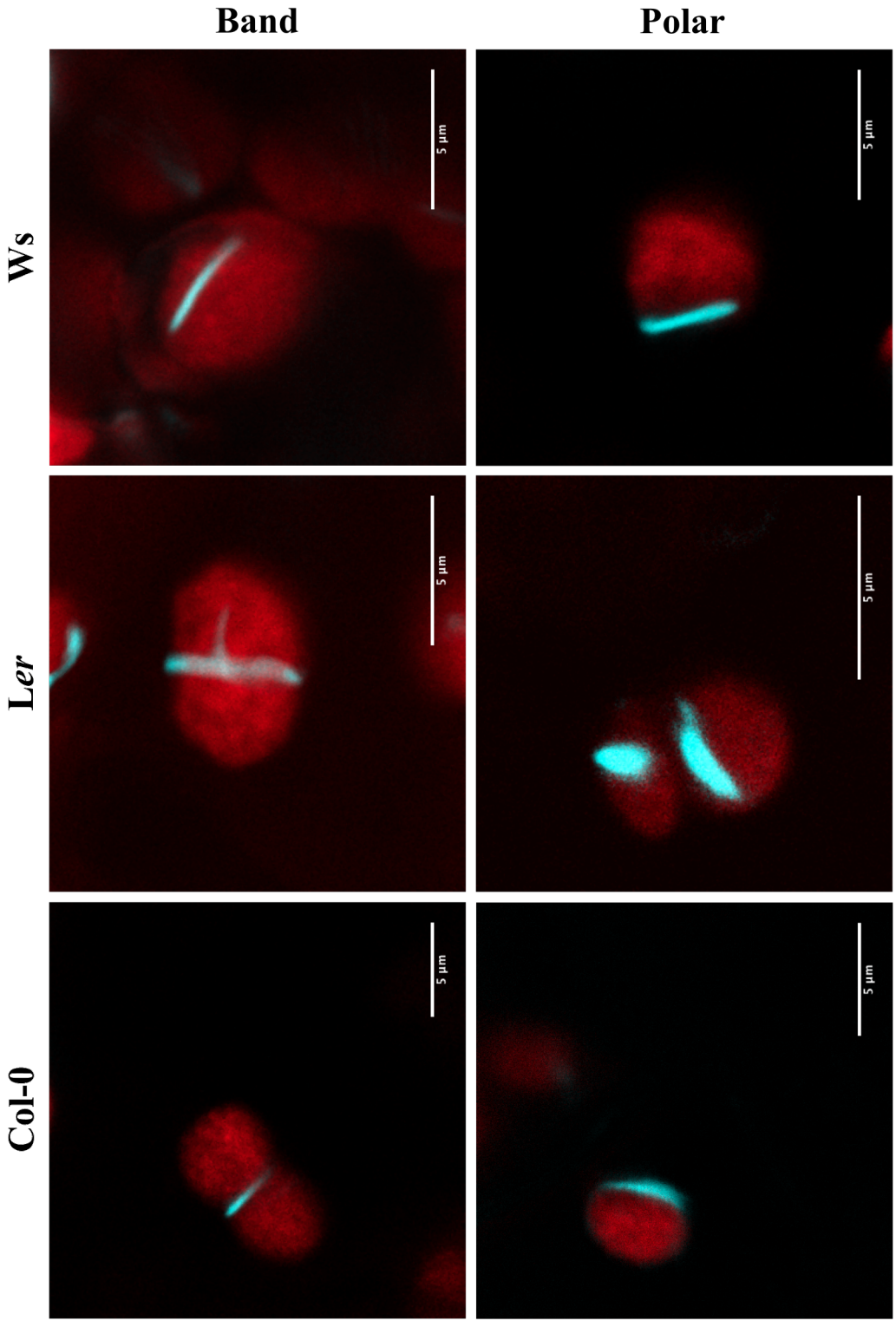
Band
Polar
Ws
Ler
Col-0
5 µm

identified in a screen for plants resistant to a toxic analog of phenylalanine (Huang *et al.,* 2010). The mutation results in a single amino acid substitution in the ACT regulatory domain of ADT2 making the enzyme insensitive to feedback inhibition by phenylalanine (Huang *et al.,* 2010). Homozygous *adt2* mutant plants were grown from seed and chloroplast morphology was examined.

Chloroplast morphology in the *adt2* mutant differs from wild-type *A. thaliana* Col-0 in plants of equal age (Fig. 17A-B). In the *adt2* mutants large and irregularly shaped chloroplasts can be seen, different from the small oval shaped chloroplasts in wild-type *A. thaliana*. These irregular *adt2* chloroplasts vary in size and occur in many different shapes (Fig. 17C-F). Such large and irregularly shaped chloroplasts are consistent with impaired division. Despite the presence of these irregular chloroplasts, many chloroplasts were similar to wild-type in size and shape, indicating that chloroplast division is not completely compromised in this mutant.

3.8 ADT2-CFP localization in the *adt2* mutant

To determine if ADT2 localization is affected by the *adt2* mutation agroinfiltration was used to transiently express ADT2-CFP in the rosette leaves of *adt2* plants. The localization of ADT2-CFP in *adt2* mutants was variable (Fig. 18A-F) and differed from what is observed in wild-type *A. thaliana* Col-0 (Fig. 16). In centrally constricted chloroplasts ADT2-CFP was found at the site of constriction (Fig. 18A-C). However, the appearance of the bands was often unusual, and in some chloroplasts it appeared to split or fray along its length (Fig. 18A-B). In chloroplasts without central constrictions ADT2-CFP was frequently observed as short bands (Fig. 18A,C-E) even if the chloroplasts appeared wild-type in size and shape. At times ADT2-CFP bands were not linear, but seen to bend and branch along a chloroplast (Fig. 18E). ADT2-CFP was rarely found in chloroplasts that morphologically were most severely affected and only very faint bands or small punctate structures were observed (Fig. 18F). These unusual localization patterns further suggest that chloroplast division is affected by the *adt2* mutation.

Figure 17. Chloroplast morphology in an *adt2* mutant.

To determine if chloroplast morphology is affected by the *adt2* mutation chloroplasts were examined and compared to chloroplasts in wild-type *A. thaliana* Col-0 of equal age.

(A) An overview of chloroplasts in wild-type *A. thaliana* Col-0

(B) An overview of chloroplasts in the *adt2* mutant.

(C-F) Chloroplasts in the *adt2* mutant were irregular and heterogeneous in size and shape.

Scale bars are 20 μm **(A-B)** or 5 μm **(C-F).**

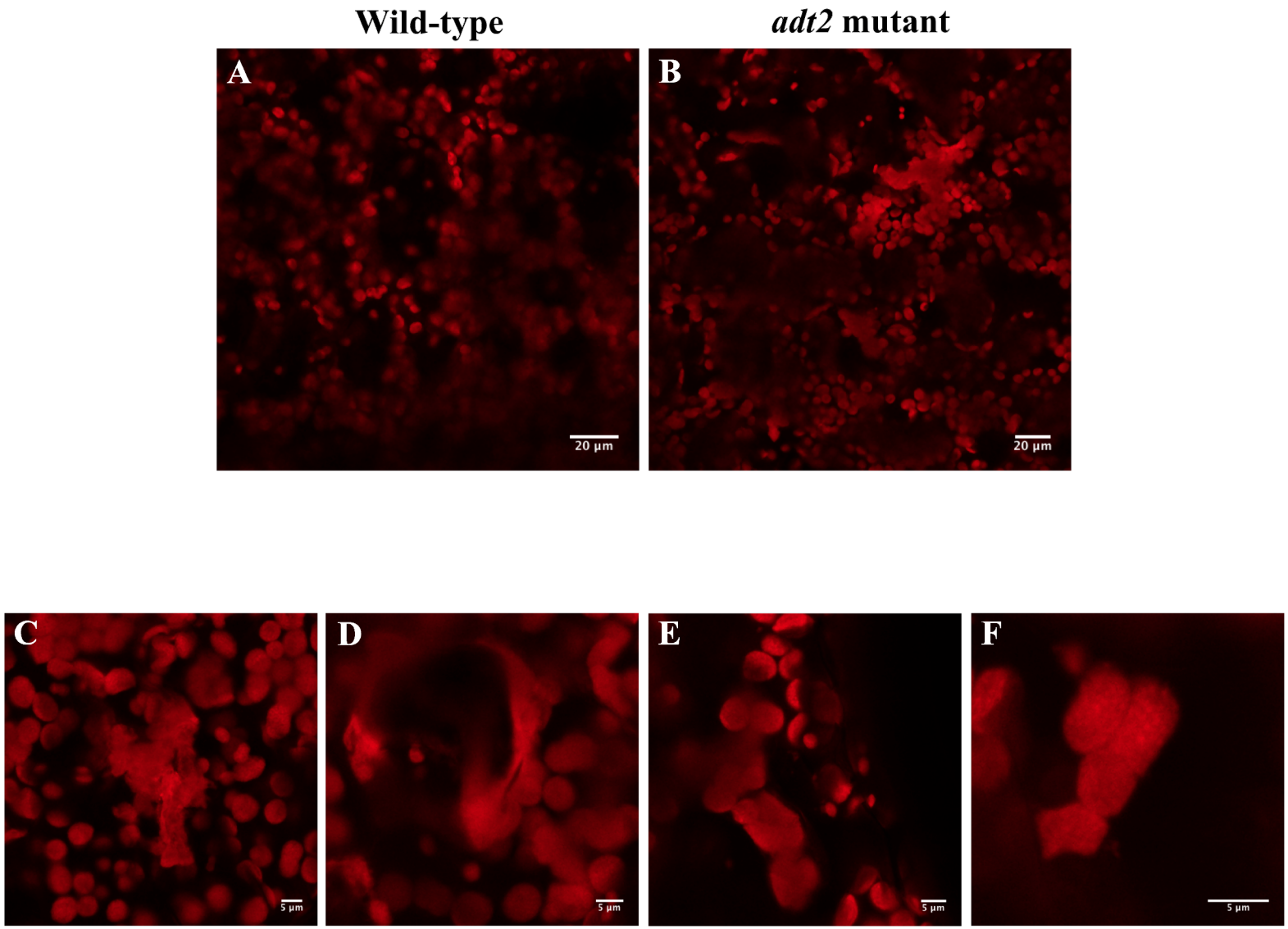
Wild-type
adt2 mutant
A
B
20 µm
20 µm
C
D
E
F
5 µm
5 µm
5 µm
5 µm

Figure 18. ADT2-CFP localization in the *adt2* mutant.

ADT2-CFP was transiently expressed in *adt2* mutant plants to determine if ADT2-CFP localization is affected by the *adt2* mutation. Images of chlorophyll fluorescence and ADT2-CFP are shown merged.

(A) ADT2-CFP is observed as a band at the equatorial plane of a constricted chloroplast (left) and as several short bands (right).

(B) ADT2-CFP is visible as a band at the equatorial plane of a constricted chloroplast.

(C) ADT2-CFP is observed as a band at the equatorial plane of a constricted chloroplast (left) and as two short bands (right).

(D) ADT-CFP localized to multiple short bands and a pole.

(E) ADT2-CFP observed as non-linear bands along chloroplasts.

(F) ADT2-CFP is observed as puncta (left arrow) and faint bands (right arrow) in severely affected chloroplasts

Scale bars are 5 μm **(A-E)** or 10 μm **(F)**.

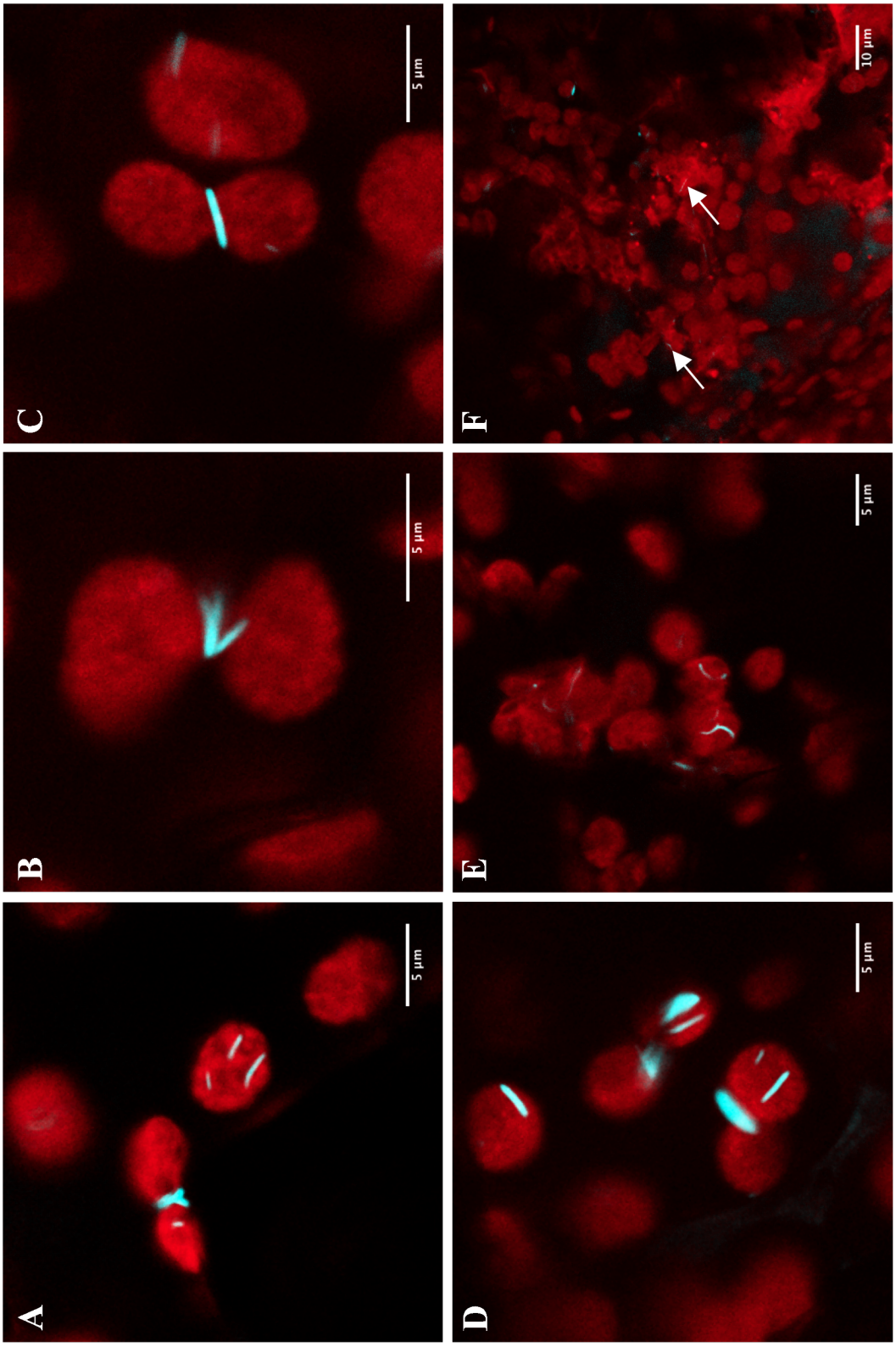
A
5 µm
B
5 µm
C
5 µm
D
5 µm
E
5 µm
F
10 µm

3.9 ADT2-CFP localization in *arc* mutants

Chloroplast division is disrupted in the *A. thaliana arc3*, *arc5* and *arc6* mutants (Pyke and Leech, 1992; 1994; Pyke *et al*., 1994). Furthermore, these disruptions occur at different stages of chloroplast division, and the relative position of FtsZ is known in each mutant (Glynn *et al.,* 2007; Vitha *et al.,* 2001; 2003). Thus, it was hypothesized that ADT2-CFP would be mislocalized in these mutants in a predictable way. The *arc* mutants are from the L*er* (*arc3* and a*rc5*) and Ws (*arc6*) accessions of *A. thaliana*, and ADT2-CFP was visualized at a pole or as a band at the equatorial plane in both accessions (Fig. 16), consistent with a role in chloroplast division. This ensures that any difference in ADT2-CFP localization in the *arc* mutants is due to the mutation and its effects on chloroplast division. Agroinfiltration was performed to express ADT2-CFP in the rosette leaves of each *arc* mutant.

In *arc3* mutants, the Z-ring can form multiple times along a single chloroplast (Glynn *et al.,* 2007), and *arc3* chloroplasts are highly irregular in size and shape (Pyke and Leech, 1992). The localization of ADT2-CFP in *arc3* mutants differs substantially from wild-type *A. thaliana* L*er*. Instead of localizing to a single band placed at the equatorial plane of the chloroplast ADT2-CFP is observed as several bands across *arc3* chloroplasts (Fig. 19A-C) resembling the location of Z-rings in *arc3* mutants (Glynn *et al.,* 2007). The bands were variable in appearance in both their linearity and thickness (Fig.19A-C). Although *arc3* chloroplasts are larger on average than those in wild-type *A. thaliana* (Pyke and Leech, 1992) the misplacement of the division ring creates a heterogeneous population of chloroplasts (Glynn *et al.,* 2007; Pyke and Leech, 1992). The smaller chloroplasts in *arc3* plants had ADT2 localization patterns that more closely resembled wild-type where ADT2-CFP was observed at a pole or as a single band (Fig. 19D). This polar localization pattern was never observed for larger chloroplasts in *arc3* mutants.

In *arc5* mutants, chloroplasts are larger in size and fewer in number compared to wild-type, and many have a central constriction corresponding to the location of the Z-

Figure 19. ADT2-CFP localization in *arc3* mutants.

ADT2-CFP was transiently expressed in *arc3* mutants to determine if ADT2-CFP localization is affected by the *arc3* mutation.

(A) Images of chlorophyll fluorescence (left) and ADT2-CFP (middle) are shown separately and merged (right). ADT2 localizes to multiple bands across the chloroplast.

(B-D) Images of chlorophyll fluorescence and ADT2-CFP are shown merged.

(B) ADT2-CFP localizes to thick linear bands across the chloroplast.

(C) ADT2-CFP localizes to highly curved bands and shorter linear bands.

(D) ADT2-CFP localizes to single central bands or to the poles of smaller chloroplasts.

Scale bars are 5 μm.

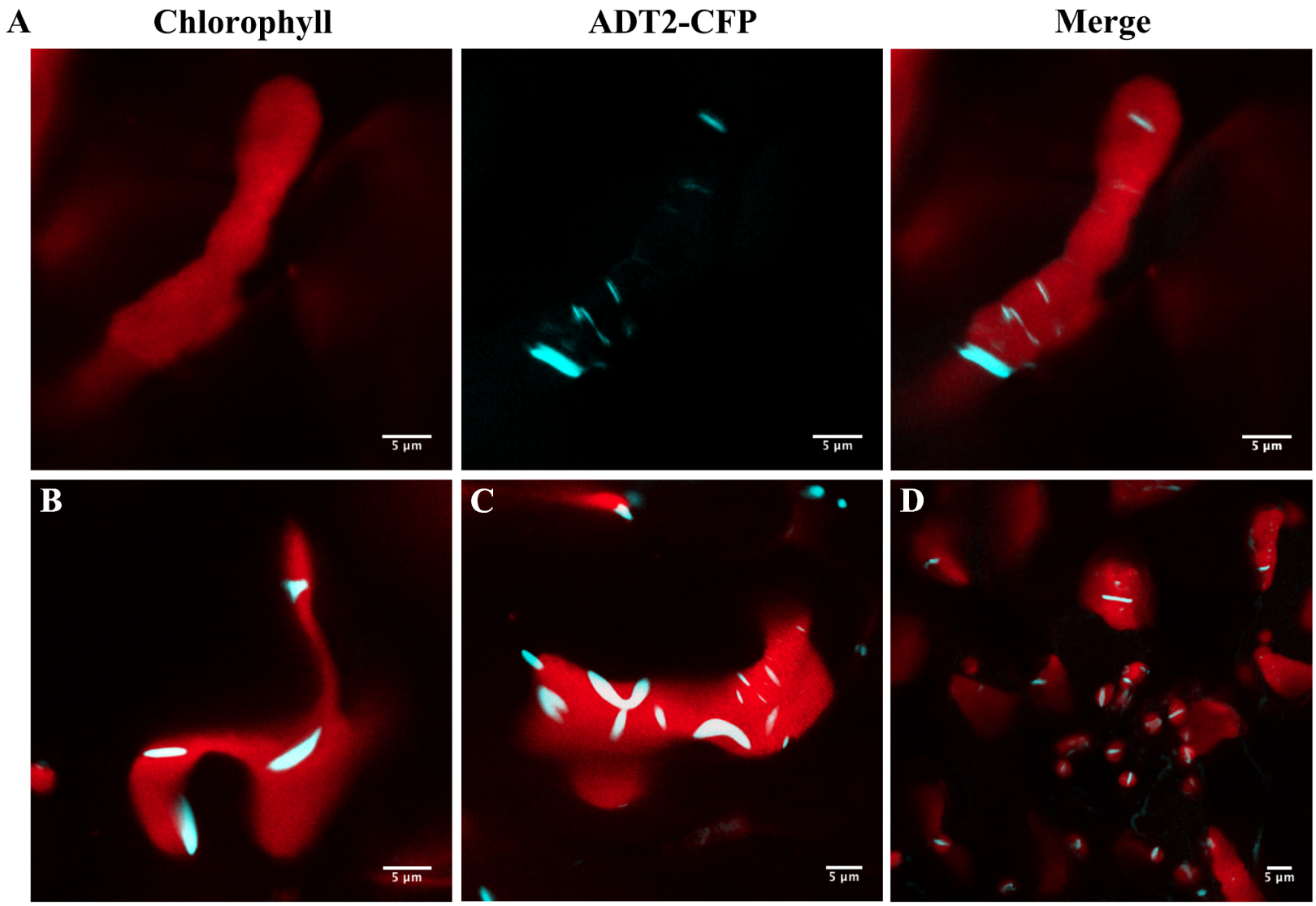
A
Chlorophyll
ADT2-CFP
Merge
5 µm
B
C
D

ring (Pyke and Leech, 1994; Vitha *et al.,* 2001). The localization of ADT2-CFP in *arc5* mutants was predominantly to a band located at the central constriction (Fig. 20A-C), consistent with the location of the Z-ring (Vitha *et al*., 2001). The appearance of ADT2-CFP bands was variable: some bands appeared straight and tightly wrapped around the constriction (Fig. 20A), while others appeared to curve along its length (Fig. 20B). On some chloroplasts ADT2-CFP was observed to localize to multiple bands on a single chloroplast (Fig. 20C), although they always appeared centered near an area of constriction. Chloroplasts that appear wild-type in size and shape were present in *arc5* mutants, and ADT2-CFP was observed as either a central band or toward a pole (Fig. 20C), similar to ADT2-CFP localization on wild-type chloroplasts. This polar localization pattern was never observed in large, centrally constricted chloroplasts. In addition, ADT2-CFP was observed in stromule-like structures (Fig. 20D) although if observed the stromules are typically longer and more convoluted in appearance than in wild-type plants.

In *arc6* plants, the Z-ring does not form, and short rod-shaped bands of FtsZ, believed to be unassembled FtsZ filaments are found throughout the stroma (Vitha *et al.,* 2003). This is associated with *arc6* chloroplasts being very large in size and few in number per cell (Pyke *et al.,* 1994). In *arc6* mutant chloroplasts ADT2-CFP localized to short bands (Fig. 21A) similar to what has been observed for FtsZ (Vitha *et al.,* 2003). However, ADT2-CFP also localized to round punctate structures usually observed near the edge of a chloroplast (Fig. 21B), although they occasionally appeared detached from chloroplasts (Fig. 21C).

3.10 Generation of an *FtsZ2-YFP* fusion construct

The localization of ADT2-CFP in arc mutants is consistent with that of FtsZ (Glynn *et al.,* 2007; Vitha *et al.,* 2001; 2003), suggesting that ADT2 and FtsZ are closely linked. Thus, it was of interest to investigate the relationship between the two proteins by determining if FtsZ localization is affected in the *adt2* mutant. To accomplish this FtsZ

Figure 20. ADT2-CFP localization in *arc5* mutants.

ADT2-CFP was transiently expressed in *arc5* mutants to determine if ADT2-CFP localization is affected by the *arc5* mutation.

(A) Images of chlorophyll fluorescence (left) and ADT2-CFP (middle) are shown separately and merged (right). ADT2 localizes to a single linear band at the central constriction.

(B-D) Images of chlorophyll fluorescence and ADT2-CFP are shown merged.

(B) ADT2-CFP localizes in a curved band along the central constriction.

(C) ADT2-CFP occasionally localized to multiple bands near the central constriction. In smaller *arc5* chloroplasts, ADT2-CFP localized to a single equatorial band or to a pole of chloroplasts (arrows).

(D) ADT2-CFP was infrequently observed as long stromule-like structures.

Scale bars are 5 μm.

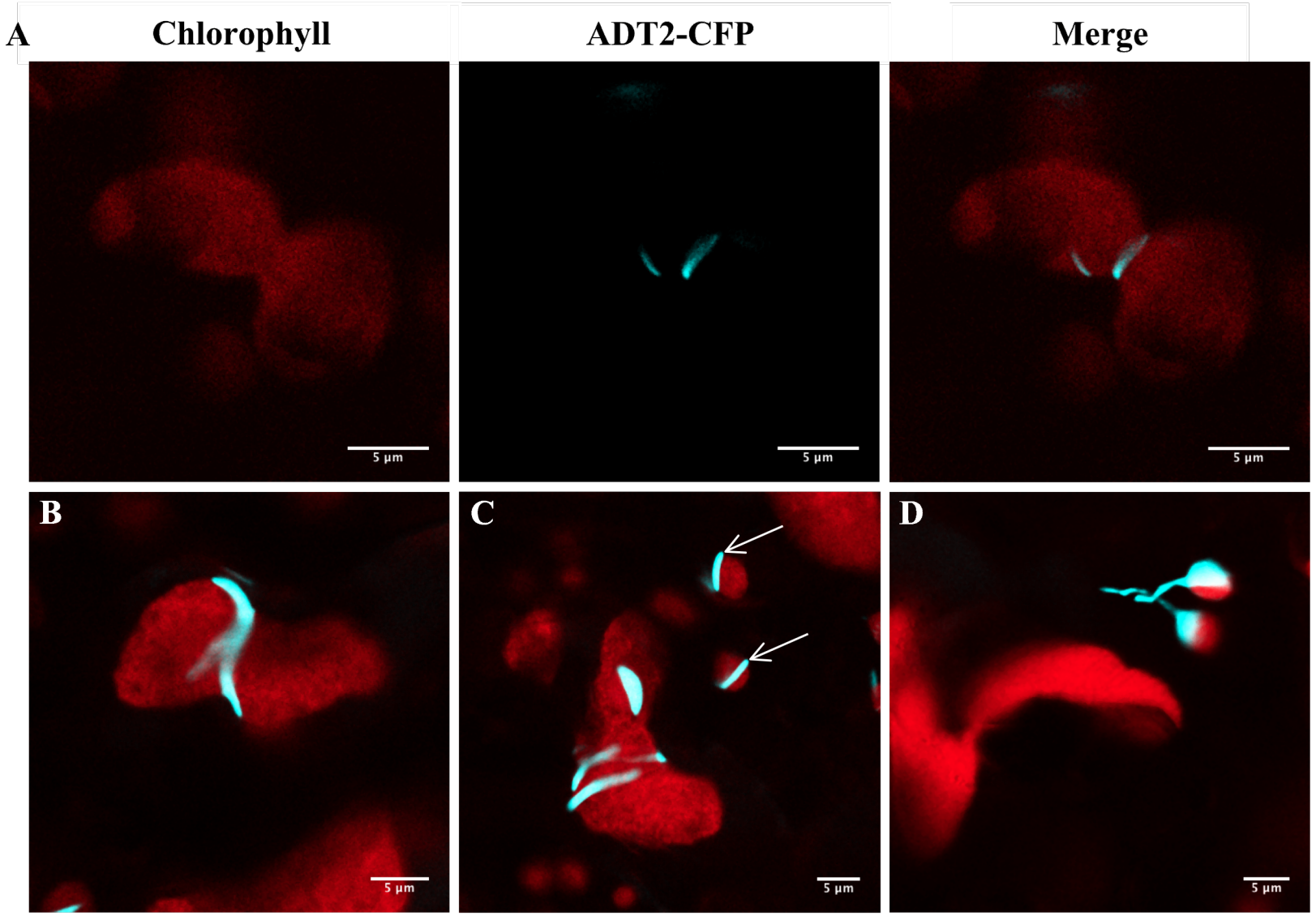
A
Chlorophyll
ADT2-CFP
Merge
5 µm
5 µm
5 µm
B
C
D
5 µm
5 µm
5 µm

Figure 21. ADT2-CFP localization in *arc6* mutants.

ADT2-CFP was transiently expressed in *arc6* mutants to determine if ADT2 localization is affected by the *arc6* mutation. Images of chlorophyll fluorescence (left) and ADT2-CFP (middle) are shown separately and merged (right).

(A) ADT2-CFP localizes to multiple short bands on *arc6* chloroplasts.

(B) ADT2-CFP is visualized as punctate structures at the periphery of the chloroplast.

(C) These punctate structures were occasionally viewed further away from the chloroplast, possibly in the cytosol.

Scale bars are 5μm **(A)** or 10 μm **(B-C)**.

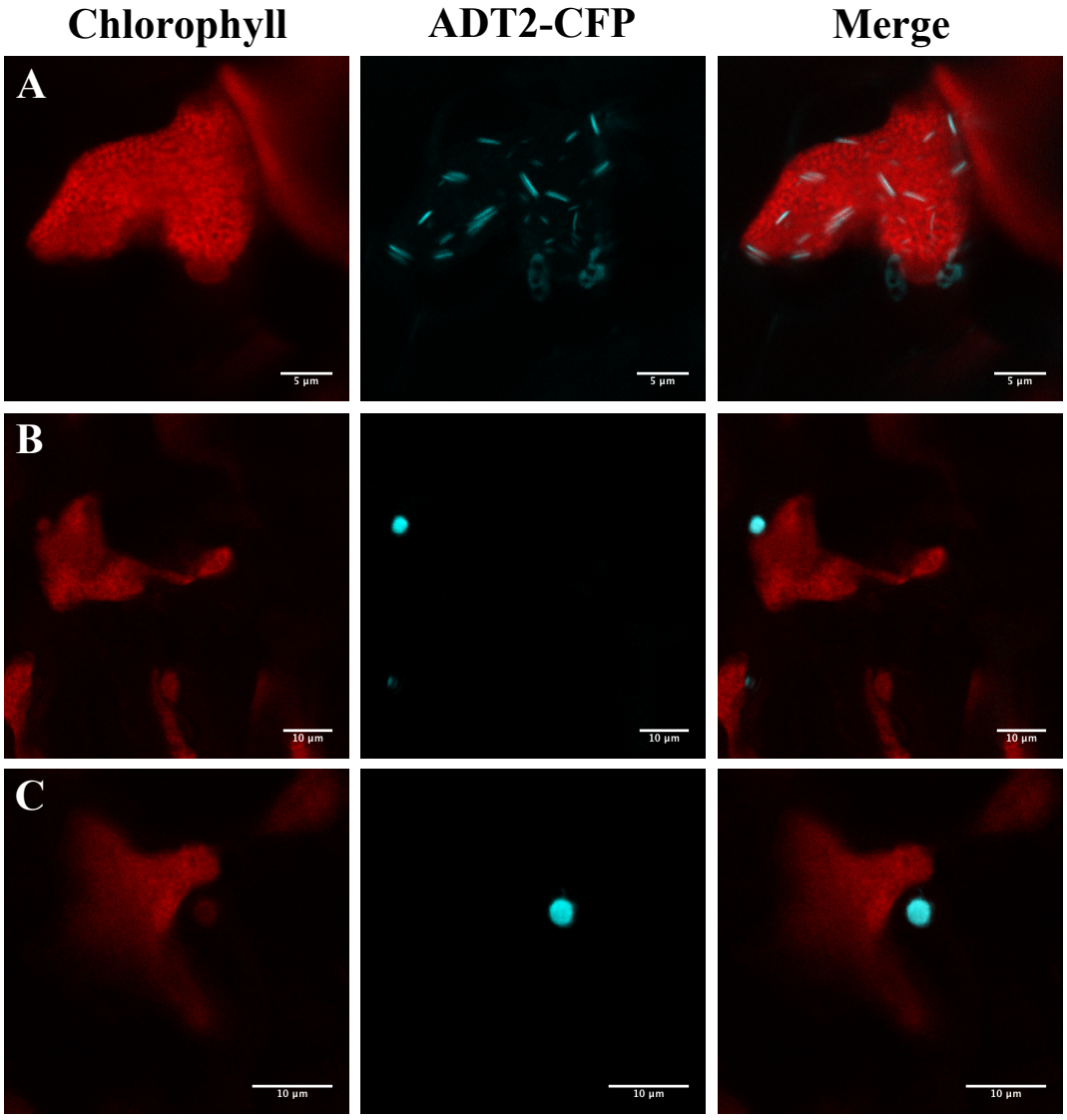
Chlorophyll
ADT2-CFP
Merge
A
B
C
5 µm
10 µm

first needed to be visualized. To allow for FtsZ visualization, *FtsZ2-1* was cloned as a *YFP* fusion construct using Gateway® technology (Fig. 22).

Gateway® technology uses enzyme mixes (BP and LR Clonase) that allow for homologous recombination between specific *attachment* (*att*) sequences (Invitrogen Corporation, 1999-2003). BP Clonase causes recombination between *att*B and *att*P sites in a BP reaction, creating *att*L sites. LR Clonase causes recombination between *att*L sites and *att*R sites, creating *att*B sites.

Plasmid pLIC6 containing *FtsZ2-1* cDNA flanked by *att*B sites (Popescu *et al.,* 2007) was propagated in *E. coli* DH10B and isolated from overnight cultures. The isolated plasmid was restriction digested with *Hind*III, cutting pLIC6 twice on either side of the *att*B flanked *FtsZ2-1* cDNA. The 2329 bp fragment containing *att*B flanked *FtsZ2-1* was excised from the gel and purified. The purified fragment was combined with the donor vector pDONR221, which encodes the *ccdB* gene (a negative selectable marker) flanked by *att*P sites. A BP reaction was performed overnight and transformed into chemically competent *E. coli* DH5α cells and transformants were selected with kanamycin. Successful transformants were identified by isolating plasmid DNA and restriction digesting it with *Ase*I. After size separation of the digestion the 2608 bp band containing *FtsZ2-1* now flanked by *att*L sites was observed, excised from the gel and purified. This purified fragment was combined with the destination vector pEarleygate101, which contains the *ccdB* gene flanked by *att*R sites. An LR reaction was performed overnight and transformed into chemically competent *E. coli* DH5α cells and transformants were selected with kanamycin. Successful transformants were identified after digestion with *Pst*I revealed the expected five band sizes (6884, 3864, 813, 547 and 345 bp; data not shown). In pEarleygate101 *FtsZ2-1* is fused to *YFP* and expression is regulated by the CaMV *35s* promoter.

Figure 22. *FtsZ2-1* cloning strategy.

FtsZ2-1 cDNA encoded in pLIC6 was used to create an *FtsZ2-YFP* fusion gene using Gateway® technology. In pLIC6 *FtsZ2-1* is flanked by *att*B sites allowing for recombination with a donor vector using Gateway® technology. The vector was digested with *Hind*III cutting pLIC6 on either side of the *att*B sites. The fragments were size separated on a gel and the 2329 bp band containing *att*B flanked *FtsZ2-1* was extracted from the gel and purified. The purified gel fragment was combined with the donor vector pDONR221 and BP Clonase was added to perform a BP reaction generating an entry vector with *FtsZ2-1* flanked by *att*L sites. The entry vector was digested with *Ase*I cutting on either side of the *att*L sites and the fragments were size separated on a gel. A 2608 bp band containing *FtsZ2-1* flanked by *att*L sites was extracted from the gel and purified. This fragment was combined with the destination vector pEarleygate101 and LR Clonase was added to perform an LR reaction. This generated an *FtsZ2-YFP* fusion construct with expression regulated in planta by the CaMV *35s* promoter.

A: *Ase*I sites; H: *Hind*III sites.

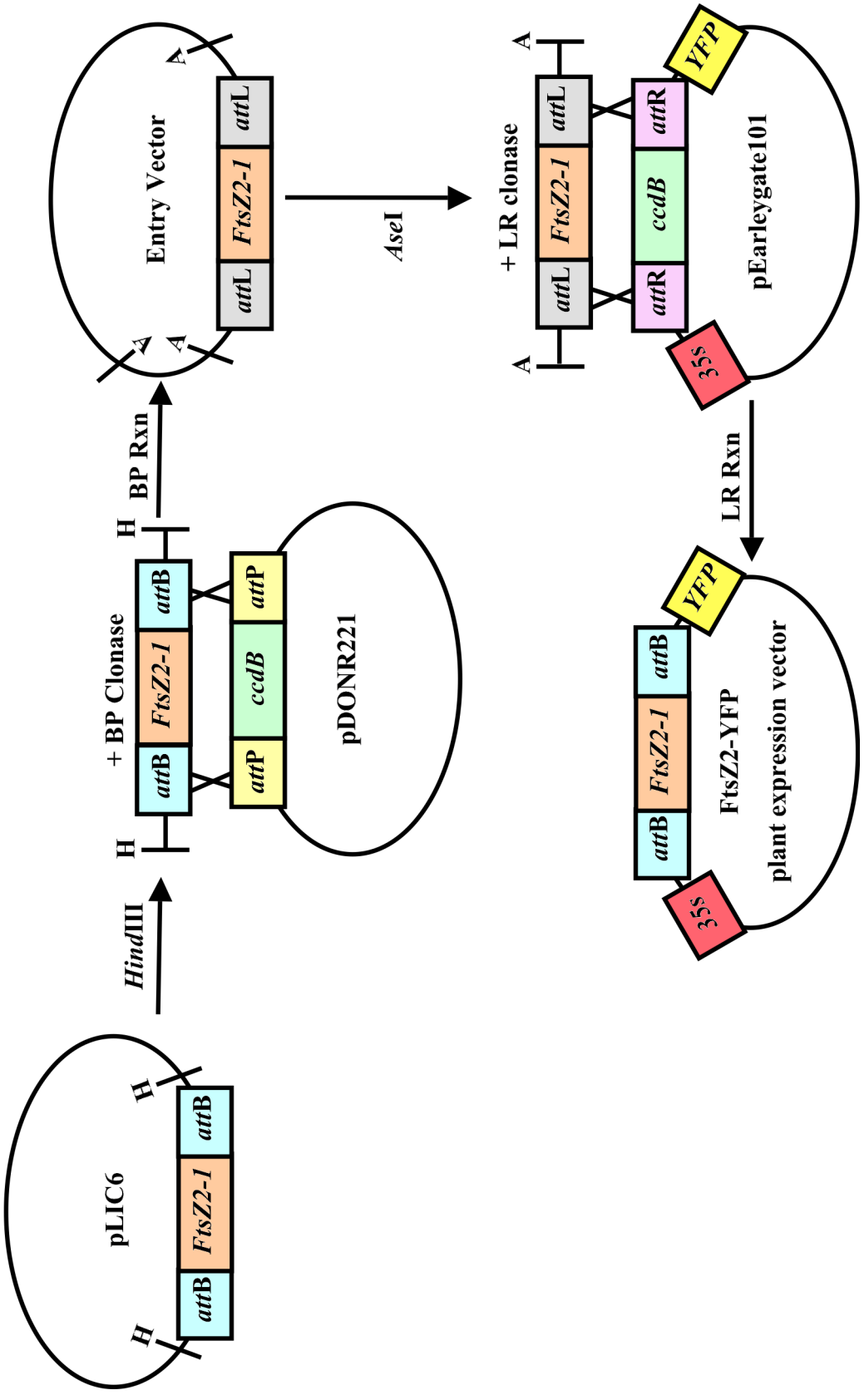
pLIC6
H
attB
FtsZ2-1
attB
H
HindIII
+ BP Clonase
H
attB
FtsZ2-1
attB
attP
ccdB
attP
pDONR221
H
BP Rxn
Entry Vector
A
A
A
attL
FtsZ2-1
attL
AseI
+ LR clonase
A
attL
FtsZ2-1
attL
A
attR
ccdB
attR
YFP
35S
pEarleygate101
LR Rxn
YFP
attB
FtsZ2-1
attB
35S
FtsZ2-YFP
plant expression vector

3.11 FtsZ2-YFP localization

Prior to expressing FtsZ2-YFP in the *adt2* mutant it must be ensured that FtsZ2-YFP localization is consistent with what has been documented in *A. thaliana* Col-0 (Vitha *et al.,* 2001), *arc3* (Glynn *et al.,* 2007), *arc5* (Vitha *et al.,* 2001) and *arc6* mutants (Vitha *et al.,* 2003). The newly generated construct was transformed into *A. tumefaciens* LBA4404 and agroinfiltrations were performed to express FtsZ2-YFP in each plant. In *A. thaliana* Col-0, FtsZ2-YFP localized as expected at the equatorial plane of chloroplasts (Fig 23A). In *arc3* plants FtsZ2-YFP localized to multiple bands across chloroplasts (Fig 23B). In *arc5* mutants FtsZ2-YFP localized to bands centered at areas of chloroplasts appearing centrally constricted (Fig 23C). Finally, in *arc6* plants FtsZ2-YFP localized to short bands appearing scattered within the chloroplasts (Fig. 23D). Therefore, FtsZ2-YFP localization was as expected in each plant. However, FtsZ2-YFP also localized to punctate structures on some chloroplasts in all plants in which it was expressed (data not shown).

To determine if FtsZ localization is affected by the *adt2* mutation FtsZ2-YFP was transiently expressed in the rosette leaves of *adt2* plants. Compared to wild-type *A. thaliana* Col-0 (Fig. 23A) FtsZ2-YFP localization was clearly different in *adt2* chloroplasts (Fig. 24A-B). Mostly, FtsZ2-YFP was found to form long curving filaments in *adt2* chloroplasts. These could either be multiple bands of FtsZ2-YFP or longer spiraling filaments that twist and loop in the stroma (Fig. 24A-B). Therefore, the location of a known chloroplast division protein is affected by the *adt2* mutation.

Figure 23. Testing FtsZ2-YFP localization.

FtsZ2-YFP was transiently expressed in *A. thaliana* Col-0 **(A)**, *arc3* **(B)**, *arc5* **(C)**, and *arc6* mutants **(D)**. All images show a merge of chlorophyll fluorescence and FtsZ2-YFP.

(A) FtsZ2-YFP localizes to a band at the equatorial plane of *A. thaliana* Col-0 chloroplasts.

(B) FtsZ2-YFP localizes to multiple bands in *arc3* chloroplasts.

(C) FtsZ2-YFP localizes to bands at the central constriction (arrow) of *arc5* chloroplasts.

(D) FtsZ2-YFP localizes to short bands consistent with the appearance of filaments in *arc6* chloroplasts.

Scale bars are 5 μm.

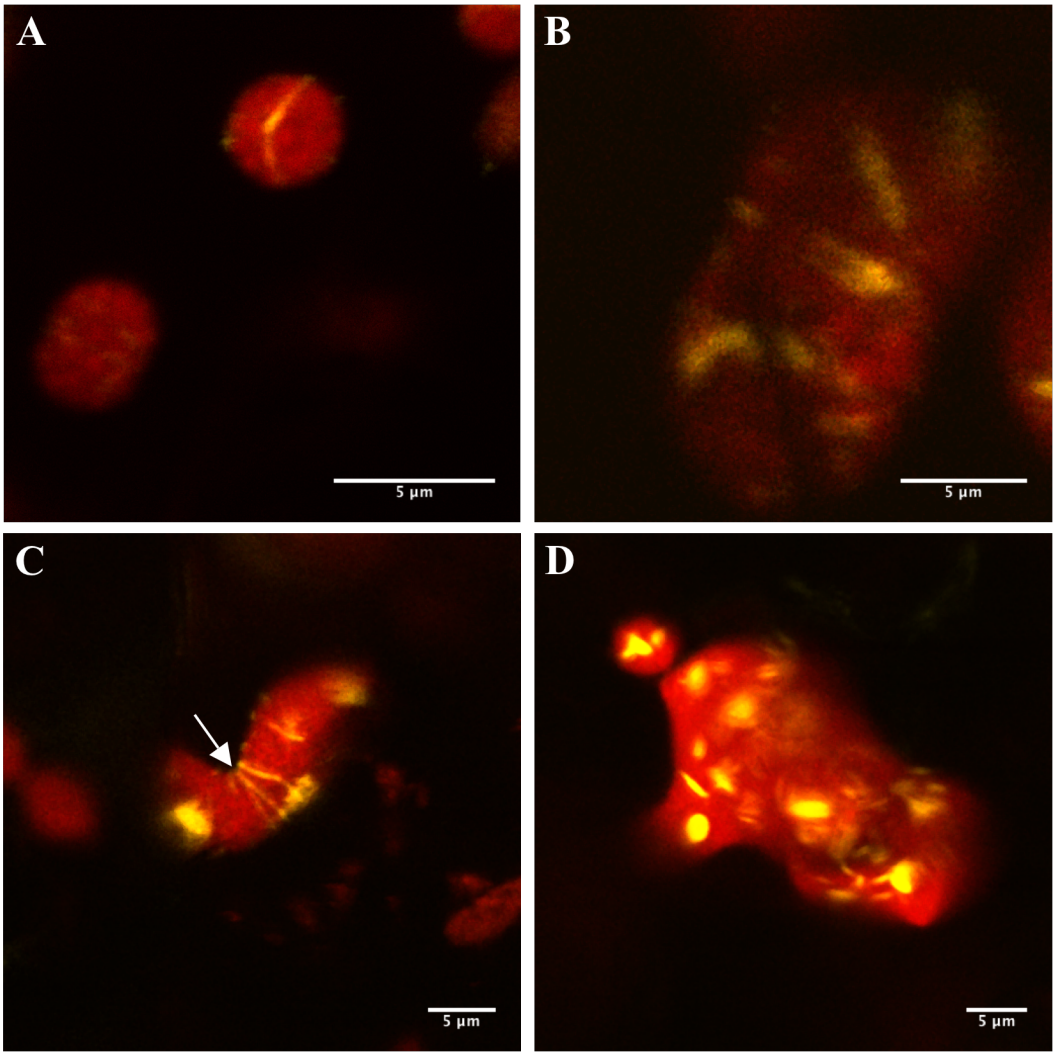
A
5 µm
B
5 µm
C
5 µm
D
5 µm

Figure 24. FtsZ2-YFP localization in *adt2* mutants.

FtsZ2-YFP was transiently expressed in *adt2* mutants to determine if its localization is altered. Images of chlorophyll fluorescence (left) FtsZ2-YFP (middle) are shown separately and merged (right).

(A) FtsZ2-YFP localizes to long, curving filaments within *adt2* mutant chloroplasts.

(B) FtsZ2-YFP appears to localize to several bands that may be long, spiraling filaments.

Scale bars are 5 μm.

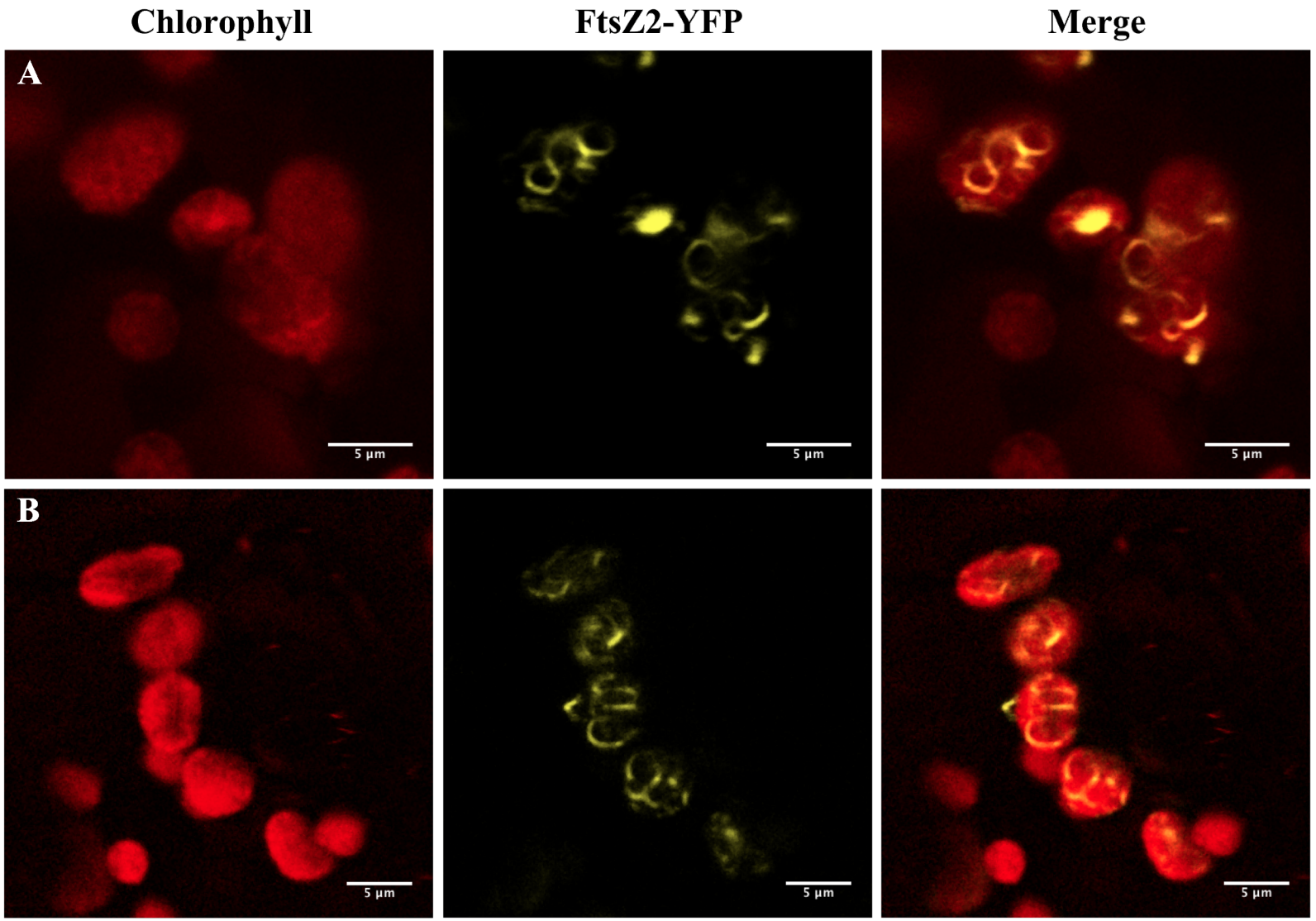
Chlorophyll
FtsZ2-YFP
Merge
A
B
5 µm
5 µm
5 µm
5 µm
5 µm
5 µm

4 Discussion

This study examined the *in planta* subcellular localization of ADTs through *Agrobacterium*-mediated transient transformation of *N. benthamiana* and *A. thaliana*. By co-localizing all six ADT-CFPs with a fluorescently tagged stromal protein it was found that most ADTs localize to stromules. The novel localization patterns of ADT5 and ADT2 were the focus of much of the remainder of this study. ADT5-CFP was co-expressed with NUP1-YFP confirming that it localizes to the nucleus. In addition, indirect evidence was provided for a stromule-mediated method of transportation of ADT5-CFP to the nucleus. Finally, the localization patterns of ADT2-CFP were found to be highly suggestive of a role in chloroplast division in all plants studied, while an *adt2* mutant has altered chloroplast morphology and FtsZ localization patterns.

4.1 ADTs localize to stromules

To determine if ADTs predominantly localize to stromules all *ADT-CFP* fusion genes were co-expressed with a fluorescent stromal marker (*TP-YFP*) in *N. benthamiana*. With the exception of ADT6-CFP (Fig. 8F), all ADT-CFPs were co-localized with TP-YFP confirming that they are localizing to stromules as opposed to aggregating outside of chloroplasts (Fig. 8A-E). In theory, any stromal protein could be present in stromules but ADTs are unique because they often appear to accumulate in them rather than in the main body of the chloroplast. While the function of stromules remains the subject of debate, it is speculated that the increase in surface area associated with stromules can increase transport of materials, including metabolites, to other areas of the cell (Natesan *et al*., 2005). Keeping this proposed function in mind, the localization of ADTs to stromules is consistent with their enzymatic function. If phenylalanine is synthesized in stromules and accumulates in them, it can be easily envisioned to be an efficient way of mediating phenylalanine transport to other areas of the cell. In the cytosol, phenylalanine is not only required for protein synthesis, but also as a precursor to the biosynthesis of phenylpropanoids such as flavonoids and lignin (Liu, 2012; Samanta *et al.,* 2011). Interestingly, abiotic stressors such as drought and salt stress known to induce stromules

(Gray *et al.,* 2012) are also associated with increased flavonoid levels in the leaves of plants (Agati *et al.,* 2011; Mewis *et al.,* 2012). This increase in flavonoids is supported at the transcriptional level as studies in rice found that enzymes in the flavonoid biosynthetic pathway are upregulated in response to salinity-induced stress (Walia *et al.,* 2005). Of particular interest to this study is an upregulation of *PHENYLALANINE AMMONIA LYASE1 (PAL1*) (Walia *et al.,* 2005). PAL1 uses phenylalanine as a substrate to catalyze the first step of phenylpropanoid biosynthesis in the cytosol (Fraser and Chapple, 2011). This suggests there is an increased demand for cytosolic phenylalaine under the same conditions known to induce stromules. Therefore, the induction of stromules in response to abiotic stress could create an increased supply of phenylalanine to be incorporated into downstream cytosolic pathways.

4.2 ADT6 is cytosolic

The only ADT-CFP fusion protein that does not localize to stromules is ADT6-CFP (Fig. 8F). The cytosolic localization of ADT6 is in contrast with previous studies detecting ADT activity solely in chloroplasts of *N. silvestris* and spinach (Jung *et al.,* 1986). While phenylalanine biosynthesis has only been characterized in the chloroplasts of higher plants, there are other enzymes that have cytosolic isoforms (Maeda and Dudareva, 2012). For example, an enzyme in the shikimate pathway, 3-hydroxy-D-arabino-heptulosonate 7-phosphate synthase (Ganson *et al.,* 1986), and chorismate mutase 2 (CM2) (Eberhard *et al.,* 1996), the last common enzyme required for the synthesis of all aromatic amino acids (Maeda and Dudareva, 2012). In the chloroplast, prephenate, which is synthesized by CM, is transaminated by PAT (Bonner and Jensen, 1985) to produce arogenate used by ADTs to synthesize phenylalanine (Cho *et al.,* 2007). While the only PAT identified in *A. thaliana* localizes to the chloroplast (Maeda *et al.,* 2011), aminotransferases often have broad substrate specificities (Maeda *et al.,* 2011; Wightman and Forest, 1978) and the presence of a cytosolic aminotransferase capable of connecting the activity of CM2 to ADT6 cannot be ruled out. While a cytosolic pathway for phenylalanine biosynthesis remains uncharacterized, the presence of one seems advantageous given the need for phenylalanine in the cytosol.

4.3 ADT5 localizes to the nucleus

To confirm that ADT5 localizes to the nucleus ADT5-CFP and NUP1-YFP were co-expressed in *N. benthamiana* and it was clearly shown that ADT5-CFP is surrounded by the nuclear membrane (Fig. 10C). Given that ADT5 also localizes to chloroplasts, this result indicates that ADT5 localizes to two different subcellular compartments. There are several proteins that localize to both plastids and nuclei (Krause *et al.,* 2012). This includes other enzymes such as phosphate-isopentyltransferase 3, an enzyme involved in cytokinin biosynthesis (Galichet *et al.,* 2008; Krause *et al.,* 2012), although like ADT5 its nuclear role is unknown (Krause *et al.,* 2012).

Chloroplasts are able to communicate with the nucleus through retrograde signaling, a process believed to occur by the release of chemical signals from the chloroplast that result in changes in nuclear gene expression (Inaba *et al.,* 2011). While retrograde signaling traditionally refers to chemical messengers, it is becoming apparent that proteins within the chloroplast can act as retrograde signals as well (Isemer *et al.,* 2012; Krause *et al.,* 2012). One such protein is WHIRLY1 from *A. thaliana*, which can move directly from plastids to the nucleus (Isemer *et al.,* 2012). In plastids, WHIRLY1 contributes to plastid genome stability by preventing illegitimate recombination (Maréchal *et al.,* 2009). In the nucleus it acts as a transcriptional activator of pathogen-response genes (Isemer *et al.,* 2012), consistent with the increased pathogen susceptibility associated with decreased WHIRLY1 DNA binding ability (Desveaux *et al.,* 2005).

The mechanism through which proteins such as WHIRLY1 are able to move from the plastid to the nucleus is not known, however, stromules are a hypothetical mode of transport (Krause *et al.,* 2012). Stromules can closely associate with nuclei and have even been observed extending into grooves of the nuclear membrane (Kwok and Hanson, 2004b). In the case of ADT5, chloroplasts with stromules containing ADT5-CFP often appeared to connect directly with the nucleus (Fig. 11). Expression of dominant negative forms of myosin XI found to inhibit stromules (Fig. 13A-B) also significantly reduced ADT5-CFP localization to the nucleus (Fig. 14), providing indirect evidence of stromule-mediated nuclear transport. As a note of caution, this result could be due to suppression

of other processes requiring myosin XI. Dominant negative inhibition of myosin XI-K reduces the movement of many organelles, including golgi stacks, peroxisomes and mitochondria (Avisar *et al.,* 2008), while in this study only stromules were examined. Myosin associated movement along actin filaments is also needed for cytoplasmic streaming (Shimmen and Yokota, 2004). If the movement of proteins in the cytoplasm was inhibited, it could be argued that this would prevent nuclear transport by other means. Regardless, the appearance of stromules directly connecting to nuclei expressing ADT5-CFP (Fig. 11) makes a stromule-mediated nuclear transport system intriguing. Although alternate, more direct approaches to study this should be used.

Currently, it is unknown what role ADT5 plays in the nucleus, but as an enzyme involved in a biosynthetic pathway it is conceivable that it acts as a transcriptional regulator of upstream or downstream genes, or of other *ADT*s. There is precedence for an enzyme to act as a transcriptional regulator of related genes. *A. thaliana* HEXOKINASE1 is involved in glucose metabolism in mitochondria, but also localizes to the nucleus where it forms part of a protein complex affecting transcription of genes involved in glucose signaling (Cho *et al.,* 2006). While it is unknown if ADT5 acts as a transcriptional regulator of genes, evidence suggests that ADT5 activity cannot be compensated for by other ADTs (Corea *et al*., 2012). Of all available T-DNA insertion knockout lines for *ADT*s, the *adt5* knockout is the only one with an obvious phenotype (Corea *et al.,* 2012). In *adt5* plants, stems lack the structural rigidity to stand erect and instead fall over, a phenotype associated with altered lignin composition (Corea *et al.,* 2012). At this point it is purely speculation if the nuclear role of ADT5 is to regulate genes in lignin biosynthesis, but ADT5's role in the nucleus should be the subject of future research.

4.4 ADT localization is identical in *A. thaliana*

Prior to this study the *in planta* localization of *A. thaliana* ADTs had only been examined in *N. benthamiana* (Bross, 2011). Transient transformation using agroinfiltration is widely used in *N. benthamiana* but has traditionally been difficult in *A. thaliana* (Wroblewski *et al.,* 2005). In this current study, reliable transformation of

A. thaliana was achieved by infiltrating 3 to 4 week old plants gently with small volumes of *A. tumefaciens*. In addition, plants were grown from seed in soil watered with 20 mM L-ascorbic acid, which seemed to decrease necrosis of leaves associated with agroinfiltration. As it was not the focus of this study, the reason for this was not addressed. However, because L-ascorbic acid can scavenge damaging reactive oxygen species (Gallie, 2013), the increased tolerance of *A. thaliana* to agroinfiltration may be due to a decrease in oxidative stress. As in *N. benthamiana*, all six ADT-CFPs in *A. thaliana* localized to stromule-like structures (Fig. 9A-E), with the exception of ADT6-CFP which appeared in the cytosol (Fig 9F). Similarly, the unique localization patterns of ADT2-CFP and ADT5-CFP are present in *A. thaliana*, localizing to bands and poles of chloroplasts (Fig. 16), and to nuclei (Fig. 10B), respectively. This was an important finding given that *A. thaliana* is the host plant of these proteins, and proves that the findings in *N. benthamiana* are not artifacts. However, it also supports *N. benthamiana* as a good model organism for determining the subcellular localization of *A. thaliana* proteins. It also demonstrates that agroinfiltration can be performed effectively in *A. thaliana*, which is significant given its wide use in plant biology and the availability of characterized mutant lines.

4.5 ADT2 localization is consistent with chloroplast division

Early observations of ADT2 subcellular localization determined that ADT2-CFP localized to a band at the equatorial plane or towards a pole of a chloroplast (Bross, 2011). The similarity of these patterns to those of chloroplast division proteins (Glynn *et al.,* 2007) led to an investigation into a possible secondary non-enzymatic role of ADT2 in chloroplast division. Initial evidence in support of this proposed function came from ADT2-CFP localization in dividing chloroplasts as indicated by an elongated and constricted appearance (Fig. 15B-C). ADT2-CFP was visualized as a band at the equatorial plane of chloroplasts both with and without areas of constriction and elongation (Fig. 15A-C), consistent with ADT2 localizing to the division plane early in the division process, similar to FtsZ and ARC6 (Vitha *et al.,* 2001; 2003). ADT2-CFP is also observed at one pole of chloroplasts (Fig. 15D). In general, chloroplast division

proteins localize to the poles of chloroplasts as a consequence of the protein's function or as a remnant of the division ring. For example, ARC3 is active towards the poles of chloroplasts and prevents Z-ring assembly there (TerBush *et al.,* 2013). On the other hand proteins including PARC6, PDV1, PDV2 and ARC5 have also been found at the poles of chloroplasts (Glynn *et al.,* 2009; Miyagishima *et al.,* 2006). As these proteins are present at the division plane during constriction their polar localization is thought to represent remnants of protein left on daughter chloroplasts post-division (Miyagishima, 2011). As ADT2-CFP is present at the division plane of highly constricted chloroplasts (Fig. 15C), ADT2-CFP localization at the poles is expected to be a post-division remnant. Given that chloroplast division is regulated by size (Pyke, 1999), chloroplasts with ADT2-CFP at a pole should be smaller than average chloroplasts if they are newly divided chloroplasts. Similarly, chloroplasts with ADT2-CFP observed as a band should be larger in size than average chloroplasts if they represent dividing chloroplasts. Compared to the average length of chloroplasts in uninfiltrated plants those with ADT2-CFP at a pole and as an equatorial band were smaller and larger, respectively (Table 1). Chloroplasts with ADT2-CFP at a pole also had a lower standard deviation (Table 1) than the other two groups, indicating that they are close in size to one another, as would be expected for newly divided chloroplasts. The standard deviation for chloroplasts with ADT2 as a band was higher than the polar chloroplasts but lower than those from uninfiltrated plants (Table 1), which makes sense because dividing chloroplasts would be at different stages of division. These results are highly suggestive of a role in chloroplast division in which ADT2 localizes to the division plane early and remains there throughout the constriction stages and thus remains on the poles of newly divided chloroplasts.

4.6 Chloroplast morphology is abnormal in *adt2* mutants

As ADT2 localization suggests a role in chloroplast division, a second independent confirmation of this role was needed. As seen in the *arc* mutants (Pyke and Leech, 1992; 1994; Pyke *et al.,* 1994), mutations in genes required for chloroplast division affect the appearance of chloroplasts. Therefore, chloroplasts in an *adt2* mutant (Huang *et al.,* 2010) were examined.

Chloroplast morphology was altered in these mutants, and chloroplasts with a wide range of shapes and sizes were found (Fig. 17B-F). This finding establishes a more direct connection between chloroplast division and ADT2 function. The phenotype of chloroplasts in division mutants often yields clues into a protein's function during this process. Chloroplasts in the *adt2* mutant were heterogeneous in size and shape, ranging from enlarged and misshapen to wild-type in size and shape. Heterogeneous populations of chloroplasts can result from mutations in genes required for correct Z-ring placement, such as *ARC3* (Pyke and Leech 1992; Shimada *et al.,* 2004; Zhang *et al.,* 2013) suggesting that ADT2 may be involved in Z-ring positioning.

The mutation responsible for these unusual chloroplasts is a point mutation that only causes a single amino acid substitution (Huang *et al.,* 2010). Compared to the *arc* mutants, which are caused by nonsense mutations (Gao *et al.,* 2003; Shimada *et al.,* 2004; Vitha *et al.,* 2003), this seems to be a subtle change. Therefore, ADT2 function is probably not abolished by this mutation but altered or reduced. This could explain why normally sized chloroplasts are relatively prevalent.

The location of the mutation in the C-terminal ACT domain (Huang *et al.,* 2010) suggests that this region may be, at least in part, required for the chloroplast division function of ADT2. It has been shown that this mutation decreases the enzyme's ability to respond to the allosteric inhibition by phenylalanine (Huang *et al.,* 2010). In bacterial PDTs the allosteric binding of phenylalanine results in a conformational change to the enzyme, changing it from an active open state to an inactive closed state (Tan *et al.,* 2008). Such a conformational change has not been studied for ADTs, although, given the amino acid sequence similarity between ADTs and PDTs (Cho *et al.,* 2007), a similar conformational change is likely in ADTs as well. While entirely hypothetical, this conformational change could be important for the chloroplast division function of ADT2. Alternatively, it could be that the single amino acid substitution changes the tertiary structure of the enzyme to such an extent that it decreases its ability to function in chloroplast division. While the abnormal chloroplast morphology in the *adt2* mutant confirms that ADT2 has a role during chloroplast division, it is interesting that ADT2 is

the only ADT for which T-DNA knockout lines do not exist (Corea *et al.,* 2012) raising the possibility that an ADT2 knockout is lethal.

4.7 ADT2 localization in *arc* mutants

The *arc3*, *arc5* and *arc6* mutants of *A. thaliana* are affected in different stages of chloroplast division and FtsZ localization is known for each (Glynn *et al.,* 2007; Vitha *et al.,* 2001; 2003). ADT2-CFP was expressed in each mutant to determine if its localization was affected by the mutations and gain insight into its position in the division process relative to FtsZ.

In *arc3* mutants, ADT2-CFP is predominantly found as multiple bands along chloroplasts (Fig. 19A-C), consistent with FtsZ localization in *arc3* plants (Glynn *et al.,* 2007). *In planta* ARC3 is a regulator of Z-ring placement, restricting the Z-ring to the equatorial plane by inhibiting FtsZ polymerization in other areas of the chloroplast (Zhang *et al.,* 2013). As ARC3 can interact with both FtsZ1 (Maple *et al.,* 2007) and FtsZ2 it likely accomplishes this through a direct interaction (Zhang *et al.,* 2013). Because ADT2 has a similar localization pattern to FtsZ in *arc3* plants it indicates that ARC3 positions ADT2 in a similar manner to FtsZ. It is unknown how ARC3 affects ADT2 localization, though several possibilities are imaginable (Fig. 25A-C). One possibility is that ADT2 directly interacts with FtsZ, so misplacement of FtsZ will cause ADT2 to be misplaced as well (Fig. 25A). It is also possible that ARC3 interacts with ADT2 and FtsZ to position each protein independent from one another (Fig. 25B). Alternatively, ADT2 and ARC3 could both interact with FtsZ for correct Z-ring placement (Fig. 25C) and ADT2 is misplaced in *arc3* mutants because the action of ADT2 alone is not sufficient for correct FtsZ positioning.

In *arc6* mutants ADT2- CFP localizes to short rod-shaped bands in the stroma (Fig. 21A) resembling previously established FtsZ localization patterns (Vitha *et al.,* 2003). These results indicate that ARC6, like ARC3, is required for the correct

Figure 25. Hypothetical models for ADT2 in chloroplast division.

The models shown are hypothetical ways that ARC3 **(A-C)** and ARC6 **(D-F)** affect ADT2 localization.

(A) ARC3 positions FtsZ and ADT2 localizes with FtsZ due to an interaction.

(B) ARC3 interacts with ADT2 and FtsZ to position each protein independently.

(C) ARC3 and ADT2 act together to position FtsZ.

(D) ARC6 anchors FtsZ, ADT2 localizes with FtsZ due to an interaction.

(E) ARC6 anchors FtsZ and ADT2 individually.

(F) ADT2 and ARC6 act together to anchor FtsZ.

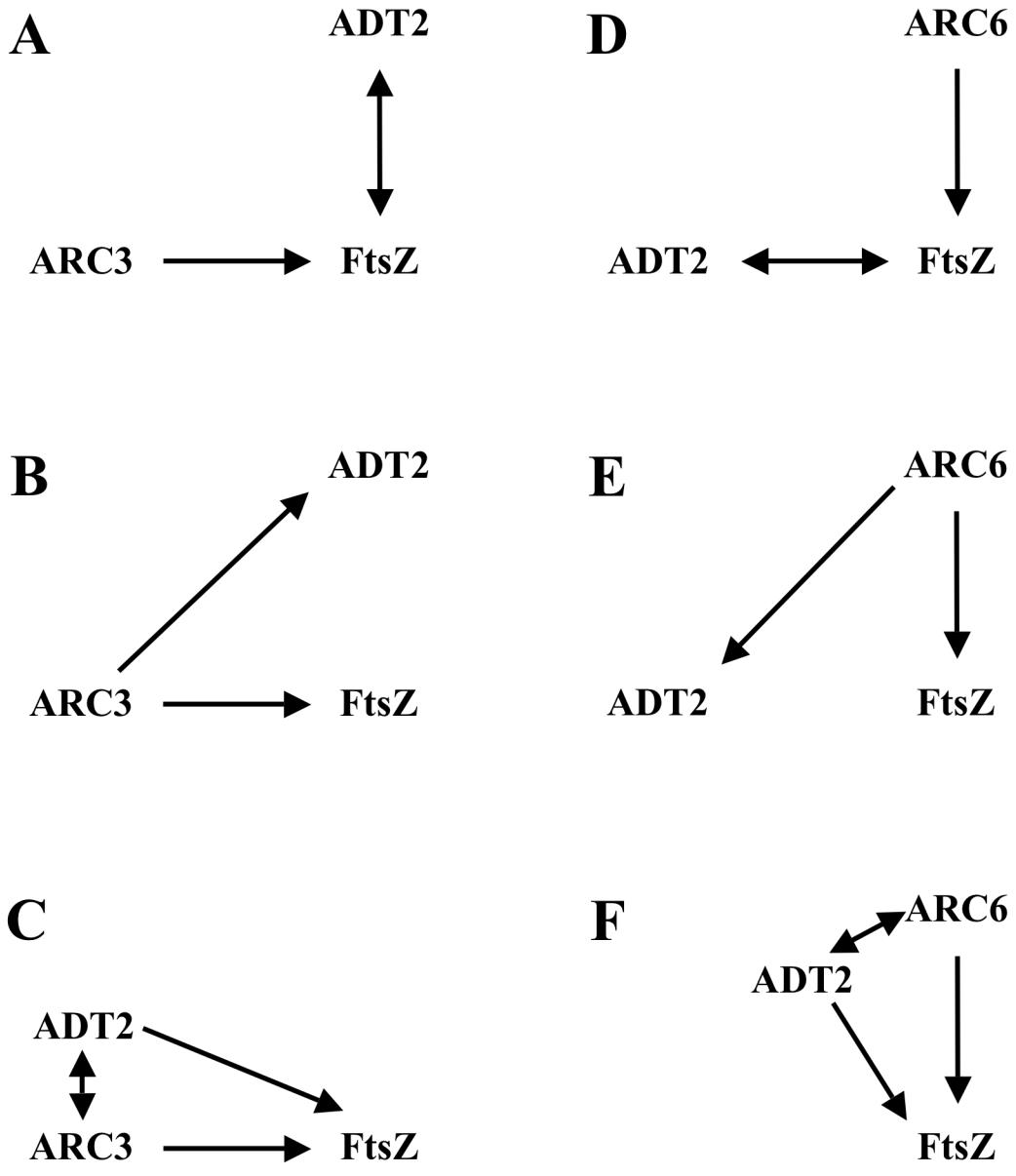
A
ADT2
ARC3
FtsZ
D
ARC6
ADT2
FtsZ
B
ADT2
ARC3
FtsZ
E
ARC6
ADT2
FtsZ
C
ADT2
ARC3
FtsZ
F
ARC6
ADT2
FtsZ

positioning of both FtsZ and ADT2. ARC6 is involved early in chloroplast division and anchors FtsZ filaments in the Z-ring (Vitha *et al.,* 2003). It is unknown how ARC6 regulates ADT2 localization, however, as was the case for ARC3, several possibilities exist (Fig. 25D-F). If ADT2 directly interacts with FtsZ, ARC6 may affect its localization indirectly (Fig. 25D). Alternatively, ARC6 could interact with ADT2 and regulate its positioning independently from FtsZ (Fig. 25E). Another possibility is that ADT2 interacts with ARC6 to anchor FtsZ (Fig. 25F) and neither protein on its own is sufficient for correct FtsZ placement. In *arc6* mutants ADT2 was also frequently observed as round puncta near the periphery of chloroplasts (Fig. 21B), and occasionally away from chloroplasts (Fig. 21C). It is not known if these patterns have functional significance or if they are artifacts of ADT2-CFP over-expression.

ARC5 provides the force needed to constrict chloroplasts during division (Gao *et al.,* 2003; Yoshida *et al.,* 2006), and in *arc5* mutants chloroplasts are enlarged and often centrally constricted (Pyke and Leech, 1994). ARC5 is recruited to the cytosolic face of the outer membrane after Z-ring placement (Gao *et al.,* 2003) acting downstream of ARC6 and ARC3. Z-ring positioning in *arc5* mutants is unaffected as FtsZ localizes to the equatorial plane (Vitha *et al.,* 2001). Consistent with FtsZ localization ADT2-CFP also localizes to the central constriction (Fig. 20A-C) indicating that ADT2 resides at the division plane in later stages of division in agreement with ADT2-CFP localization in highly constricted chloroplasts in *N. benthamiana* (Fig. 15C). The appearance of ADT2 bands around the central constrictions was variable and on occasion multiple bands were able to form (Fig. 20C) While ARC5 does not affect Z-ring placement the large size of *arc5* chloroplasts could allow multiple Z-rings to form near the constriction if ARC3 levels are sufficiently low. Alternatively, one cannot exclude the possibility that multiple bands result from over-expression of ADT2-CFP. In addition to being at the central constriction of *arc5* chloroplasts, ADT2-CFP occasionally localized to long, convoluted stromule-like structures (Fig. 20D). While all three of these *arc* mutants are known to have an increased frequency of stromules in certain tissues (Holzinger *et al.,* 2008), *arc5* was the only *arc* mutant where a stromule pattern was seen. While the reason for this is

not known, it was infrequently observed in *arc5* mutants, and thus it may only be due to chance that it was not observed in the *arc3* and *arc6* mutants. The infrequent observation of ADT2-CFP in stromules of *arc* mutant chloroplasts could be due to inefficient chloroplast division, and hence division proteins remain at the site of constriction for a longer period of time preventing ADT2 from accumulating in stromules.

4.8 The relationship between FtsZ and ADT2

ADT2 localization in *arc3*, *arc5*, and *arc6* mutant plants suggests a close relationship between FtsZ and ADT2. To examine this *FtsZ2-1* was cloned as a *YFP* fusion gene, to determine if a known chloroplast division protein is affected by the *adt2* mutation. Prior to expression in the *adt2* mutant it was expressed first in wild-type *A. thaliana* Col-0, *arc3*, *arc5* and *arc6* mutants to ensure that FtsZ2-YFP localization is consistent with previous studies (Glynn *et al.,* 2007; Vitha *et al.,* 2001; 2003). In each case FtsZ2-YFP localized to the expected areas of chloroplasts (Fig. 23A-D). In *arc5* mutants multiple bands of FtsZ2-YFP were seen at the central constriction (Fig. 23C), as was observed with over-expression of ADT2-CFP in *arc5* mutants (Fig. 20C). In all plants, FtsZ2-YFP was also found in punctate structures (data not shown) that could be artifacts of over-expression, although FtsZ puncta have been previously observed (Johnson *et al.,* 2013).

The localization of FtsZ2-YFP in the *adt2* mutant (Fig. 24A-B) was found to differ substantially from wild-type *A. thaliana*. FtsZ2-YFP formed long curving filaments in the stroma of *adt2* chloroplasts (Fig. 24A-B). In some chloroplasts FtsZ2-YFP appeared to assemble into multiple rings (Fig. 24B), although due to the length and curvature of FtsZ2-YFP filaments observed these might represent filaments spiraling inside the chloroplast. Interestingly, long spiraling filaments of FtsZ are also seen in plants over-expressing ARC6 (Vitha *et al.,* 2003), although a link between ADT2 and ARC6 has not been established and will require further study. The abnormal localization of FtsZ2-YFP in the *adt2* mutant suggests that ADT2 is required for proper Z-ring placement. This is consistent with the heterogeneous populations of chloroplasts

observed in the *adt2* mutant, because mutations in genes needed for proper Z-ring placement such as ARC3 (Zhang *et al.,* 2013) also result in heterogeneously sized chloroplasts (Pyke and Leech, 1992).

The *adt2* mutant is the only plant line in this study where the localization of ADT2-CFP (Fig. 18A-F) did not reflect that of FtsZ2-YFP (Fig. 24A-B). ADT2-CFP was never observed in long filaments, instead its pattern was variable. Although it was not clear if ADT2-CFP over-expression is able to rescue the phenotype, several images were obtained where ADT2-CFP was found at the division plane of constricted *adt2* chloroplasts (Fig. 18A-C). The appearance of the ADT2-CFP band along the constriction, as well as the appearance of the constricted chloroplasts themselves were often unusual. Constricted chloroplasts appeared to divide asymmetrically and bands of ADT2-CFP often appeared to fray along their length (Fig. 18A-B) or were not centered at the constriction (Fig. 18C). While not quantifiable, these constricted chloroplasts were seen more often when ADT2-CFP was being expressed. One could argue that if the mutant adt2 protein retains some of its chloroplast division function it may be interacting with a known chloroplast division protein, blocking ADT2-CFP from rescuing the phenotype.

4.9 Summary and future directions

The localization of ADTs to stromules is intriguing given their enzymatic function and proposed functions of stromules in increasing metabolite transport (Natesan *et al*., 2005). Further research into a link between stromules and metabolite transport will need to be performed before the significance of ADT stromule localization can be established. As *ADT-CFP* fusion genes were overexpressed using the CaMV *35s* promoter, future studies should look at the localization patterns using native ADT promoters to ensure these results are not artifacts of overexpression. The creation of stably transformed plant lines would also be beneficial, as it would extend our observation of ADTs from leaves to other tissues. Alternatively, antibodies could be developed against each ADT to directly detect their localization without using a fusion protein.

In this study ADT5 was confirmed to localize to the nucleus in addition to chloroplasts. Although the nuclear role of ADT5 remains unknown, as a component of a biosynthetic pathway it could act as a transcriptional regulator of genes in the shikimate pathway or phenylpropanoid pathway. If ADT5 is a transcription factor it should be able to recognize specific DNA sequences. It would be worthwhile to determine if ADT5 can bind DNA through chromatin immunoprecipitation, and if it can the sequences it binds to should be determined. Comparative transcriptional profiling between *adt5* knockout plants and wild-type *A. thaliana* could also be informative. It would be interesting to determine if there are changes in transcript levels in the absence of ADT5. Genes involved in lignin biosynthesis would be particularly interesting given the altered lignin content in *adt5* plants (Corea *et al.,* 2012).

Through stromule inhibition indirect evidence of stromule-mediated transport of ADT5 to the nucleus was provided in this study. Future studies will be needed to provide more direct and conclusive evidence. Transport of fluorescently labeled proteins between plastids connected by stromules was demonstrated using a fluorescence recovery after photo-bleaching (FRAP) approach (Köhler *et al.,* 1997; Kwok and Hanson 2004a). By photo-bleaching one plastid fluorescence was shown to recover at the expense of the other plastid, indicating that fluorescently labeled protein could move from one plastid to another. A similar FRAP based study could be performed with ADT5 by photo-bleaching a nucleus and determining if fluorescence could recover at the expense of stromule-connected chloroplasts. Alternatively, the development of photo-convertible fusion proteins such as EosFP (Wiedenmann *et al.,* 2004) could be used. EosFP normally fluoresces green light but after excitation with ultraviolet light this changes to red light in a process known as photo-conversion. If *ADT5* is cloned as an *EosFP* fusion gene, photo-conversion could be used to specifically photo-convert a stromule connected to the nucleus, and then it can be observed if the change in fluorescent colour emitted by EosFP travels to the nucleus.

This study provides strong evidence for an involvement of ADT2 in chloroplast division. The similarities between ADT2 localization and that of FtsZ suggest that these

proteins are tightly linked. To further investigate this, ADT2-CFP should be expressed in FtsZ mutant plants, as localization patterns would provide insight as to how ADT2 behaves in the absence of FtsZ. Because there are multiple forms of FtsZ, it would be interesting to determine its localization patterns when different FtsZ isoforms are absent. This would further our knowledge as to how different FtsZ isoforms are related to ADT2. What is critically lacking in our understanding of ADT2 in chloroplast division is how it interacts with other division proteins. For example, yeast two-hybrid assays should be performed between ADT2 and other known chloroplast division proteins. This would be of particular interest for ARC3, ARC6 and FtsZ1 and FtsZ2, given that ARC3 and ARC6 affect ADT2 localization in a similar manner to FtsZ. If interactions are found they should be taken from yeast into a plant and bi-molecular fluorescence complementation could be performed to determine if these interactions occur *in planta*. Random or targeted mutations should also be induced in ADT2 to determine the region of the enzyme responsible for its chloroplast division role. Finally, other species of plants should be used to determine if ADT2's chloroplast division function is conserved.

5 References

Agati, G., Biricolti, S., Guidi, L., Ferrini, F., Fini, A., Tattini, M. (2011) The biosynthesis of flavonoids is enhanced similarily by UV radiation and root zone salinity in *L. vulgare* leaves. *J. Plant Physiol.* **168**: 204-212.

Avisar, D., Prokhnevsky, A.I., Makarova, K.S., Koonin, E.V., Dolja, V.V. (2008) Myosin XI-K is required for rapid trafficking of golgi stacks, peroxisomes, and mitochondria in leaf cells of *Nicotiana benthamiana*. *Plant Physiol.* **146**: 1098-1108.

Bevan, M. (1984) Binary *Agrobacterium* vectors for plant transformation. *Nucleic Acids Res.* **12**: 8711-8721.

Bonner, C.A., Jensen, R.A. (1985) Novel features of prephenate aminotransferase from cell cultures of *Nicotiana silvestris*. *Arch. Biochem. Biophys*. **238**: 237-246.

Bross, C.D. (2011) Characterizing substrate specificity and subcellular localization of argenate dehydratases from *Arabidopsis thaliana*. M.Sc. Thesis. University of Western Ontario, Department of Biology.

Cho, M.H., Corea, O.R.A., Yang, H., Bedgar, D.L., Laskar, D.D., Anterola, A.M., Moog-Anterola, F.A., Hood, R.L., Kohalmi, S.E., Bernards, M.A., Kang, C., Davin, L.B., Lewis, N.G. (2007) Phenylalanine biosynthesis in *Arabidopsis thaliana*: identification and characterization of arogenate dehydratases. *J. Biol. Chem.* **282:** 30827-30835.

Cho, Y., Yoo, S., Sheen, J. (2006) Regulatory functions of nuclear hexokinase1 complex in glucose signaling. *Cell.* **127**: 579-589.

Clough, S.J., Bent, A.F. (1998) Floral dip: a simplified method for *Agrobacterium*-mediated transformation of *Arabidopsis thaliana*. *Plant J.* **16**: 735-743.

Corea, O.R.A., Ki, C., Cardenas, C.L., Kim, S., Brewer, S.E., Patten, A.M., Davin, L.B., Lewis, N.G. (2012) Arogenate dehydrase isoenzymes profoundly and differentially modulate carbon flux into lignins. *J. Biol. Chem.* **287**: 11446-11459.

Crawley, C.D. (2004) Characterization of six *PREPHENATE DEHYDRATASE*-like genes in *Arabidopsis thaliana*. M.Sc. Thesis. University of Western Ontario, Department of Biology.

Desveaux, D., Maréchal, A., Brisson, N. (2005) Whirly transcription factors: defense and beyond. *Trends Plant Sci.* **10**: 95-102.

Earley, K.W., Haag, J.R., Pontes, O., Opper, K., Juehne, T., Song, K., Pikaard, C.S. (2006) Gateway-compatible vectors for plant functional genomics and proteomics. *Plant J.* **45**: 616-629.

Eberhard, J., Ehrler, T.T., Epple, P., Felix, G., Raesecke, H.R., Amrhein, Schmid, J. (1996) Cytosolic and plastidic chorismate mutase isoenzymes from *Arabidopsis thaliana*: molecular characterization and enzymatic properties. *Plant J.* **10**: 815-821.

Eberhard, J., Raesecke, H.R., Schmid, J., Amrhein, N. (1993) Cloning and expression in yeast of a higher plant chorismate mutase. *FEBS Lett.* **334**: 233-236.

Ehlting, J., Mattheus, N., Aeschliman, D.S., Li, E., Hamberger, B., Zhuang, J., Kaneda, M., Mansfield, S.D., Samuels, L., Ritland, K., Ellis, B.E., Bohlmann, J., Douglas, C.J. (2005) Global transcript profiling of primary stems from *Arabidopsis thaliana* identifies candidate genes for missing links in lignin biosynthesis and transcriptional regulators of fiber differentiation. *Plant J.* **42**: 618-640.

Escobar, M.A., Dandekar, A.M. (2003) *Agrobacterium tumefaciens* as an agent of disease. *Trends Plant Sci*. **8**: 380-386.

Fernstrom, J.D., Fernstrom, M.H. (2007) Tyrosine, phenylalanine, and catecholamine synthesis in the brain. *J. Nutr.* **137**: 1539S-1547S.

Fraser, C.M., Chapple, C. (2011) The phenylpropanoid pathway in *Arabidopsis*. The *Arabidopsis* Book **9**: e0152

Galichet, A., Hoyerová, K., Kamínek, M., Gruissem, W. (2008) Farnesylation directs *At*IPT3 subcellular localization and modulates cytokinin biosynthesis in *Arabidopsis*. *Plant Physiol.* **146**: 1155-1164.

Gallie, D.R. (2013) L-ascorbic acid: a multifunctional molecule supporting plant growth and development. *Scientifica.* **2013**: 1-24.

Ganson, R.J., D'Amato, T.A., Jensen, R.A. (1986) The two-isozyme system of 3-deoxy-d-arabino-heptulosonate 7-phosphate synthase in *Nicotiana silvestris* and other higher plants. *Plant Physiol.* **82**: 203-210.

Gao, H., Kadirjan-Kalbach, D., Froehlich, J.E., Osteryoung, K.W. (2003) ARC5, a cytosolic dynamin-like protein from plants is part of the chloroplast division machinery. *Proc. Nat. Acad. Sci. USA.* **100**: 4328-4333.

Gelvin, S.B. (2003) *Agrobacterium*-mediated plant transformation: the biology behind the "gene-jockeying" tool. *Microbiol. Mol. Biol. R.* **67**: 16-37.

Glynn, J.M., Froehlich, J.E., Osteryoung, K.W. (2008) *Arabidopsis* ARC6 coordinates the division of the inner and outer chloroplast membranes through interaction with PDV2 in the intermembrane space. *Plant Cell*. **20**: 2460-2470.

Glynn, J.M., Miyagishima, S., Yoder, D.W., Osteryoung, K.W., Vitha, S. (2007) Chloroplast division. *Traffic*. **8**: 451-461.

Glynn, J.M., Yang, Y., Vitha, S., Schmitz, A.J., Hemmes, M., Miyagishima, S., Osteryoung, K.W. (2009) PARC6, a novel chloroplast division factor, influences FtsZ assembly and is required for recruitment of PDV1 during chloroplast division in *Arabidopsis*. *Plant J.* **59**: 700-711.

Gray, J.C., Hansen, M.R., Shaw, D.J., Graham, K., Dale, R., Smallman, P., Natesan, S.K.A., Newell, C.A. (2012) Plastid stromules are induced by stress treatments acting through abscisic acid. *Plant J.* **69**: 387-398.

Gray, J.C., Sullivan, J.A., Hibberd, J.M., Hansen, M.R. (2001) Stromules: mobile protrusions and interconnections between plastids. *Plant Biol.* **3**: 223-233.

Gray, J.C., Sullivan, J.A., Newell, C.A. (2011) Visualization of stromules on *Arabidopsis* plastids. *Methods Mol. Biol.* **774**: 73-85.

Gunning, B.E.S. (2005) Plastid stromules: video microscopy of their outgrowth, retraction, tensioning, anchoring, branching, bridging, and tip-shedding. *Protoplasma.* **225**: 33-42.

Hanahan, D. (1983) Studies on transformation of *Escherichia coli* with plasmids. *J. Mol. Biol.* **166**: 557-580.

Hanson, M.R., Sattarzadeh, A. (2011) Stromules: recent insights into a long neglected feature of plastid morphology and function. *Plant Physiol*. **155**: 1486-1492.

Herrmann, K.M., Weaver, L.M. (1999) The shikimate pathway. *Annu. Rev. Plant Physiol. Plant Mol. Biol*. **50**: 473-503.

Hoekema, A., Hirsch, P.R., Hooykaas, P.J.J., Schilperoort, R.A. (1983) A binary plant vector strategy based on separation of *vir* and T-region of the *Agrobacterium tumefaciens* Ti-plasmid. *Nature*. **303**: 179-180.

Holtsmark, I., Lee, S., Lunde, K.A., Auestad, K., Maple-Grøden, J., Møller, S.G. (2013) Plastid division control: the PDV proteins regulate DRP5B dynamin activity. *Plant Mol. Biol*. **82**: 255-266.

Holzinger, A., Kwok, E.Y., Hanson, M.R. (2008) Effects of *arc3*, *arc5* and *arc6* mutations on plastid morphology and stromule formation in green and nongreen tissues of *Arabidopsis thaliana*. *Photochem. Photobiol*. **84**: 1324-1335.

Huang, T., Tohge, T., Lytovchenko, A., Fernie, A.R., Jander, G. (2010) Pleiotropic physiological consequences of feedback-insensitive phenylalanine biosynthesis in *Arabidopsis thaliana*. *Plant J.* **63**: 823-835.

Inaba, T., Yazu, F., Ito-Inaba, Y., Kakizaki, T., Nakayama, K. (2011) Retrograde signaling pathway from plastid to nucleus. *Int. Rev. Cell. Mol. Biol.* **290**: 167-204.

Invitrogen Corporation. (1999-2003) Gateway® technology a universal technology to clone DNA sequences for functional analysis and expression in multiple systems. (tools.invitrogen.com/content/sfs/manuals/gatewayman.pdf).

Isemer, R., Mulisch, M., Schäfer, A., Kirchner, S., Koop, H., Krupinska, K. (2012) Recombinant Whirly1 translocates from transplastomic chloroplasts to the nucleus. *FEBS Lett.* **586**: 85-88.

Ishida, H., Yoshimoto, K., Izumi, M., Reisen, D., Yano, Y., Makino, A., Ohsumi, Y., Hanson, M.R., Mae, T. (2008) Mobilization of RuBisCO and stroma-localized fluorescent proteins of chloroplasts to the vacuole by an *ATG* gene-dependent autophagic process. *Plant Physiol.* **148**: 142-155.

Johnson, C.B., Tang, L.K., Smith, A.G., Ravichandran, A., Luo, Z., Vitha, S., Holzenburg, A. (2013) Single particle tracking analysis of the chloroplast division protein FtsZ anchoring to the inner envelope membrane. *Microsc. Microanal.* **19:** 507-512.

Jung, E., Zamir, L.O., Jensen, R.A. (1986) Chloroplasts of higher plants synthesize L-phenylalanine via L-arogenate. *Proc. Natl. Acad. Sci. USA*. **83**: 7231-7235.

Köhler, R.H., Cao, J., Zipfel, W.R., Webb, W.W., Hanson, M.R. (1997) Exchange of protein molecules through connections between higher plant plastids. *Science.* **276**: 2039-2042.

Köhler, R.H., Hanson, M.R. (2000) Plastid tubules of higher plants are tissue-specific and developmentally regulated. *J. Cell Sci.* **113**: 81-89.

Koncz, C., Schell, J. (1986) The promoter of TL-DNA gene 5 controls the tissue-specific expression of chimaeric genes carried by a novel type of *Agrobacterium* binary vector. *Mol. Gen. Genet.* **204**: 383-396.

Krause, K., Oetke, S., Krupinska, K. (2012) Dual targeting and retrograde translocation: regulators of plant nuclear gene expression can be sequestered by plastids. *Int. J. Mol. Sci.* **13**: 11085-11101.

Kwok, E.Y., Hanson, M.R. (2003) Microfilaments and microtubules control the morphology and movement of non-green plastids and stromules in *Nicotiana tabacum*. *Plant J.* **35**: 16-26.

Kwok, E.Y., Hanson, M.R. (2004a) GFP-labeled RuBisCO and aspartate aminotransferase are present in plastid stromules and traffic between plastids. *J. Exp. Bot*. **55**: 595-604.

Kwok, E.Y., Hanson, M.R. (2004b) Plastids and stromules interact with the nucleus and cell membrane in vascular plants. *Plant Cell Rep.* **23**: 188-195.

Kwok, E.Y., Hanson, M.R. (2004c) *In vivo* analysis of interactions between GFP-labeled microfilaments and plastid stromules. *BMC Plant Biol.* **4**: 2.

Leuchtenberger, W., Huthmacher, K., Drauz, K. (2005) Biotechnological production of amino acids and derivatives: current status and prospects. *Appl. Microbiol. Biotechnol*. **69**: 1-8.

Liberles, J.S., Thórólfsson, M., Martínez, A. (2005) Allosteric mechanisms in ACT domain containing enzymes involved in amino acid metabolism. *Amino Acids.* **28**: 1-12.

Liu, C. (2012) Deciphering the enigma of lignification: precursor transport, oxidation, and the topochemistry of lignin assembly. *Mol. Plant*. **5**: 304-317.

Lu, Q., Tang, X., Tian, G., Wang, F., Liu, K., Nguyen, V., Kohalmi, S.E., Keller, W.A., Tsang, E.W.T., Harada, J.J., Rothstein, S.J., Cui, Y. (2010) *Arabidopsis* homolog of the yeast TREX-2 mRNA export complex: components and anchoring nucleoporin. *Plant J.* **61**: 259-270.

Maeda, H., Dudareva, N. (2012) The shikimate pathway and aromatic amino acid biosynthesis in plants. *Annu. Rev. Plant Biol.* **63**: 73-105.

Maeda, H., Yoo, H., and Dudareva, N. (2011) Prephenate aminotransferase directs plant phenylalanine biosynthesis via arogenate. *Nat. Chem. Biol.* **7**: 19-21.

Maple, J., Vojta, L., Soll, J., Møller, S.G. (2007) ARC3 is a stromal Z-ring accessory protein essential for plastid division. *EMBO Rep*. **8**: 293-299.

Maréchal, A., Parent, J., Véronneau-Lafortune, Joyeux, A., Lang, B.F., Brisson, N. (2009) Whirly proteins maintain plastid genome stability in *Arabidopsis. Proc. Natl. Acad. Sci. USA*. **106**: 14639-14698.

Mewis, I., Khan, M.A.M., Glawischnig, E., Schreiner, M., Ulrichs, C. (2012) Water stress and aphid feeding differentially influence metabolite composition in *Arabidopsis thaliana* (L.). *PLOS ONE*. **7**: e48661.

Miyagishima, S. (2011) Mechanism of plastid division: from a bacterium to an organelle. *Plant physiol*. **155**: 1533-1544.

Miyagishima, S., Froehlich, J.E., Osteryoung, K.W. (2006) PDV1 and PDV2 mediate recruitment of the dynamin-related protein ARC5 to the plastid division site. *Plant Cell*. **18**: 2517-2530.

Miyagishima, S., Kabeya, Y. (2010) Chloroplast division: squeezing the photosynthetic captive. *Curr. Opin. Microbiol.* **13**: 738-746.

Natesan, S.K.A., Sullivan, J.A., Gray, J.C. (2005) Stromules: a characteristic cell-specific feature of plastid morphology. *J. Exp. Bot.* **56**: 787-797.

Natesan, S.K.A., Sullivan, J.A., Gray, J.C. (2009) Myosin XI is required for actin associated movement of plastid stromules. *Mol. Plant*. **2**: 1262-1272.

Nelson, B.K., Cai, X., Nebenführ. (2007) A multicolored set of in vivo organelle markers for co-localization studies in *Arabidopsis* and other plants. *Plant J*. **51**: 1126-1136.

Osteryoung, K.W., Stokes, F.D., Rutherford, S.M., Percival, A.L., Lee, W.Y. (1998) Chloroplast division in higher plants requires members of two functionally divergent gene families with homology to bacterial *ftsZ*. *Plant Cell.* **10**: 1991-2004.

Osteryoung, K.W., Vierling, E. (1995) Conserved cell and organelle division. *Nature*. **376**: 473-474.

Peremyslov, V.V., Proknevsky, A.I., Avisar, D., Dolja, V.V. Two class XI myosins function in organelle trafficking and root hair development. *Plant Physiol.* **146**: 1109-1116.

Popescu, S.C., Popescu, G.V., Bachan, S., Zhang, Z., Seay, M., Gerstein, M., Snyder, M., Dinesh-Kumar, S.P. (2007) Differential binding of calmodulin-related proteins to their targets revealed through high-density *Arabidopsis* protein microarrays. *Proc. Nat. Acad. Sci. USA*. **104**: 4730-4735.

Pyke, K.A. (2013) Divide and shape: an endosymbiont in action. *Planta*. **237**: 381-387.

Pyke, K.A. (1999) Plastid division and development. *Plant Cell.* **11**: 549-556.

Pyke, K.A., Leech, R.M. (1992) Chloroplast division and expansion is radically altered by nuclear mutations in *Arabidopsis thaliana*. *Plant Physiol.* **99**: 1005-1008.

Pyke, K.A., Leech, R.M. (1994) Genetic analysis of chloroplast division and expansion in *Arabidopsis thaliana*. *Plant Physiol*. **104**: 201-207.

Pyke, K.A., Rutherford, S.M., Robertson, E.J., Leech, R.M. (1994) *arc6*, a fertile *Arabidopsis* mutant with only two mesophyll cell chloroplasts. *Plant Physiol*. **106**: 1169-1177.

Rasband, W.S. (1997-2013). ImageJ, version 1.45s. U.S. National Institutes of Health, Bethesda, Maryland , USA. (imagej.nih.gov.ij).

Reddy, A.S.N., Day, I.S. (2001) Analysis of the myosins encoded in the recently completed *Arabidopsis thaliana* genome. *Genome Biol.* **2**: 0024.1-0024.17.

Rippert, P., Puyaubert, J., Grisollet, D., Derrier, L., Matringe, M. (2009) Tyrosine and phenylalanine are synthesized within the plastids in *Arabidopsis*. *Plant Physiol.* **149**: 1251-1260.

Samanta, A., Das, G., Das, S.K. (2011) Roles of flavonoids in plants. *Int. J. Pharm. Sci. Tech.* **6**: 12-35.

Sambrook, J., Russell, D. (2001) Molecular cloning: a laboratory manual (3rd edition). Cold Spring Harbor Laboratory Press, Cold Spring Harbor, New York.

Schattat, M., Barton, K., Baudisch, B., Klösgen, R.B., Mathur, J. (2011) Plastid stromule branching coincides with contiguous endoplasmic reticulum dynamics. *Plant Physiol.* **155**: 1667-1677.

Shimada, H., Koizumi, M., Kuroki, K., Mochizuki, M., Fujimoto, H., Ohta, H., Masuda, T., Takamiya, K. (2004) ARC3, a chloroplast division factor, is a chimera of prokaryotic FtsZ and part of eukaryotic phosphatidylinositol-4-phosphate 5-kinase. *Plant Cell Physiol.* **45**: 960-967.

Shimmen, T., Yokota, E. (2004) Cytoplasmic streaming in plants. *Curr. Opin. Cell Biol.* **16**: 68-72.

Silhavy, D., Molnár , A., Lucioli, A., Szittya, G., Hornyik, C., Tavassa, M., Burgyán, J. (2002) A viral protein suppresses RNA silencing and binds silencing-generated 21- to 25-nucleotide double-stranded RNAs. *EMBO J.* **21**: 3070-3080.

Statchel, S.E., Messens, E., Van Montagu, M., Zambryski, P. (1985) Identification of the signal molecules produced by wounded plant cells that activate T-DNA transfer in *Agrobacterium tumefaciens*. *Nature.* **318**: 624-629.

Tan, K., Li, H., Zhang, R., Gu, M., Clancy, S.T., Joachimiak, A. (2008). Structures of open (r) and closed (t) states of prephenate dehydratase (PDT) – implication of allosteric regulation by L-phenylalanine. *J. Struct. Biol.* **162**: 94-107.

TerBush, A.D., Osteryoung, K.W. (2012) Distinct functions of chloroplast FtsZ1 and FtsZ2 in Z-ring structure and remodeling. *J. Cell Biol.* **199**: 623-637.

TerBush, A.D., Yoshida, Y., Osteryoung, K.W. (2013) FtsZ in chloroplast division: structure, function and evolution. *Curr. Opin. Cell Biol*. **25**: 461-470.

The *Arabidopsis* Genome Initiative. (2000) Analysis of the genome sequence of the flowering plant *Arabidopsis thaliana*. *Nature*. **408**: 796-815.

Tzin, V., Galili, G. (2010) New insights into the shikimate and aromatic amino acids biosynthesis pathways in plants. *Mol. Plant.* **3**: 956-972.

Udenfriend, S., and Cooper, J.R. (1952) The enzymatic conversion of phenylalanine to tyrosine. *J. Biol. Chem.* **194**: 503-511.

Vitha, S., Froehlich, J.E., Koksharova, O., Pyke, K.A., van Erp, H., Osteryoung, K.W. (2003) ARC6 is a J-domain plastid division protein and an evolutionary descendant of the cyanobacterial cell division protein Ftn2. *Plant Cell.* **15**: 1918-1933.

Vitha, S., McAndrew, R.S., Osteryoung, K.W. (2001) FtsZ ring formation at the chloroplast division site in plants. *J. Cell Biol.* **153**: 111-119.

Voinnet, O., Rivas, S., Mestre, P., Baulcombe, D. (2003) An enhanced transient expression system based on suppression of gene silencing by the p19 protein of tomato bushy stunt virus. *Plant J*. **33**: 949-956.

Walia, H., Wilson, C., Condamine, P., Liu, X., Ismail, A.M., Zeng, L., Wanamaker, S.I., Mandal, J., Xu, J., Cui, X., Close, T.J. (2005) Comparative transcriptional profiling of two contrasting rice genotypes under salinity stress during the vegetative growth stage. *Plant Physiol.* **139**: 822-835.

Wiedenmann, J., Ivanchenko, S., Oswald, F., Schmitt, F., Röcker, C., Salih, A., Spindler, K., Nienhaus, G.U. (2004) EosFP, a fluorescent marker protein with UV-inducible green-to-red fluorescence conversion. *Proc. Natl. Acad. Sci. USA*. **101**: 15905-15910.

Wightman, F., Forest, J.C. (1978) Properties of plant aminotransferases. *Phytochemistry*. **17**: 1455-1471.

Wise, A.A., Liu, Z., Binns, A.N. (2006). Three methods for the introduction of foreign DNA into *Agrobacterium*. *Methods Mol. Biol*. **343**: 43-54.

Wroblewski, T., Tomczak, A., Michelmore, R. (2005) Optimization of *Agrobacterium*-mediated assays of gene expression in lettuce, tomato and *Arabidopsis*. *Plant Biotechnol. J.* **3**: 259-273.

Xiang, C., Han, P., Lutziger, I., Wang, K., Oliver, D.J. (1999) A mini binary vector series for plant transformation. *Plant Mol. Biol*. **40**: 711-717.

Yang, Y., Li, R., Qi, M. (2000) *In vivo* analysis of plant promoters and transcription factors by agroinfiltration of tobacco leaves. *Plant J.* **22**: 543-551.

Yoshida, Y., Kuroiwa, H., Misumi, O., Nishida, K., Yagisawa, F., Fujiwara, T., Nanamiya, H., Kawamura, F., Kuroiwa, T. (2006) Isolated chloroplast division machinery can actively constrict after stretching. *Science.* **313**: 1425-1438.

Yoshida, Y., Kuroiwa, H., Misumi, O., Yoshida, M., Ohnuma, M., Fujiwara, T., Yagisawa, F., Hirooka, S., Imoto, Y., Matsushita, K., Kawano, S., Kuroiwa, T. (2010) Chloroplasts divide by contraction of a buncle of nanofilaments consisting of polyglucan. *Science*. **329**: 949-953.

Zhang, M., Schmitz, A.J., Kadirjan-Kalback, D.K., TerBush, A.D., Osteryoung, K.W. (2013) Chloroplast division protein ARC3 regulates chloroplast FtsZ-ring assembly and positioning in *Arabidopsis* through interaction with FtsZ2. *Plant Cell*. **25:** 1787-1802.

Zupan, J., Muth, T.R., Draper, O., Zambryski, P. (2000) The transfer of DNA from *Agrobacterium tumefaciens* into plants: a feast of fundamental insights. *Plant J.* **23**: 11-28.

6 Curriculum Vitae

TRAVIS R. HOWES, B. Sc. (Hons.)

EDUCATION

2011-2013 **Master of Science Candidate**, Cell and Molecular Biology
Department of Biology
University of Western Ontario, London, Ontario, Canada

2007-2011 **Bachelor of Science (Hons.)**, double major: genetics, medical cell biology
University of Western Ontario, London, Ontario, Canada

AWARDS, HONORS AND SCHOLARSHIPS

2013 **Best oral presentation: honorable mention**
2013 Canadian Society of Plant Biologists Annual Meeting
June 25th-28th 2013, University of Laval, Québec City, Québec, Canada

2012-2013 **Graduate student teaching award nominee**
University of Western Ontario, London, Ontario, Canada

2012 **Best poster presentation**
8th Canadian Biotechnology Conference (IAPB)
May 14th-17th, University of Guelph, Guelph, Ontario, Canada

2011-2013 **Western Graduate Research Scholarship**
University of Western Ontario, London, Ontario, Canada

2011 **Western Gold Medal**
Highest average for a double major with genetics
University of Western Ontario, London, Ontario, Canada

2010 **Suncor Energy Scholarship**
Suncor Energy, Mississauga, Ontario, Canada

2009-2011 **Dean's Honor List**
University of Western Ontario, London, Ontario, Canada

2007 **Western Scholarship of Distinction**
University of Western Ontario, London, Ontario, Canada

TEACHING AND WORK EXPERIENCE

2011-2013 **Teaching Assistant**
Biology 3595a: Advanced genetics
Biology 4562b: Genes and genomes II
University of Western Ontario, London, Ontario, Canada

2011 **Water Laboratory Summer Student**
Public Health Ontario, London, Ontario, Canada

ORAL PRESENTATIONS (* denotes presenter)

2013 **Howes, T.R.***, Bross, C.D., and Kohalmi, S.E.
In planta examination of the subcellular localization of AROGENATE DEHYDRATASES.
2013 Canadian Society of Plant Biologists Annual Meeting
June 25th-28th 2013, University of Laval, Québec City, Québec, Canada

2012 Kohalmi, S.E.*, Ahmad, T., Bross, C.D., Corea, O.R.A., Hood, R.L., **Howes, T.R.**, Styranko, D.M.
Six arogenate dehydratases synthesize phenylalanine in *Arabidopsis thaliana*.
51st Annual Meeting of the Phytochemical Society of North America
August 11th-15th, University of Western Ontario, London, Ontario, Canada

POSTER PRESENTATIONS (*denotes presenter)

2013 Rad, S.A.*, **Howes, T.R.**, and Kohalmi, S.E.
Identification of sequences required for nuclear targeting of ADT5
2013 Canadian Society of Plant Biologists Annual Meeting
June 25th-28th 2013, University of Laval, Québec City, Québec, Canada

2012 **Howes, T.R.***, Bross, C.D., and Kohalmi, S.E.
Determining subcellular localization of AROGENATE DEHYDRATASES using CFP fusion proteins.
51st Annual Meeting of the Phytochemical Society of North America
August 11th-15th, University of Western Ontario, London, Ontario, Canada

2012 **Howes, T.R.*,** Bross, C.D., and Kohalmi, S.E.
Subcellular localization of AROGENATE DEHYDRATASES suggest differential functional roles
8th Canadian Plant Biotechnology Conference (IAPB)
May 14th-17th, University of Guelph, Guelph, Ontario, Canada

ASSOCIATION MEMBERSHIPS

2013-present Canadian Society of Plant Biologists
2012-2013 Phytochemical Society of North America
2012-2013 International Association for Plant Biotechnology